

Static back-pressure effects on the performance of a dual-fuel engine

Wieger Peet

Delft University of Technology

Thesis for the degree of MSc in Marine Technology in the specialization of
Marine Engineering

Static back-pressure effects on the performance of a dual-fuel engine

By

Wieger Peet

Performed at

TU Delft

This thesis **MT.21.001.m** is classified as confidential in accordance with the
general conditions for projects performed by the TUDelft.

15 oktober 2021

Thesis exam committee

Chair/Responsible Professor: Ir. K. Visser, TU Delft

Staff Member: Dr. Ir. P. de Vos, TU Delft

Staff Member: Dr. A. Coraddu MSc, TU Delft

Author Details

Studynumber: 4230329

Author contact e-mail: wieger.peet@gmail.com

An electronic version of this thesis can be found at <http://repository.tudelft.nl>

Abstract

The use of fossil fuels and their impact on humans and nature is becoming a bigger concern worldwide. An interesting concept to lower polluting emissions coming from maritime engines is the combined use of a dual-fuel engine and an underwater exhaust system. In the dual-fuel engine natural gas is used as the main fuel type. It is seen as a cleaner alternative to the traditional fossil fuels that are being used. In order to ignite the air-gas mixture in the cylinder a small amount of diesel fuel (pilot fuel) is used, therefore making it a dual-fuel engine. Some advantages of using an underwater exhaust system are no direct emissions into the atmosphere, increased space on decks and reduced noise from the exhaust. However the downside is that such a system causes back-pressure effects which can deteriorate engine performance. So far research on these back-pressure effects on a dual-fuel type engine is lacking, therefore this thesis focuses on the static back-pressure effects on a dual-fuel engine.

For this purpose experiments were performed on a constant pressure turbocharged, 4-stroke dual-fuel engine. Engine performance and emissions were recorded for load points along the propeller and generator curve for three cases of back-pressure. The back-pressure was controlled by a butterfly valve in the exhaust pipe of the engine. Due to the fact that this butterfly valve could only be controlled manually, the back-pressure during the experiments could not be kept at a constant level. Also the engine experienced an absolute back-pressure of 1.15 bar with the valve fully open which was already quite high. And in the natural gas that was used a substantial amount of hydrogen was present.

An existing diesel engine model (DE-B) that was developed at the TU Delft was then adapted to turn it into a dual-fuel engine model. It is a mean value first principle (MVFP) model. This dual-fuel MVFP model was then matched to the tested engine by using the experimental data. After the matching the model was used to test levels of back-pressure that could not be reached experimentally, due to engine limits, to see the effect on engine performance at these levels. The results were then analysed to see what the critical engine parameters are for the limits of the engine.

The experimental results showed that at low power more pilot fuel is needed to combust the gaseous fuel. It was also clear that there was a changing combustion efficiency for the gaseous fuel along the propeller curve. For the part load conditions the combustion efficiency was lower than at low or high power. For the generator curve the total efficiency was more constant, but always lower than the efficiency of the propeller curve. The results also showed that with increasing back-pressure the fuel consumption decreased for both the pilot and gaseous fuel, with the exception of the gaseous fuel flow at part load for the propeller curve. The recorded emissions showed lower levels of O_2 , CO and unburned hydrocarbons and higher levels of CO_2 and NO_x with increased back-pressure. Looking at the emissions in combination with the fuel flows, they showed signs of improved combustion efficiency with increased back-pressure. Increasing the back-pressure caused lower pressures and temperatures at the inlet side of the engine and higher pressures and temperatures at the outlet side. So for the thermal loading of the engine the outlet side is the critical one. The tested dual-fuel engine had a waste-gate installed. The model runs with higher levels of back-pressure showed that the pressure on the inlet side could become so low, that the pressure at which this waste-gate becomes active is no longer reached. This causes high pressures and temperatures before the turbine and high temperatures of the exhaust valve. The model also showed that at high levels of back-pressure the flow through the turbine becomes too low and not enough air is being put into the engine, so the air-excess ratio becomes too low, making the air-excess ratio also an important parameter for the engine limits. Finally it was shown how the dual-fuel MVFP model can be used to define acceptable limits of back-pressure for the air-excess ratio, exhaust valve and outlet receiver temperature.

The main recommendation for further research is to investigate the combustion efficiency of the gaseous fuel. Both the fact that at part load the efficiency was at its worst and the lower fuel consumption when back-pressure was increased need to be looked at. This will also help with improving the current dual-fuel MVFP model. Next to that it would be interesting to see what happens with different types of gaseous fuel and how the engine performs under a fluctuating back-pressure as induced by waves.

Contents

Abstract	iii
1 Introduction	1
1.1 Existing literature	1
1.1.1 Underwater exhaust system	1
1.1.2 Back-pressure effect on engine	2
1.1.3 Dual-fuel engine	4
1.2 Model investigation	6
1.3 Research objective	7
1.4 Plan of approach	7
1.4.1 Dual-fuel engine model	7
1.4.2 Calibration of the dual-fuel MVFP model	8
1.4.3 Validation of the dual-fuel MVFP model	8
1.4.4 Experimental results	8
1.4.5 Model extrapolation	9
1.4.6 Limit cases	9
2 MVFP model and adaptations	10
2.1 DE-B model	10
2.1.1 In-cylinder process	10
2.2 Model adaptations	12
2.2.1 Comparing tool	12
2.2.2 Fluid properties	12
2.2.3 Composition of gas in the system	13
2.2.4 Properties blocks	13
2.2.5 Cylinder: Gas exchange	14
2.2.6 Cylinder: Seiliger cycle	14
2.2.7 Volume and heat elements	14
2.2.8 Waste-gate	14
3 Matching of the dual-fuel MVFP model	16
3.1 Matching procedure	16
3.2 Calibration of the dual-fuel MVFP model	17
3.2.1 Propeller curve	17
3.2.2 Generator curve	22
3.3 Verification of the dual-fuel MVFP model	27
3.3.1 Propeller curve	27
3.3.2 Generator curve	35
4 Experiments	44
4.1 Experiment set-up and collected data	44
4.2 Experimental results - Propeller curve	46
4.2.1 Inlet side	46
4.2.2 Exhaust side	47
4.2.3 Fuel consumption	48
4.2.4 Emissions	50
4.3 Experimental results - Generator curve	53
4.3.1 Inlet side	53
4.3.2 Exhaust side	54
4.3.3 Fuel consumption	55
4.3.4 Emissions	57
4.4 Conclusion of experimental results	59
5 Dual-fuel MVFP model extrapolation	61

6	Limit cases	67
6.1	Engine envelope	67
6.2	Engine limits with back-pressure	67
7	Conclusions and recommendations	70
7.1	Conclusions	70
7.2	Recommendations	71
	References	72
	List of Figures	74
	List of Tables	75

1 Introduction

Diesel engines are used all over the world to generate power or they are being used as a prime mover for e.g. cars, trucks and ships. Since their invention they have been improved in order to enhance their performance, lower the fuel consumption or lower the emissions. In recent years the use of fossil fuels and their impact on both humans and nature has become more of a concern. Since diesel engines are still commonly used in the maritime sector, the International Maritime Organization (IMO) has introduced more rules and regulations about their emissions. For instance, since January 2016 the regulations about the emission of NO_x have been improved and as of January 2020 a global sulfur cap has been introduced (1). In order to meet these regulations, engines are equipped or retrofitted with exhaust gas after-treatment systems. Examples of these systems are scrubbers or Selective Catalytic Reactors (SCR). The downside of these systems is that they create a pressure loss in the exhaust pipes, which deteriorates the engine performance. This loss of pressure is called back-pressure.

The GasDrive project is a novel ship propulsion concept where a Solid Oxide Fuel Cell (SOFC), natural gas engine and underwater exhaust system with nano-hull coatings are used together to achieve higher propulsion efficiency and ultra-low emissions. One of the objectives of GasDrive is to allow for zero-direct emissions to the atmosphere by exhausting below the waterline and then using the exhaust gas from the underwater exhaust for gas lubrication using nano-materials to reduce drag. This will help in further improving the system efficiency (2). The use of underwater exhaust systems is a technology that has been investigated in recent years. One of the perks of this system is that there are no direct emissions to the atmosphere. But the gasses coming out of the engine experience more resistance, because of the pressure created by the water at the outlet, which adds to the back-pressure experienced by the engine.

One of the main concerns in the GasDrive project is the effect of static and dynamic back-pressure on engine performance including the effects on emissions. The aim of this research is to get a better understanding of the effect of static back-pressure on a dual-fuel engine. In the next section a description of the existing literature will be given. Then in section 1.2 the different types of simulation models will be discussed and in section 1.3 it will be explained what knowledge is missing and a more detailed description of the research objective is given.

1.1 Existing literature

In this section the existing literature will be discussed. It has been divided into three topics. First the underwater exhaust system will be discussed: what are the advantages of such a system, but also what the challenges are when such a system is being used. Next the effects of back-pressure on engine performance and emissions will be discussed. Lastly the workings of a dual fuel engine will be given, as well as the differences compared with a conventional diesel engine.

1.1.1 Underwater exhaust system

As mentioned above, the GasDrive project aims to use an underwater exhaust system. Such a system has been introduced on some small vessels in order to reduce noise and odors from the engine (3). Moreover a snorkel system was introduced in 1938 for submarines, which allowed the diesel engines to be used while the submarine was at periscope depth (4). But for large vessels the emissions normally are expelled into the atmosphere through some after treatment systems, like a scrubber. The use of an underwater exhaust system for these vessels is a recent development in the maritime industry. The advantages of such a system are (2)(5):

- Reduced noise from the exhaust, so vessels can operate more silently in harbours for example. Also the noise on working decks will be lower.
- No direct emissions into the atmosphere (although emissions do still exist).
- More space on working decks, since there is no need for a funnel going through the vessel.
- Reduced exhaust gas interference on working decks.
- Decreased risk of detection for naval vessels by reducing the hotspot detection.
- Improved aesthetics for luxury vessels, because of the elimination of bulky and un-appealing exhaust funnels through the decks.

The downside of the use of such a system is that the gasses expelled from the engine experience more resistance to their flow. This resistance comes from the pressure exerted by the water at the outlet. The resistance a moving fluid experiences by obstructions against its direction of flow is called back-pressure (3). So in addition to the static back-pressure due to the after treatment systems, an additional back-pressure is created due to the waves at the outlet. This back-pressure from the waves consists of a static and a dynamic part. The static part is due to the mean depth of the exhaust below the water surface and the dynamic part comes from the pulsating water waves, which have a varying amplitude and period depending on the ocean conditions the vessel is experiencing. The cumulative flow resistance in the exhaust system measured at the turbine outlet is the back-pressure experienced by the engine (5). The effect this back-pressure has on the engine is discussed in section 1.1.2.

1.1.2 Back-pressure effect on engine

As mentioned in the previous section, the use of an underwater exhaust system will increase the back-pressure on the engine. This back-pressure is defined as the cumulative flow resistance in the exhaust system measured at the turbine outlet for a turbocharged engine (or at the exhaust manifold in case of a naturally aspirated engine). For a certain mechanical loading, the back-pressure will increase the thermal loading of the engine and will also increase the fuel consumption. This is due to the fact that the engine needs to do more pumping work to expel the gasses from the cylinder. Another effect that may appear is a decrease in turbocharger efficiency, which leads to a change in the air-to-fuel ratio. In some cases this can cause the engine to start smoking, because there is not enough combustion air in the cylinder, leading to incomplete combustion. So even though it is known that back-pressure has an influence on the performance of the engine, there are not many studies focusing on high back-pressure on marine engines, especially due to an underwater exhaust system (5).

For instance Karuppusamy et. al. (6) investigated the effect on engine performance when a catalytic converter is installed. As stated before, the introduction of such after-treatment systems adds to the back-pressure experienced by the engine. This is recognised by the authors and therefore they first performed a CFD analysis to see the effect of different designs of the catalytic converter. They looked at two flow characteristics, the vorticity within the catalytic converter and the created back-pressure. A lower vorticity makes the catalytic converter more effective and a lower back-pressure means that the engine experiences less effect of the installation of the catalytic converter. Based on this CFD analysis they build the catalytic converter which had the best compromise between these parameters. Next they performed tests on a single cylinder four stroke diesel engine with and without the catalytic converter to see the effect on engine performance. The results show a decrease in brake thermal efficiency and an increase in brake specific fuel consumption and fuel flow rate. Even though these results comply with what is expected when an after-treatment system is introduced, it is hard to draw more conclusions. Since only one catalytic converter design is tested and there may be other effects, than just back-pressure, which causes these results.

Joardder et. al. (7) performed experiments on a 4-stroke single cylinder naturally aspirated direct injection diesel engine. They increased the back-pressure at different engine speeds and engine loads, to see the effect on both engine performance and emissions. Their results show that at low engine speed the back-pressure has no significant effect on engine performance for all load conditions. At higher engine speeds the performance remains constant to a certain level of back-pressure, after that it causes a decrease in performance. The brake specific fuel consumption is constant at low engine speed, but at higher speeds it increases a little. Looking at the emissions, their experiments show that CO emissions are higher at low rpm for all load conditions but at higher engine speeds and loads the CO emissions decreased with increased back-pressure. For the NOx emissions it is found that with increased back-pressure these emissions are lowered for all conditions. However these experiments were performed with a naturally aspirated diesel engine and the results will be different when a turbocharged diesel engine is used due to differences in, amongst other things, air-to-fuel ratio, charge pressure and exhaust temperature.

Hield (4) used the Ricardo Wave engine modelling software to simulate the effects of both steady-state and fluctuating back-pressure on a turbocharged diesel engine used in submarines. His work shows that the engine must work harder to expel the gasses from the cylinder. This causes a reduction in the pressure ratios across the turbine and compressor causing a decrease in mass flow of air through these components and therefore the air available to the engine. In order to keep the brake power output the same, the fuel flow must increase in order to create the extra power needed to overcome these pumping losses in the engine. This means that the brake specific fuel consumption increases compared to an

engine working in atmospheric conditions. The reduced air flow and extra required power also causes the exhaust gas temperatures to increase. This increases the thermal loading of the engine and can lead to thermal failure of pistons, cylinder head and valves. His study also shows that the response of the engine due to dynamic back-pressure is highly non-linear, mostly caused by the changes in operating points of the compressor and turbine. The downside of his work is that there is no experimental data to validate the results from the Ricardo Wave model.

In order to overcome the lack of experimental validated research and to better understand the effects of (high) back-pressure on marine diesel engines, some studies were carried out in earlier stages of the GasDrive project. Sapra et. al. (5) performed a combination of experiments and model simulations to investigate the effects of high back-pressure on engine performance, and to define acceptable limits of back-pressure. The experiments were carried out on a 4-stroke, pulse turbocharged, medium speed diesel engine at different loads and engine speeds, against different cases of static back pressure. Next a Mean Value First Principle (MVFP) model was adopted (and validated using the results of the experiments) in order to describe the engine performance. A more detailed description of a MVFP model is given in section 1.2. After validation the MVFP model was used to define back-pressure limits, based on the concepts of smoke limit and thermal overloading of the engine. The MVFP model was also used to model different cases, which could not be studied experimentally, such as high back-pressure (up to 1 meter of water-column), different valve overlaps and constant pressure vs pulse turbocharged capabilities. The study showed that air-excess ratio, exhaust valve and exhaust receiver temperatures are the most critical parameters with high back-pressure. This is also why the smoke limit and thermal overloading were chosen as the limiting cases of back-pressure for the engine. The effect on fuel consumption, although it does increase with increasing back-pressure, was found to be small. The effect of back-pressure on air-excess ratio, exhaust valve and exhaust receiver temperatures was higher at low engine speeds, so the limits of the engine will be reached sooner (at a lower value of back-pressure) in this region of the engine envelope. Also, when a constant pressure turbocharger is used, an engine with a smaller valve overlap is able to sustain higher levels of back-pressure compared to an engine with a larger valve overlap. The model also showed that a pulse turbocharged engine with a small valve overlap is better at withstanding back-pressure compared to an engine with a (modern) constant pressure turbocharger with the same valve overlap.

Singh (3) continued the work done by Sapra et. al. by looking at the effect of dynamic back-pressure on the engine performance and emissions. As mentioned in section 1.1.1, when using an underwater exhaust system, the water at the outlet creates an extra back-pressure effect on the engine. This back-pressure effect consists of a static and a dynamic part, the former is due to the mean depth below the water surface of the exhaust and the latter is due to the fluctuating ocean waves. In this study, similar to the work of Sapra et. al., a combination of experiments and model simulations was carried out in order to investigate the effect of the dynamic back-pressure. The experiments were done on the same engine (a 4-stroke pulse turbocharged marine engine), but in addition to a static back-pressure the engine was tested with a step up, single and multiple back-pressure waves in order to understand the dynamic back-pressure (with different amplitudes and wave periods). Then the MVFP model was further adopted, verified and used to simulate engine performance for cases which could not be investigated experimentally. The emissions of the engine were also recorded during the experiments in order to see what the effect the dynamic back-pressure has on them. The study showed that an increase in wave amplitude of both single and multiple back-pressure waves increases the thermal loading of the engine. The same goes for an increase in the wave period of the back-pressure waves. Looking at the maximum exhaust receiver temperature, multiple back-pressure waves will lead to a higher maximum temperature when compared to a single wave with the same length and period. When comparing the dynamic back-pressure waves to the static back-pressure, the effect of the dynamic waves on engine performance was not severe. Meaning that an engine designed for a certain level of static back-pressure could handle waves with a higher amplitude. Finally the emissions that were recorded show an increase in NO, CO, CO₂ and SO₂ when the back-pressure (both static and dynamic) is increased for all load conditions. But the amount of O₂ decreases with increasing back-pressure.

The studies above show that there is a good understanding what the effect of back-pressure is on engine performance. And also that there are verified models which can be used to simulate the engine performance. But all the studies were carried out, both experimentally and/or with the use of modelling software, on (turbocharged) diesel engines. The GasDrive project aims to use a dual-fuel engine, which has a different performance compared to a normal diesel engine and may therefore react differently to back-pressure. It is also possible that the limit cases (like the smoke limit and thermal overloading of the

engine) for a dual-fuel engine are different because other parameters are more important for this type of engine. In the next section the workings of a dual-fuel engine are discussed as well as the difference in performance when compared to a diesel engine.

1.1.3 Dual-fuel engine

Diesel engines are widely used as a power source in transportation and power generation systems. They are preferred because they have a high thermal efficiency, they can operate at high compression ratios allowing them to use low energy-content fuels and because they have low emissions of unburned hydrocarbons, CO and CO₂ compared to spark ignition engines (8)(9). The downside of these engines is that they emit harmful pollutants like NO_x and particulate matter. Because the rules and regulations for emissions from engines are becoming more stringent in recent years and because the reserves of fossil fuels are getting lower, there has been an increasing interest in improving these engines. Recently natural gas is seen as a clean fuel alternative for diesel fuels. Generally natural gas is used in spark ignited engines, but this type of engine can not run with high compression ratios because of the occurrence of knocking. Therefore the thermal efficiency of these engines is lower compared to diesel engines (9)(10). A promising technique to overcome these issues is the dual-fuel concept. In a dual-fuel engine a mixture of air and gaseous fuel is put in the cylinder and compressed. This mixture does not autoignite due to its high autoignition temperature. Therefore a small amount of diesel (called pilot fuel) is injected at the end of the compression stroke to ignite the mixture (9)(11)(12). The combustion energy release for such a dual-fueling technique can have three (overlapping) components: 1. pilot diesel combustion, 2. gaseous fuel combustion in the immediate vicinity of the ignition and combustion centers of the pilot fuel and 3. any pre-ignition reaction activity and the turbulent flame propagation within the lean charge (8). Natural gas can be used as gaseous fuel in such an engine, because it has a high octane number, so it could be used in engines with high compression ratios (like standard diesel engines) without the occurrence of knock. It is also widely available, mixes uniformly with air resulting in good combustion and has lower emissions of NO_x and particulate matter compared to diesel fuels (9)(10)(12)(13). Another upside to this technique is that existing diesel engines can easily be converted into dual-fuel operation and one can choose to switch between dual-fuel and full diesel operation without interrupting the power output (11)(12)(13). The downside to the dual-fuel technique is that at low loads the engine is fed with a very lean air-gas mixture which is hard to ignite and slow to burn. This means that a considerable amount of natural gas passes through the engine without being burned, leading to higher levels of unburned hydrocarbons and CO emissions and a low thermal efficiency at low loads (9)(10)(12)(13).

Diesel vs Dual-fuel operation

In the section above the dual-fuel concept is explained and some of the perks of using such a system are given. But in order to get a good understanding of the influence of using the dual-fuel mode on the engine performance and emissions it is necessary to do experiments. Two papers have been found in which experiments were carried out first running the engine in 'normal' diesel mode and then in dual-fuel mode, looking at the performance and emissions. Mustafi et. al. (8) used a Lister Petter PHW1, single cylinder, four-stroke, direct injection, stationary diesel engine to perform the experiments. The engine was run at a constant rpm and at two different loads (low and high load). After running on diesel fuel only, they performed experiments with different types of gaseous fuels (one of them was natural gas). Loubar et. al. (12) performed their experiments on a similar engine, a single cylinder air cooled Lister Petter (TS1), 4-stroke, direct injection diesel engine. Measurements were carried out at four different rpm's and four different loads. Both papers show similar trends when comparing the engine performance and emissions of diesel and dual-fuel mode. These effects are summarised below.

At low load and/or low rpm it was observed that the cylinder pressure for dual-fuel mode was lower than the conventional diesel mode. At low loads, when in dual-fuel mode, the air-fuel mixture in the cylinder is very lean, which affects the pre-ignition conditions resulting in a delayed and lowered combustion pressure. Increasing the engine speed (at the same load condition) improved the pressure because the air-fuel mixture is well prepared and the engine is warmer, resulting in a faster flame speed. When the engine was running at high loads the pressure in the cylinder becomes higher for dual-fuel operation compared to diesel operation. Looking at the pressure peak, a similar trend was found. At low loads the pressure peak for dual-fuel mode was somewhat lower, but increases when the load is increased and surpasses the peak pressure for diesel operation. However the peak for dual-fuel mode appears later in the cycle because of the increased ignition delay.

The heat release rate in the case of dual-fuel combustion is more rapid and a higher maximum energy

release rate is observed in comparison to diesel operation. This is due to the combined combustion of the pilot fuel and the gaseous fuel in the direct vicinity of the pilot fuel. At low loads the difference is more clearly seen during the final phase of combustion, which is because of the late combustion of the gaseous fuel. This is also why at low loads the measured combustion pressure is lower, because this late combustion of the gaseous fuel happens during the expansion stroke. At higher loads the difference in heat release rate is bigger, in favour of dual-fuel mode, which means that there is an improvement of the combustion of the gaseous fuel.

When looking at the brake specific fuel consumption (BSFC), so not taking into account the difference in lower heating value between natural gas and diesel, it is found that at low loads the total BSFC for dual-fuel operation is higher than for diesel operation. This means that there is a poor utilization of the gaseous fuel. The reason for this poor utilization is a combination of low temperatures (at low loads) and a poor air-gas mixture in combustion chamber, resulting in a bad and slow combustion of the gaseous fuel. As the load increases the total BSFC goes down for both fueling modes, however at medium to high loads the improvement of the gaseous fuel utilization leads to a relative better improvement of the total BSFC, and for that range of loads the total BSFC is lower for the dual-fuel mode than the diesel mode. However when comparing the brake specific energy consumption (BSEC) the difference between dual-fuel and diesel mode is insignificant.

Both papers found that the use of the dual-fuel mode leads to a reduction in particulate matter (PM), especially at high loads. In general the more carbon a fuel contains the more likely it is that soot will be formed during combustion. Since natural gas, where methane is the main component, has less carbon molecules compared to neat diesel, PM is less likely to be formed. Another effect that helps the reduction of PM is that in the dual-fuel mode there is a bigger chance of PM oxidation.

The formation of NO_x is a harmful pollutant in the emissions of engines. The formation of NO_x is influenced mainly by two parameters, high oxygen concentration and a high charge temperature. At low loads the charge temperature is almost equal for both fuel modes, but the higher concentration of oxygen in conventional diesel leads to more NO_x formation for this fuel mode. However at higher loads the NO_x formation for the dual-fuel mode can become higher than for conventional diesel mode. This is because at these loads the charge temperature for the dual-fuel mode is higher, due to a higher heat released in the early premixed combustion stage as a result of the improved gaseous fuel combustion. The better combustion, and therefore a lower fuel consumption, also leads to a higher oxygen concentration, increasing the NO_x formation at these loads. The same trend was found when the engine speed was increased.

The emission of unburned hydrocarbons (UHC) is always higher for the dual-fuel mode. This is due to the fact that some of the natural gas passes through the engine without taking part in the combustion process. The total hydrocarbon (THC) emissions showed a similar trend for all tested engine speeds. At low loads, as mentioned earlier, there is a bad and slow combustion of the gas-air mixture and therefore not all the natural gas is being burned. As the load increases so do the THC emissions, because even though the gaseous fuel participation increases the combustion quality is not enough to lower the THC emissions. For high loads the higher charge temperature level and richer gaseous fuel result in a further improvement in the combustion process, and for these loads the THC emissions are lowered for the dual-fuel mode, but are never as low as for conventional diesel mode.

The formation of CO is dependent of the unburned gaseous fuel and the mixture temperature. At low loads the CO emissions are higher for dual-fuel mode, but as the load increases the concentration of CO decreases for this fuel mode due to a better fuel utilization. However for conventional diesel mode at high loads the (locally) rich mixture leads to bad combustion for this mode and a sharp increase of CO emissions can be seen. At these loads the CO emission for dual-fuel mode is significantly lower.

The greenhouse gas that is most produced by humans is CO_2 . Because natural gas is mostly made of methane it has one of the lowest carbon contents among hydrocarbons and therefore a potential in lowering the CO_2 emissions. At low loads, because of the small participation of the gaseous fuel, this difference in CO_2 emission between the fuel modes is not significant. But at higher loads this difference becomes more clearly, showing the decrease of the CO_2 emissions by using natural gas.

The section above gives a good overview of why the dual-fuel concept is seen as an interesting way to improve the diesel engine. But it also highlights some issues with this concept, where a conventional diesel engine works better. Most of these issues appear in the low load region of the engine envelope. There have been many researches into improving the dual-fuel concept, with an extra interest in this low load region. Some of the engine parameters that have been investigated are: exhaust gas recirculation (EGR) and intake heating (10)(14); natural gas injection timing, pressure and position (9)(13)(15)(16)

and pilot fuel pressure and timing (9)(17)(18). The results show that improving some of these parameters can improve the combustion and reduce emissions (especially at low loads). Introducing EGR/intake heating can reduce the emission of THC, NO_x and improve engine efficiency. Optimizing the injection timing and/or injection strategy of both pilot fuel and natural gas can also improve engine performance.

The literature study above shows that there is a lot of knowledge about the dual-fuel engine and how to improve this concept. But it also shows that there has not been an (experimental) investigation into the effects on engine performance and emissions when back-pressure is applied to this type of engine. Since the GasDrive project aims to combine a dual-fuel engine with an underwater exhaust, which causes back-pressure, it is necessary to know how this type of engine reacts when back-pressure is applied. This will therefore be the basis of this master thesis. In section 1.3 the research objective will be further explained.

1.2 Model investigation

In order to better understand and predict engine performance simulation programs are used. The type of simulation model is dependant on the level of detail required from the model, computational time and accuracy. Geertsma et. al. (19) categorised the different types of models by the level of dynamics considered and the underlying physical detail as follows:

- **Zero order models**, they use a purely mathematical equation derived from a number of measurement points or from a look-up table to represent engine torque and fuel consumption. The dynamics of a turbocharger are not included. This type of model is very simple and requires little details.
- **First order models**, this type is very similar to a zero order model, but contain a state variable representing either the turbocharger pressure or the turbocharger speed. These models can be based on complex underlying physical models, on mathematical equations derived from a number of measurement points, or on look-up tables, which require even more measurement points and therefore require extensive experimental data.
- **Mean Value First Principal (MVFP) models**, here air and exhaust gas flow dynamics are included. They require a large set of parameters and a good calibration. They are used when the in-cylinder details are not the main concern of the research. The focus of these models is on engine parameters like exhaust temperature or pressure and air-fuel ratio. The in-cylinder process is simulated by a mean value model. A gas exchange model and the Seiliger cycle can be used to calculate the exhaust gas conditions.
- **Zero-dimensional crank angle models**, they determine the thermodynamic state of the air and combustion gas in the cylinder, using a crank angle rotation scale, for the closed cylinder process, assuming a single homogeneous ideal gas in the cylinder. They are combined with a heat release model using Wiebe functions, a two-zone combustion model or a multi-zone combustion model based on the level of detail required from the model.
- **One-dimensional fluid dynamics models**, these predict the air flow, pressure and temperature along the flow path of the air across the engine. But this type of model requires too much computational time when simulating the engine performance of a ship's operational profile.
- **Multi-zone combustion models and CFD models**, they model the combustion process and the gas flow in the various engine components in three dimensions. These models can be used to gain detailed insight into the processes of soot formation, NO_x formation, heat radiation and convective heat transfer in the cylinder during combustion. So they give a detailed insight in the in-cylinder process, however they require a high computational time so their use for a propulsion system analysis is limited.

The purpose of this research (both this thesis on dual-fuel engines and the GasDrive project as a whole) is to get a better understanding of engine performance and emissions with externally applied back-pressure. So the focus is on overall engine parameters such as exhaust gas temperature, inlet receiver pressure and fuel consumption. The in-cylinder process details are less important. Therefore a mean value first principle (MVFP) model including a gas exchange model and an analytical compressor-turbine model was chosen. Such a model has already been developed at the Netherlands Defence Academy

(NLDA) and the TU-delft for a standard diesel engine. During the previous stages of the GasDrive project this MVFP model (called the DE-B model) was used and optimised by Sapra et. al. (5) (20) and Singh (3) to investigate the effects of static and dynamic back-pressure on a diesel engine. This DE-B model will also be used in this research, with some adaptations in order to simulate a dual-fuel engine instead. In section 2.1 the MVFP model is explained in more detail.

1.3 Research objective

As mentioned earlier, the GasDrive project is a novel ship propulsion concept where a solid oxide fuel cell (SOFC), natural gas engine and underwater exhaust system with nano-hull coatings are used together to achieve higher propulsion efficiency and ultra-low emissions. The natural gas engine uses a small amount of diesel fuel (pilot fuel) to ignite the air-gas mixture in the cylinder, making it a dual-fuel type engine. The underwater exhaust system causes back-pressure effects due to the waves at the outlet. One of the main concerns in the GasDrive project is the effect of static and dynamic back-pressure on engine performance including the effects on emissions. The literature study in section 1.1 shows that there is a good understanding of the effects of static and dynamic back-pressure on a conventional diesel engine. There is also extensive literature available about the workings of a dual-fuel engine and how to enhance the performance. But the effect of back-pressure on this type of engine is yet to be investigated, and because it is important for the GasDrive project to know this, it will be the research objective of this master thesis. For this purpose experiments were performed at the Harbin Engineering University, China on a dual-fuel engine to study the effects of static back pressure. The following research question and sub questions will be answered during this study:

What is the influence of static back-pressure on the performance and emissions of a dual-fuel engine?

1. How can the experiments performed at Harbin Engineering University be used?
 - How were the experiments performed?
 - What data was collected?
 - Which of the collected data can be used?
2. Which parameters change when applying back-pressure on a dual-fuel engine?
 - What happens when back-pressure is increased?
 - What happens at different engine loads?
 - Which engine parameters are crucial for the performance of the dual-fuel engine?
 - What happens with the emissions of the dual-fuel engine?
3. How can the Diesel Engine models be used to describe the performance of a dual-fuel engine?
 - Which of the available models should be used?
 - What needs to be adopted in this model to describe the performance of a dual-fuel engine?
 - Using the adopted model, can limiting cases be defined for back-pressure on a dual-fuel engine?

In the next section the plan of approach to answer these questions will be explained.

1.4 Plan of approach

In the previous section the research objective of this thesis was described and a research question and sub questions were given. This section will explain the plan of approach that was used to answer these questions.

1.4.1 Dual-fuel engine model

Section 1.2 explained the different types of models that can be used. It also explained that since the focus of this thesis is on main engine parameters the use of a mean value first principle model was the right choice, and that there already is such a model available, the DE-B model. However this model is made for a conventional diesel engine and at the moment is not able to calculate with two types of fuel simultaneously, which is necessary for a dual-fuel engine model. So the first step will be to explore the existing DE-B model and see what adaptations needs to be made to turn it into a dual-fuel mean value first principle model and then implementing these changes.

1.4.2 Calibration of the dual-fuel MVFP model

The adopted DE-B model (now a dual-fuel MVFP model) will be used to investigate the performance of a dual-fuel engine. The aim is to get a better understanding of the effects of back-pressure and the limitations of the engine under those conditions. Therefore the model will also be used to simulate conditions that can not be tested experimentally. In order to do so, the model first needs to be calibrated and matched to the test engine. For the calibration of the model the experimental results when there was no extra back-pressure applied will be used.

The model uses a certain set of parameters that needs to be defined. These parameters can be divided into three categories (3)(5):

- **Known parameters;** these are the parameters which are known from the engine specification. For instance the number and the dimensions of the cylinders.
- **Arbitrary set parameters;** some parameters are hard to get from the engine, so they are expressed non-dimensionally as a function of a known parameter. An example are the valve diameters, which can be expressed as a percentage of the bore diameter.
- **Unknown parameters;** these parameters are used to simulate a certain phenomenon of the real engine. They are estimated using the measurement data. For example the ' μ -phi' parameter is used to determine the flow through the engine. It is set such that the compressor size in the model corresponds to the air-swallow characteristic of the compressor of the test engine.

For the model to work correctly it is also necessary that all the sub-models that are used are calibrated as well. This is also known as system matching, and for the most parts this has already been done for the existing DE-B model. The turbocharger model however, does need to be matched to the test engine. The analytical compressor and turbine models require some parameters that need to be estimated. The matching of the turbocharger model can be divided into three parts (5):

1. Matching the engine inlet flow to the compressor flow, at the correct inlet pressure and engine and compressor speed. This is the matching of the air-swallow characteristic of the compressor.
2. Matching the engine exhaust flow to the turbine flow, at the correct exhaust pressure and temperature and engine and turbine speed. This is the matching of the turbine characteristic.
3. Matching the turbine and compressor power. This is the Büchi balance, which links the inlet and outlet pressures given the turbine and compressor inlet temperatures.

In this manner the dual-fuel MVFP model will be matched and calibrated to the test engine. The next section will explain how the calibrated model is then validated using the other measured data.

1.4.3 Validation of the dual-fuel MVFP model

After calibrating and matching the dual-fuel MVFP model to the results of the test engine with no back-pressure, the model will be used to predict the engine performance when back-pressure is applied. If the model is able to predict the engine performance with a satisfactory accuracy, it will be used to simulate engine performance at set-points which could not be investigated experimentally in order to find limit cases for back-pressure on the dual-fuel engine.

During the experiments it was decided to establish measurement series based on one specific position of the back-pressure valve. This meant that at lower ratings the engine experienced less back-pressure during the experiment than at higher ratings. This is explained in more detail in section 4.1. Therefore during the validation of the model the back-pressure as recorded during the experiment series will be used as input in the model. After validating using the experimental results, the model will be used to run at the same set points for the low and high back-pressure cases, but now with the back-pressure at the same value for all set-points.

1.4.4 Experimental results

The data recorded during the experiments will not only be used to validate and calibrate the model, but will also be analysed themselves. This will help with gaining insight into the behaviour of a dual-fuel engine under back-pressure and to see if this behaviour complies with what was found during the literature study in section 1.1. One of the reasons to use natural gas as a fuel is that it is seen as a cleaner alternative to standard fossil fuels (9)(10)(12)(13). During the experiments the emissions were recorded as well, so an analysis of this data will be useful.

1.4.5 Model extrapolation

If the dual-fuel MVFP model is calibrated in a satisfactory manner, it will be used to see what happens if the back-pressure is truly kept constant over the range of engine power, as this was not achieved during the experiments. Together with the experimental results the model will help to give insight into two case types:

- The first case is what happens when an engine is designed to withstand a certain level of back-pressure at max engine rating, but then runs at a lower rating (i.e. experiences less back-pressure than the design condition). Or to look at it another way, when an after-treatment system is installed it causes a back-pressure effect. It can be seen as an obstruction in the exhaust line, similar to the valve used in the experiments. So this will also give an insight in the effect of installing an after-treatment system to a dual-fuel engine.
- The second case is what happens to engine performance at lower engine ratings when the engine experiences more back-pressure at these set-points.

Then the model can be used to see what happens when the back-pressure is increased to levels that could not be applied during the experiments. This will help with gaining insight into the important engine parameters when looking at the limits of the engine.

1.4.6 Limit cases

In order for the engine not to be overloaded with a too high level of back-pressure it is necessary to know what the limits of the engine are. The experiments, the model extrapolation and literature will highlight the important engine parameters when looking for these limits. The model will then be used to calculate the limit values for these parameters when no back-pressure is applied. Then the back-pressure will be increased in the model to see when these engine limits are being reached.

2 MVFP model and adaptations

In section 1.2 it was explained why a mean value first principle (MVFP) model was chosen to simulate the engine performance. This chapter will explain how the chosen existing DE-B model is build up as well as taking a closer look into the in-cylinder process simulation. Then the adaptations that were made to the model to turn it into a dual-fuel MVFP model will be explained.

2.1 DE-B model

The DE-B model is made in Matlab/Simulink. Within the model the different engine components such as inlet receiver, cylinder and outlet volume are modelled as a series of volume elements. The various volume elements are connected to one-another via resistance elements. A schematic overview of the MVFP model is shown in figure 1. The back-pressure is implemented in the red box.

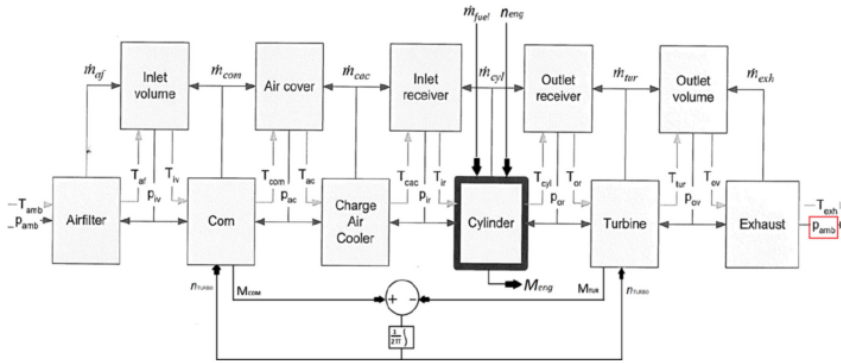


Figure 1: Mean Value First Principle model (5)

The volume elements use the net mass flow to calculate the instantaneous mass (conservation of mass) and the instantaneous temperature by using the net energy flow (conservation of energy). The instantaneous pressure is calculated using the ideal gas law. The resistance elements calculate the mass flow by using the momentum equation as a function of pressure difference. Meanwhile empirical sub-models calculate the compressor and turbine characteristics. A more detailed overview of the model, the equations used and the in-cylinder process model based on the Seiliger cycle can also be found in (21)(22)(23)(24).

2.1.1 In-cylinder process

The in-cylinder process is complex and a detailed model for this process will take a long computational time. Since the aim of this project is on overall engine parameters and to shorten the computational time, the DE-B model uses a mean value model to simulate the in-cylinder process. A lot of research has been done using different techniques to simulate the in-cylinder process.

Ding (25) showed that the Seiliger cycle is an effective way to characterise the combustion of diesel engines. The Seiliger process uses finite combustion stages to characterise the in-cylinder process and the Seiliger parameters can be used to calculate the engine performance. Figure 2 shows the six-point Seiliger cycle and the definition of the Seiliger parameters.

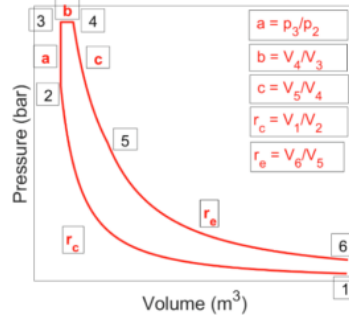


Figure 2: Seiliger cycle and parameters

The Seiliger parameters can be determined using the in-cylinder pressure data. Figure 3 shows the flow chart on how to obtain these parameters. This method was used and proven by Ding (25) and Ding et. al. (26). First the in-cylinder pressure data is used as input into a Heat Release Rate (HRR) calculation method. The outcome of the HRR is smoothened using multiple Wiebe functions. The smoothened HRR outcomes are then used as input to find the in-cylinder parameters. Next the Seiliger parameters are calculated using the equivalence criteria between the Seiliger cycle and the in-cylinder process of the real engine. In the 'Seiliger fit model' the Seiliger combustion parameters are calculated using a Newton-Raphson multi-variable root finding method. This is an iterative process that finds the Seiliger parameters for a certain set of conditions. A more detailed description of this Newton-Raphson method can be found in (25) and (26). The last part uses the Seiliger combustion parameters to express the in-cylinder combustion.

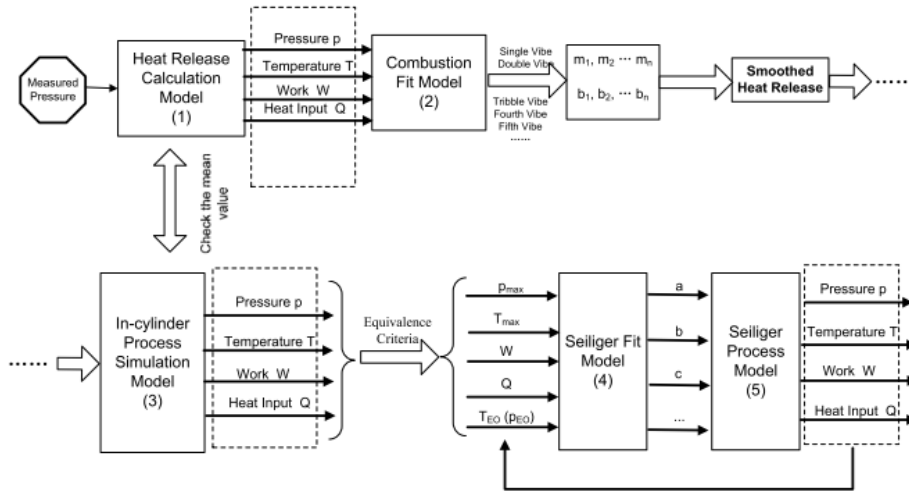


Figure 3: Flow chart of procedure to obtain Seiliger parameters (26)

The DE-B model calculates the Seiliger parameters itself, but it needs some initial calibration. So with the above explained method the Seiliger parameters can be determined based on the experimental data, and then they will be used to calibrate the in-cylinder process in the DE-B model. Combining this method of obtaining Seiliger parameters with a Mean Value First Principle model was also done by Sui et. al. (27). After finding the Seiliger parameters and implementing them into the model, it showed that this combination was able to predict overall engine parameters with a good accuracy and calculation time. Sapra et. al. (28) also used a similar procedure as in figure 3, but then for hydrogen-natural gas (H-NG) combustion. They also compared Seiliger-based and Wiebe-based models for H-NG combustion. Their research shows that the Seiliger-based approach is more accurate to simulate the H-NG combustion in the cylinder. Since the fuel used for this research is a combination of diesel and H-NG, the Seiliger approach to model the in-cylinder process will be used here as well.

2.2 Model adaptations

The DE-B model, as described in the previous section, now needs to be converted into a dual-fuel engine model. The DE-B model uses the pressure, temperature and composition of the gas in the system to calculate the instantaneous properties. The gas in the original system consists of air and the stoichiometric gas from burning diesel fuel. For the composition of the gas the DE-B model calculates the air mass fraction in the system, the remaining part is considered to be stoichiometric gas from the fuel. In the dual-fuel system there will also be stoichiometric gas from burning natural gas. This means that there will be a third gas species in the mix, and this needs to be added to the model.

The addition of a new gas species is the starting point of the adaptations to the model. The following sections will explain the steps that were taken.

2.2.1 Comparing tool

The original model runs two identical diesel engines at the same time. It was chosen to change one of these diesel engines and turn it into a dual-fuel engine and to use the other engine as comparison. During this stage the flow of gaseous fuel was set to zero, so the dual-fuel engine should give the same result as the original model. During each model run the data of 258 signals is recorded in Matlab/Simulink for each engine. Checking all the signals manually would take too much time, so in order to check if the changes to the model were implemented correctly a comparing tool was developed. The data of the 258 signals of both engines were compared and if there was a difference, the error was expressed as a percentage of the value from the original diesel engine. The tool also gave the location (signal number and time-step) of the maximum error in the system. In this way it could quickly be seen if the adaptation to the model was implemented correctly and if not, where the error occurred in the system.

2.2.2 Fluid properties

In order for the model to use natural gas as a fuel, the properties of this fuel and the stoichiometric gas created by it must be determined. This is done in the file `fluid_properties.m`. First the volume and mass fractions of the fuel gas are calculated, based on the measured composition of the gas. This composition can be seen in table 1.

Compound	Volume fraction
CH4	0.79220150
C2H6	0.03666489
C3H8	0.0002429
C4H10	0.00004875
H2	0.07146203
CO	0.02680111
CO2	0.04702819
N2	0.02555062

Table 1: Composition of natural gas used as fuel

Based on this composition and the corresponding mass fractions the properties for the gaseous fuel were calculated, such as the gas constant, Lower Heating Value (LHV) en stoichiometric ratio. The formulas used in this part can all be found in (22) and (23). Table 2 shows the main properties of both the pilot fuel and the natural gas used in the model.

	DMA	Natural gas
Mass fractions:		
x_C	0.8650	0.6452
x_H	0.133	0.2035
x_S	0.002	-
Mass [kg/kmol]	194.3977	17.5049
Gas constant [J/kg/K]	42.7706	474.9818
C/H ratio [-]	6.5038	3.1709
Density at 15°C [kg/m ³]	843	545.3787
LHV [kJ/kg]	42771	46055
Stoichiometric ratio [-]	14.6674	14.5442

Table 2: Properties of both fuel types

The last step is to calculate the composition and properties of the stoichiometric gas from the gaseous fuel. This is done in the same way as for the diesel fuel, because the compounds of the stoichiometric gasses are the same for both fuels (with the exception of SO₂, as there is no sulfur in the gaseous fuel). Their reference values are calculated based on the reference values of the base elements, so the structure within the model to calculate the properties remains the same. The main properties are given in table 3

	DMA stoichiometric gas	Natural gas stoichiometric gas
Mass fractions:		
x_N ₂	0.7003	0.7025
x_Ar	0.0119	0.0119
x_CO ₂	0.2023	0.1521
x_H ₂ O	0.0759	0.1170
x_SO ₂	0.00025505	-
Mass [kg/kmol]	29.3188	28.3080
Gas constant [J/kg/K]	283.5889	293.7152

Table 3: Properties of the stoichiometric gasses from both fuel types

2.2.3 Composition of gas in the system

As mentioned earlier, in the original model the composition of the gas in a certain system was determined by calculating the air mass fraction. The remaining part was the stoichiometric gas. So in the original model it was enough to keep track of the air mass fraction in the system, as this would automatically determine the stoichiometric gas mass fraction. In the dual-fuel model this no longer applies, since we have three different species now. In the dual-fuel model the composition is given by x , x_{sg} and x_{fg_sg} , being the mass fractions of air, stoichiometric gas from the pilot fuel and stoichiometric gas from the gaseous fuel respectively. This means that the traces for x_{sg} and x_{fg_sg} need to be added to the model. A similar approach was used and proven to work by previous research (29)(30).

It has to be said that knowing 2 out of the 3 mass fractions would be enough to determine the properties (similar to the original model), but for reasons of clarity it was chosen to calculate all 3 the fractions throughout the model. It made checking for implementation errors easier, if a species undergoes an individual change it can easily be picked out of all the traces in the model and having the complete composition in one overview was preferred.

2.2.4 Properties blocks

The model uses the pressure, temperature and composition of the gas in the system to calculate its instantaneous properties. This is done by using a library which contains several blocks which are used throughout the model. In these blocks the overall properties are calculated by multiplying the mass fraction of a species with its individual property and then adding them together. This means that the overall structure of these blocks remained the same. The only changes were adding an input port for x_{sg} and x_{fg_sg} and adding a third term to all the formulas. The following 5 blocks were changed in this manner:

- Properties block

- Gas constant
- Spec heats
- Spec energy
- Spec entropy

As the output ports of these blocks remained the same, the old blocks can now easily be swapped for the new blocks without changing the structure of the model (with the exception of adding the `x_sg` and `x_fg` traces to the input ports of course).

2.2.5 Cylinder: Gas exchange

The gas exchange part of the model takes care of: the intake of fresh air into the cylinder, the expulsion of combustion gasses (including blow-down), scavenging and it calculates the trapped condition. These processes are modeled using several sub-systems. In most cases the only change was to update the properties blocks in these sub-systems. A structural change was made when calculating the air access ratio and the trapped mass condition:

- The total air access ratio is now calculated by dividing the total air in the cylinder by the total stoichiometric gas from complete combustion of the two fuels.
- For the trapped mass it was chosen to add the mass of the gaseous fuel to the trapped mass (as calculated in the original model). This simplification was made because the mass of the gaseous fuel is a small portion of the total trapped mass. It made implementation easier and previous studies have shown that the error due to this simplification is not significant (29)(30).

2.2.6 Cylinder: Seiliger cycle

As explained in section 2.1.1 the six point Seiliger cycle is used to model the combustion in the cylinder. The first step here is to calculate the parameters `a` and `b`. The only structural change in the model for these parameters was to add the mass of the gaseous fuel in the calculation of the total heat by combustion. Next the 5 stages of the Seiliger cycle are modelled individually. During each stage the initial conditions for the next stage are calculated as well as the energy released in the current stage. A difference between the two fuels occurs in the sub-system which covers the mass and composition change during a stage. In this sub-system part of the fuel available is burned (which creates stoichiometric gas). The pilot fuel is injected and immediately fully burned during the first combustion stage as this is a very small amount of fuel, only used to start the combustion process. The burning of the gaseous fuel is spread over the three combustion stages in the Seiliger process. Another difference is that the gaseous fuel is already present in the cylinder at the trapped condition. This means that the mass of the pilot fuel used in the first stage is added to the total mass in the cylinder, but the mass of the gaseous fuel is not. In the other sub-systems only the properties blocks were changed.

2.2.7 Volume and heat elements

Engine components outside the cylinder are modelled by a volume and a heat element. The volume element calculates the mass, composition, temperature and pressure in the engine component. The heat element calculates the heat loss to the wall. The only structural change in these elements is in the calculation of the composition, in the other blocks of these elements it was sufficient to only update the properties blocks. In the calculation for the composition, the mass balance is used to determine the instantaneous composition. This mass balance has now been divided into two parts: one for the diesel stoichiometric gas and one for the gaseous fuel stoichiometric gas. In this manner both mass fractions are calculated separately and adding them together determines the air mass fraction (being the remaining part of the total mass fraction).

2.2.8 Waste-gate

One way to improve the part load performance of an engine is to optimise the turbocharger for part load. This means that the turbine is designed with a smaller throat area so that at part load (or engine speed) there will be more pressure built up to drive the turbine. But at higher engine speeds the turbine can no longer handle the flow, so part of this flow needs to be led around the turbine through a waste-gate (22).

The engine used during the experiments had such a waste-gate installed, so this needs to be added to the model. In the original DE-B model a sub model for such a waste-gate was already implemented. So all that needed to be done here was to update the properties block in this sub model. During the matching of the dual-fuel MVFP model some iterations will be necessary to get the inputs for this sub-model correct.

3 Matching of the dual-fuel MVFP model

This chapter will show how the dual-fuel MVFP model, as described in chapter 2, was matched to the tested engine. First the matching procedure will be explained. Then the results of the calibration by using the experimental data will be shown in section 3.2. And in section 3.3 the dual-fuel MVFP model will be verified.

3.1 Matching procedure

The dual-fuel MVFP model is made in Matlab/Simulink. For each engine component, as shown in figure 1, there is a file containing the parameters for that component. As mentioned in section 1.4 these parameters can be divided into three categories (3)(5):

- **Known parameters;** these are the parameters which are known from the engine specification. For instance the number and the dimensions of the cylinders.
- **Arbitrary set parameters;** some parameters are hard to get from the engine, so they are expressed non-dimensionally as a function of a known parameter. An example are the valve diameters, which can be expressed as a percentage of the bore diameter.
- **Unknown parameters;** these parameters are used to simulate a certain phenomenon of the real engine. They are estimated using the measurement data. For example the ' μ -phi' parameter is used to determine the flow through the engine. It is set such that the compressor size in the model corresponds to the air-swallow characteristic of the compressor of the test engine.

Defining these parameters in the correct files is basically the start of the calibration. However for the model to work correctly it is also necessary that all the sub-models that are used are matched to the tested engine as well. This is also known as system matching, and for the most parts this has already been done for the existing DE-B model. The turbocharger and waste-gate model however, do still need to be matched to the test engine. The analytical compressor and turbine models require some parameters that need to be estimated. The matching of the turbocharger model can be divided into three parts (5):

1. Matching the engine inlet flow to the compressor flow, at the correct inlet pressure and engine and compressor speed. This is the matching of the air-swallow characteristic of the compressor.
2. Matching the engine exhaust flow to the turbine flow, at the correct exhaust pressure and temperature and engine and turbine speed. This is the matching of the turbine characteristic.
3. Matching the turbine and compressor power. This is the Büchi balance, which links the inlet and outlet pressures given the turbine and compressor inlet temperatures.

As not all the parameters required for both the turbocharger and waste-gate models are known they need to be calibrated as well. This means that the system matching and model calibration are done simultaneously.

When a parameter was changed the model was run to see the influence on the outcomes. Of course changing a single input parameter can have an influence on more than one outcome parameter. For instance when changing something in the turbine part of the turbocharger, this will also have an influence on the behaviour of the compressor (as the two are linked), this in turn may affect the air flow to the engine which changes the combustion etc. So the whole matching procedure consists of many iterations and gaining experience on working with the model. Broadly speaking the procedure was done in the following steps:

1. **Input of known parameters and first estimate of arbitrary parameters;** all parameters that are definitely known, such as number of cylinders, were implemented first. These did not need to be changed once they were put in. For the arbitrary set parameters a first estimate was made based on available data and literature. Most of these parameters were not changed much afterwards either because the estimate was quite accurate, or because without further information no basis for a change could be formed, or their influence on the outcome of the model was very small. A few of these parameters were changed slightly during the iterations of the following steps, for instance the amount of cooling by the charge air cooler.

2. **Defining in-cylinder parameters;** the 3 main in-cylinder parameters that were calibrated during this step were the mu-phi parameter and the the Seiliger parameters a and b. The mu-phi parameter is used to calibrate the flow through the engine, but also has an influence on the compressor size. The Seiliger parameters a and b within the model can be calibrated by changing 2 factors in their formulas. One is a consistent part (called $X_{a,c}$ and $X_{b,c}$) and one is a part dependant on engine speed (called $X_{a,n}$ and $X_{b,n}$). Changing parameter a determines the maximum in-cylinder pressure and changing parameter b determines the heat addition in the second combustion phase (and ultimately the temperature of the gas coming our of the cylinder). Once Seiliger parameter a and b are know, the model automatically calculates Seiliger parameter c. A more in-depth analysis and the formulas of this step in the calibration can be found in (20).
3. **Compressor and turbine parameters input;** during this step the compressor and turbine properties were calibrated. For instance the efficiency, pressure ratio, temperature ratio and the shape parameters were changed. In this file the amount of gas that is diverted to the waste-gate was implemented too. Again an in-depth analysis is written in (20) and all formulas can also be found in (22).
4. **Input of waste-gate parameters;** once the turbocharger was defined the waste-gate has to be implemented. At a certain inlet pressure the waste-gate is opened and part of the flow coming out of the cylinder is by-passed around the turbine. The size of the waste,the inlet pressure at which it is activated and the gain of the waste-gate model needed to be calibrated.
5. **Specific fuel consumption calibration;** the last step was to adjust the SFC and SFGC. Within the dual-fuel MVFP model this is done by manipulating some mechanical losses in the engine. These losses are modelled as frictional losses. These frictional losses can be adjusted to reduce the error between the calculated and measured specific fuel consumptions (20).

It has to be said that exactly following these steps will not necessarily result in a well matched engine model. There were a lot of iterations of these steps (especially between the in-cylinder and turbocharger calibration) and many smaller changes in other parts of the model. It is merely an illustration of the most important steps that were taken, as describing the whole matching procedure (which took weeks of time and experience in working with these models) would be to cumbersome.

3.2 Calibration of the dual-fuel MVFP model

This section will show the results of the calibration of the dual-fuel MVFP model. For this purpose the experimental data without added back-pressure were used. The calibration results have been divided into two parts, section 3.2.1 will show the propeller curve outcomes and section 3.2.2 the generator curve outcomes.

3.2.1 Propeller curve

This section will focus on the propeller curve, the exact measurement points of this curve during the experiments can be seen in figure 55a (the MCR was used for both the propeller and generator curve measurements for this case). In order to give a clear oversight of the calibration, it was chosen to show the results by following the flow through the engine and finishing with the fuel figures.

Engine power

Figure 4 shows the engine power vs rpm. It is clear that the model calculates the correct engine power at the shaft at the right rpm ('Pb model' is the same as 'Power test'). So the engine output of the model is matched correctly.

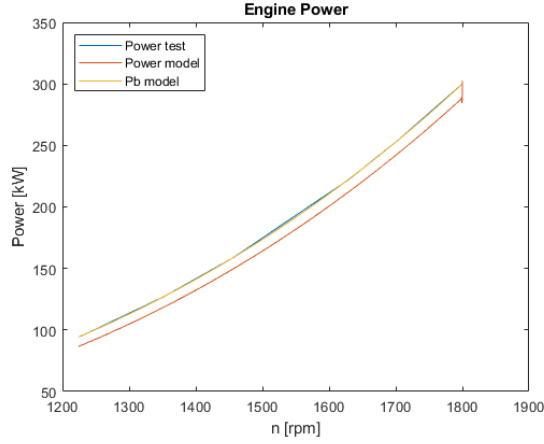


Figure 4: Engine power

Compressor

Figure 5 shows the compressor outlet pressure and temperature. It can be seen that the outlet temperature matches quite well. The outlet pressure is somewhat lower than the experimental data, especially at low loads, but this difference is less than 10 % so the error is not too large. It does however influence the pressure ratio, see figure 6b, which is too low in comparison. But this difference is also an effect of the too high turbine inlet pressure (figure 9a) as this affects the turbine performance and, since the compressor is driven by the turbine, this will decrease the compressor performance too. Even though the compressor characteristic does not match well, the outlet values of the compressor model are quite good, and since these values are more important for this research it was chosen to continue with these values for the compressor.

Lastly figure 6a shows the flow through the compressor and through the engine at the corresponding compressor pressure ratio. It can be seen that they are the same, so the air-swallow characteristic of the engine and the compressor in the model are matched.

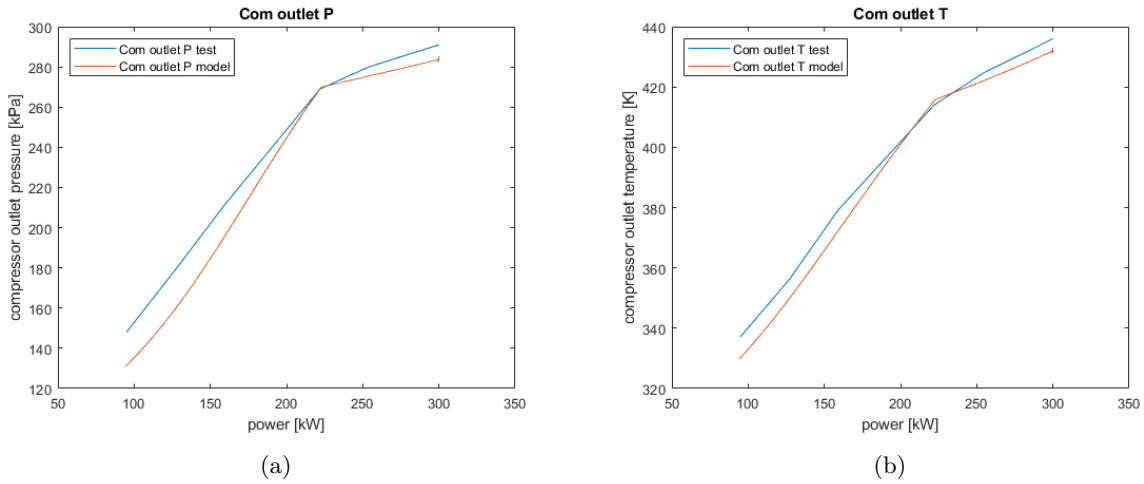


Figure 5: Compressor outlet pressure (a) and temperature (b)

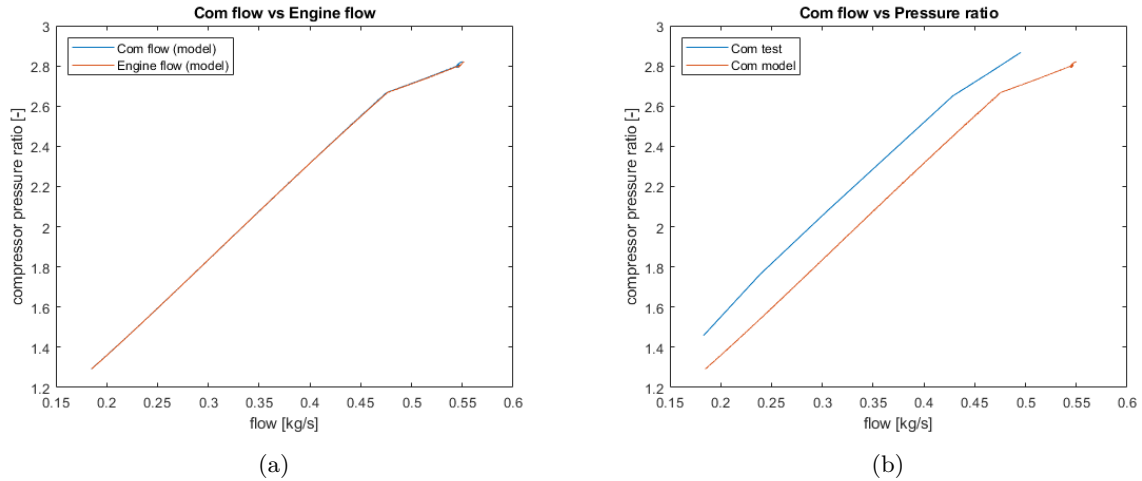


Figure 6: Compressor flow vs. engine flow (a) and compressor flow vs. pressure ratio (b)

Inlet receiver

After the compressor the air flow goes through a charge air cooler before entering the inlet receiver. It is important that the inlet receiver values are correct as they in term determine the trapped conditions within the cylinder. The inlet receiver pressure is also the determining factor for when the waste-gate will become active. Figure 7 shows that both the inlet receiver pressure and temperature are matching rather well. The point at which the waste-gate becomes active is around 220 kW (the point where the curve starts to flatten). For the model this is nearly the same as well as the decrease of the steepness of the curve, so the waste-gate is calibrated nicely.

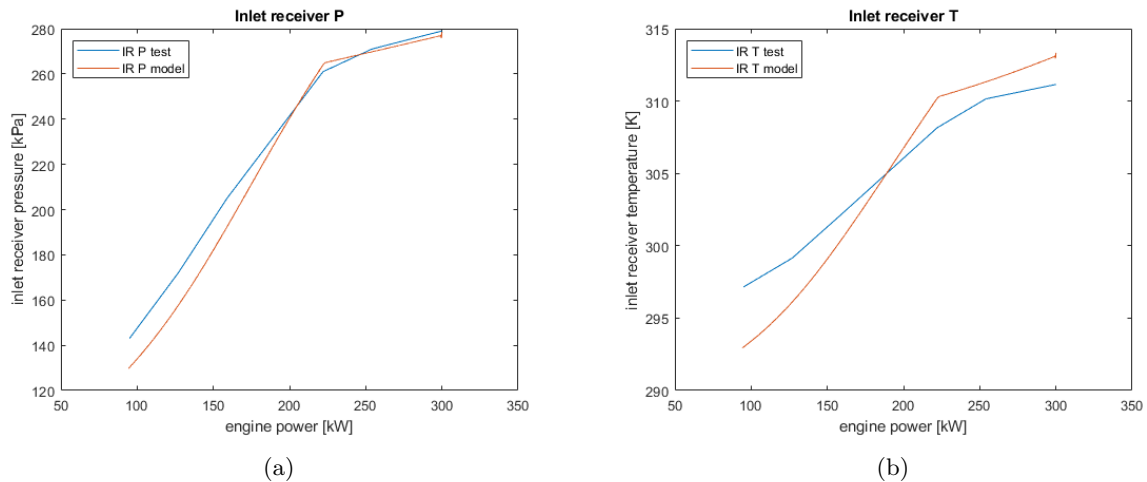


Figure 7: Inlet receiver pressure (a) and temperature (b)

In-cylinder: Seiliger parameters

As stated earlier for the in-cylinder process the Seiliger cycle is being used. The cycle and the definitions of the Seiliger parameters can be seen in figure 2. In section 3.1 it was explained that in the model the Seiliger parameters a and b can be calibrated and the model will then calculate parameter c. In figure 2 it can be seen that the maximum in-cylinder pressure is determined by the parameter a. So that is why the maximum in-cylinder pressure was chosen as the reference value for the calibration of parameter a. Figure 8a shows this comparison and it can be seen that this matches well.

At point 4 in the Seiliger cycle (so after parameter b is used) the maximum temperature is reached (21). The higher this maximum temperature, the higher the temperature at the end of the cycle and therefore the higher the temperature in the exhaust. The amount of heat input during stage 3-4 in the cycle within the model is based on the total amount of heat input into the cylinder by the fuel. The part of this total heat input that is used in this stage of the cycle is determined by the parameter b. So for the calibration of this parameter 2 reference values are used. The first one is the heat input into the cylinder

(figure 8b) and the second one is the turbine inlet temperature (figure 9b). The heat input in the model is higher at high loads. This difference is due to the fact that the fuel flows are not perfectly matched (this will be discussed later), but could also come from the fact that the calculated Lower Heating Value of the gaseous fuel is slightly higher than it was during the experiments (fuel flow in figure 12a is lower but heat input is higher, so therefore a higher LHV). However the turbine inlet temperature does not deviate much (maximum error is less than 5 %), so it seems that the calibration of Seiliger parameter b was done rather well. The exact in-cylinder process is not the focus of this thesis, but more the overall engine parameters like the temperatures, so since this is matching quite well it was chosen to continue even though the exact heat input is not perfect (and therefore the Seiliger parameter b might in fact be different for the tested engine).

A small note by figure 8b, the lines for 'Qcomb model' and 'Qf model' are exactly the same and therefore the line for 'Qcomb model' can not be seen in the figure. This is because the combustion efficiency (calculated by a sub-model based on Woschni formulas using the air access ratio) is 1 for the whole range. This basically means that at no point the air access ratio was lower than the smoke limit for the pilot fuel.

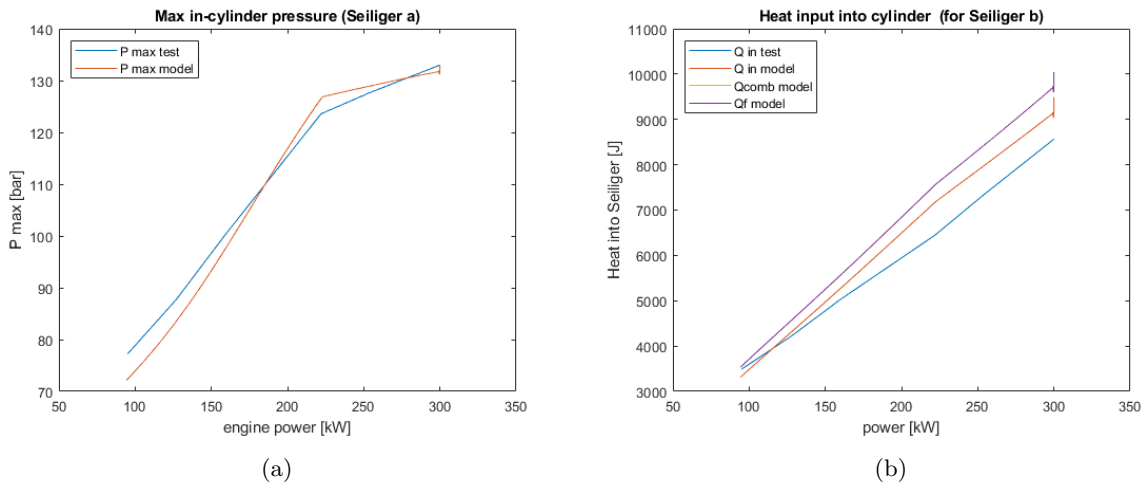


Figure 8: Maximum in-cylinder pressure (a) and heat input into Seiliger cycle (b)

Turbine

The turbine inlet pressure and temperature from figure 9 have been mentioned in the parts above. The temperature does not deviate much, the inlet pressure however is much higher at medium to high loads than the measured values. This higher inlet pressure causes a lower pressure ratio across the turbine in the model. This lowers the turbine performance and in extension the compressor performance. It was tried to lower this inlet pressure, but then it either did not match at lower engine loads or the values on the inlet side did not match at all anymore and could not be improved to a satisfactory level. So there is some room for improvement in the model here. However since at the moment most of the other values, especially those that are of interest (the exhaust temperatures for example as these are a limiting factor for the engine), are matching rather well it was chosen to continue with this too high turbine inlet pressure.

What the turbine inlet pressure does show is that the point at which the waste-gate becomes active is indeed correct. Also the steepness of the curve after this point is almost the same as for the tested engine, so again it seems that the waste-gate parameters are implemented correctly.

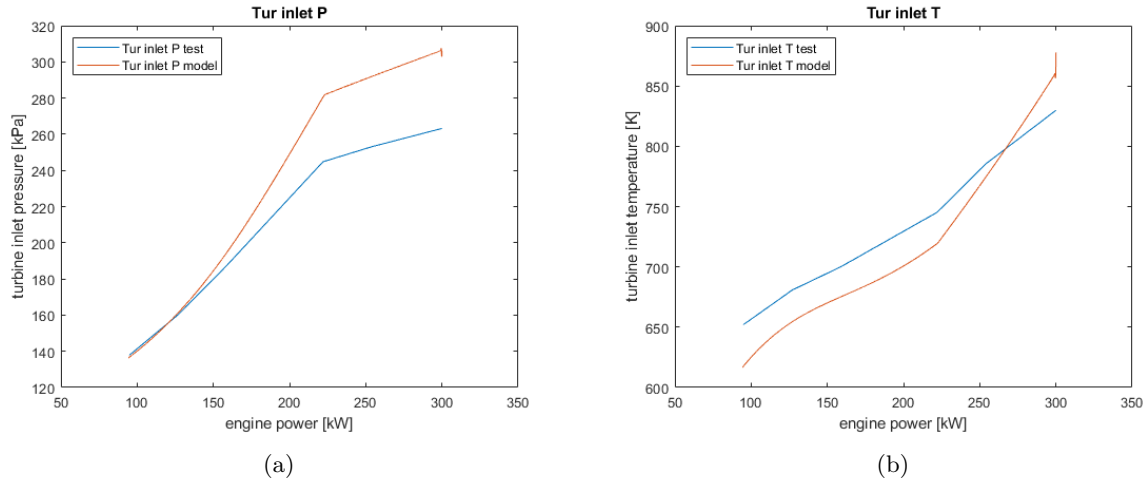


Figure 9: Turbine inlet pressure (a) and temperature (b)

The turbine outlet pressure, as seen in figure 10a, is matching well. This is because this is the back-pressure that is put into the model. The small deviation is due to the fact that in the model uses a time scale to run the model. So the input is the pressure at the beginning and at the end of the run and in between the model gradually changes this outlet pressure over time, whereas during the experiments the engine was run at certain loads and the back-pressure did not change linearly between these points, see section 4.1 for a more detailed discussion about this issue with back-pressure during the experiments. The turbine outlet temperature in figure 10b is matching nicely, with only a small overshoot at maximum engine power, but this error is less than 5 %.

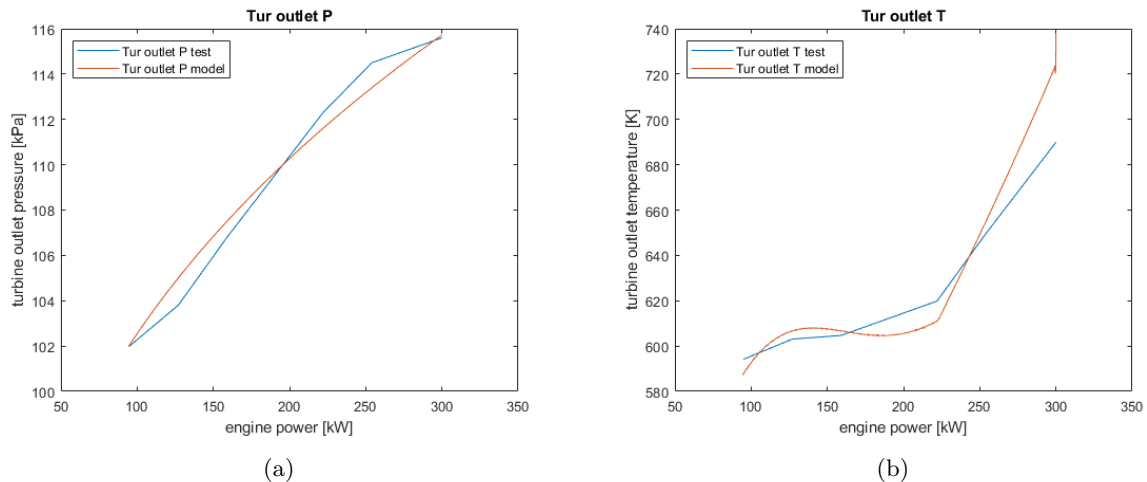


Figure 10: Turbine outlet pressure (a) and temperature (b)

Figure 11 shows the turbine flow and the corresponding pressure ratio. The pressure ratio becomes too high at a certain point, which is caused by the too high turbine inlet pressure. This also reduces the flow through the turbine at a certain moment, which can clearly be seen. At lower flow/pressure ratio's it is matched.

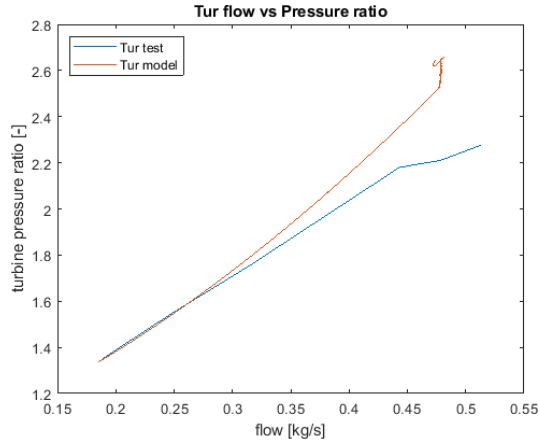


Figure 11: Turbine flow vs. pressure ratio

Fuel

Figure 12a shows that, with exception of very high power range, the fuel flow for both the pilot and gaseous fuel for the model are lower than for the tested engine, although the difference is small. This also leads to a difference in specific fuel consumption's, see figure 12b. What is especially noteworthy here is the increase in specific pilot fuel consumption (blue line in the graph) for the tested engine at low loads. This will also be discussed in section 4.2.3, but it seems that for the tested engine the combustion efficiency changes over the range of engine power. This is a rather strange and so far (looking at the literature study) unknown phenomena. At this point this behaviour is very hard to implement into the model without further research.

The small vertical off-shoot at maximum engine power (which can also be seen in some other figures) is coming from the way the governor for the fuel rack works in the model. It adjusts the fuel rack position so that the error between the required and the real rpm of the engine is zero. As soon as the model starts to run the required rpm is changing and there for an error occurs. The governor reacts to this error (controlled by a PID controller) and this causes a small overshoot in the first couple of seconds of the run. This causes this 'overshoot' to appear in the data, but is something that does not happen in real life.

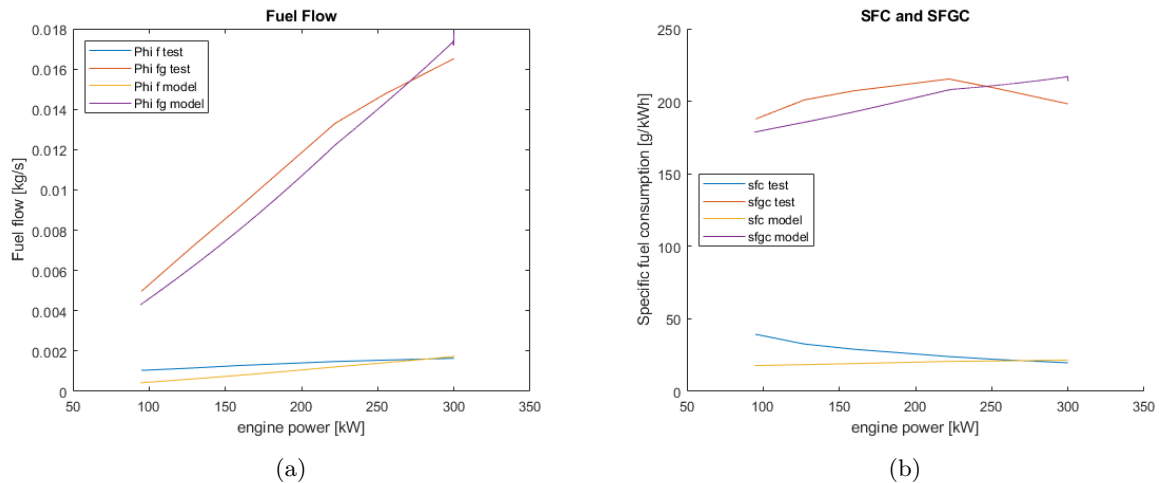


Figure 12: Fuel flows (a) and specific fuel and specific gaseous fuel consumption (b)

3.2.2 Generator curve

After the calibration along the propeller curve, the model was run along the generator curve to see how it matches at this point in the engine envelope. The input parameters for the engine components are the same as for the propeller curve. This section will show these results, again following the flow through the engine.

Engine power

Figure 13 shows the engine power vs torque (as the rpm is the same for all points). It is perfectly matched, so the engine output of the model is correct as it was for the propeller curve.

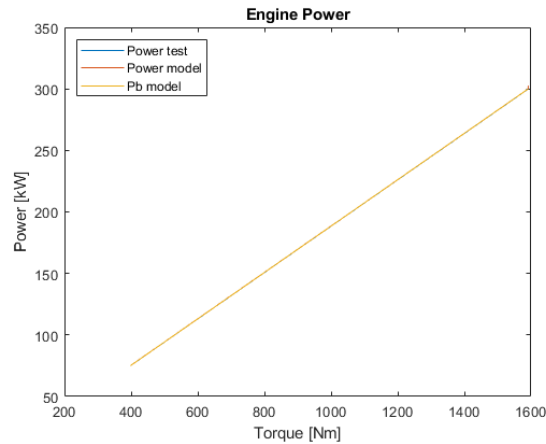


Figure 13: Engine power

Compressor

The compressor outlet values in figure 14 are matching rather well. The biggest difference is at part load, but this is mainly due to the fact that only a few points were tested experimentally and these points are linearly connected in the graph. In figure 15a it can be seen that the air swallow characteristic of the compressor and the engine in the model are still matched. The compressor flow vs pressure ratio, figure 15b, is not matched. Again this is mainly due to the too high turbine inlet pressure (see figure 18a) which causes an error in turbocharger performance. Comparing figures 6b and 15b shows that there is a shift in the flow vs pressure ratio of the compressor. Although the model and the test results are not matched, it seems that this shift is rather similar for both the model and test results. This, in combination with the fact that the outlet values are quite correct, gives reason to believe that the compressor characteristic itself is implemented rather well.

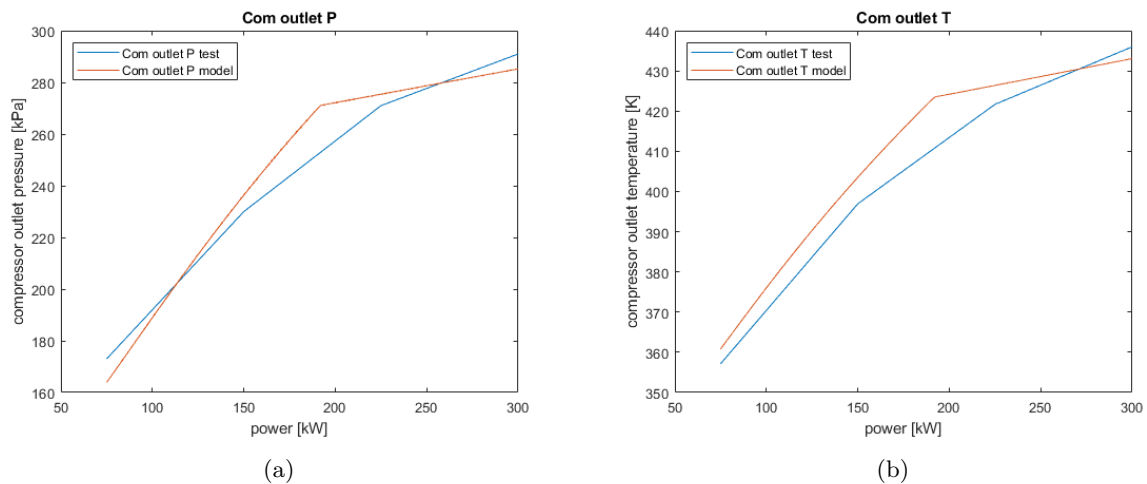


Figure 14: Compressor outlet pressure (a) and temperature (b)

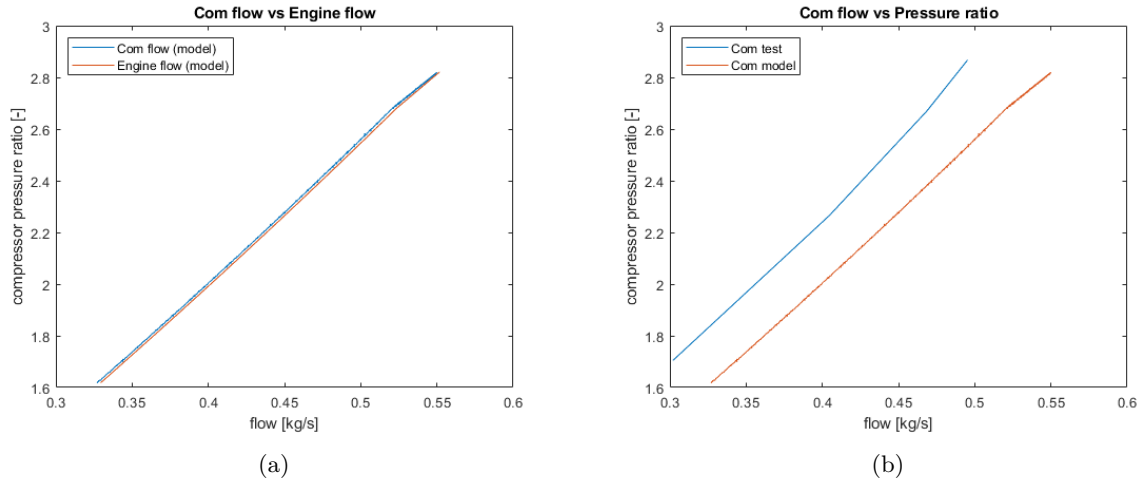


Figure 15: Compressor flow vs. engine flow (a) and compressor flow vs. pressure ratio (b)

Inlet receiver

The values for the inlet receiver are, similar to the compressor curve, matching rather well too. The temperature difference is only a few degrees. Again for the pressure difference at part load the linear connection between the tested points makes the error look larger than it in fact may be.

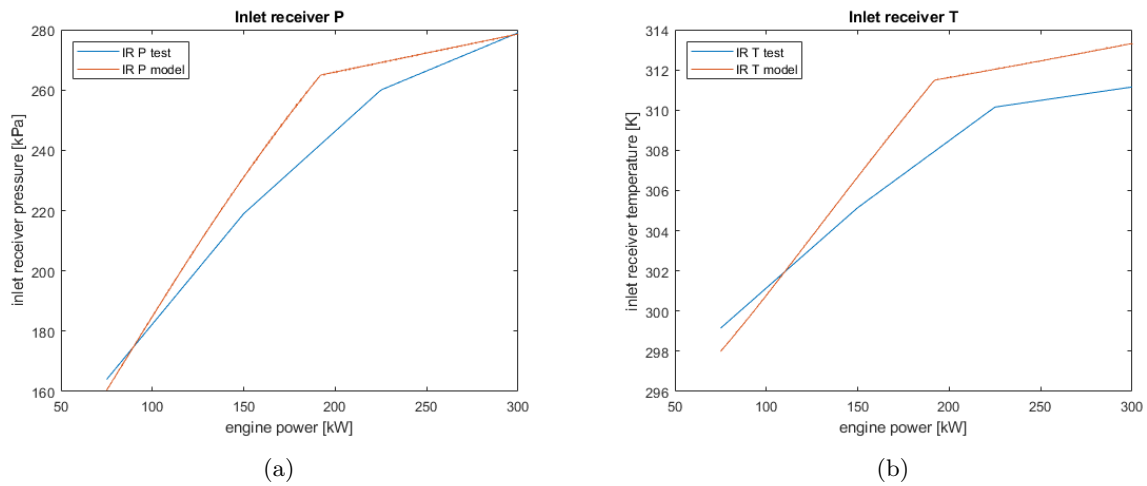


Figure 16: Inlet receiver pressure (a) and temperature (b)

In-cylinder: Seiliger parameters

For the calibration of Seiliger parameter a the maximum in-cylinder pressure is the reference value and for Seiliger parameter b the heat input and turbine inlet temperature were chosen. In the previous section it is explained why. It can be seen in figure 17a that the maximum in-cylinder pressure is matching well. Similar to the compressor outlet pressure and inlet receiver pressure, the apparent error at part load is due to the linear connection between the (few) experimentally tested points along the generator curve. The heat input into the cylinder, figure 17b, is higher in the model although the trend over the power range is rather similar. This difference is caused by a difference in fuel flow (figure 21a) and probably a difference in calculated and real lower heating value of the gaseous fuel. The turbine inlet temperature as seen in figure 18b is matching nicely, so it seems that at the moment, despite the higher heat input, the overall in-cylinder process output is good and both parameters are matched well.

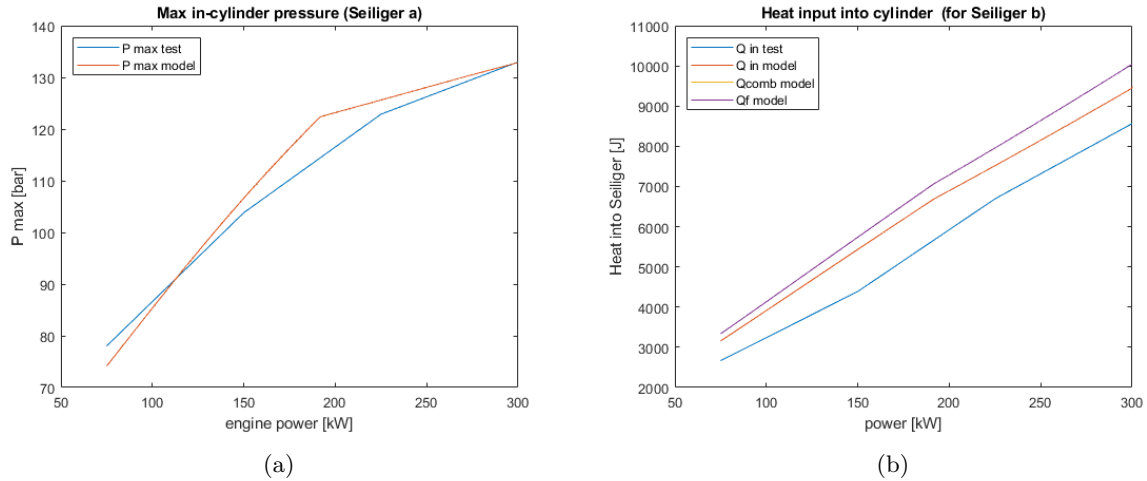


Figure 17: Maximum in-cylinder pressure (a) and heat input into Seiliger cycle (b)

Turbine

Looking at the turbine inlet and outlet pressure (figures 18a and 19a respectively) it can be seen that they do not match. For the propeller curve the turbine inlet pressure became too high at high engine loads (or high rpm). As the rpm is now continuously at its maximum level this error is even worse. As was explained in the previous section, the difference in turbine outlet pressure is due to the fact that in the model this outlet pressure is the back-pressure input, and in the model only the start and end pressure are given as an input and in between the model gradually changes this back-pressure where during the experiment this was not the case. The error in these turbine pressures causes that the pressure ratio in the model is not correct, which affects the turbine performance (and thus the turbocharger performance as a whole). However looking at the turbine temperatures, figures 18b and 19b, they are matching really well. And as stated earlier the thermal loading of the engine (and especially of the turbine) is an important limiting factor. So for the moment it was chosen to continue since these values are quite well matched.

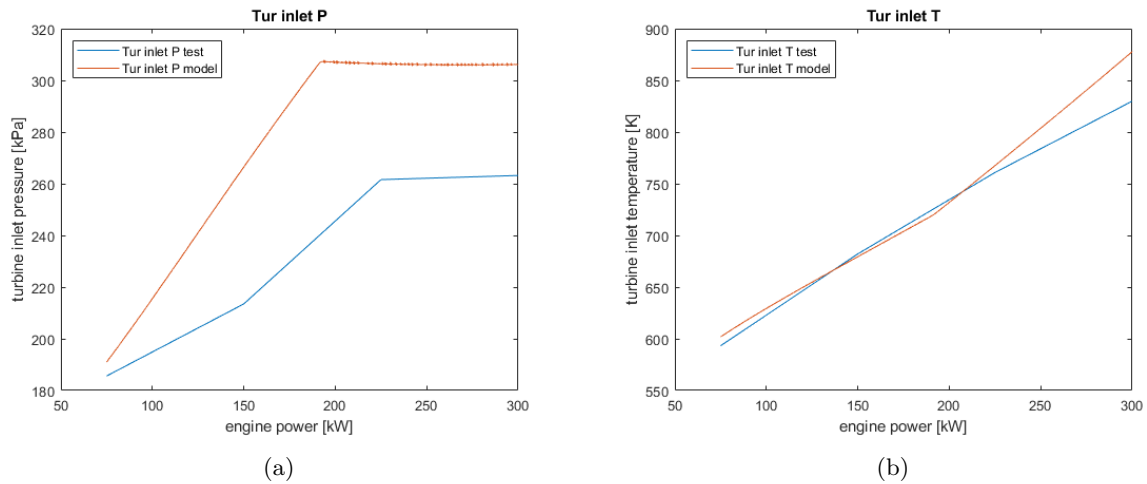


Figure 18: Turbine inlet pressure (a) and temperature (b)

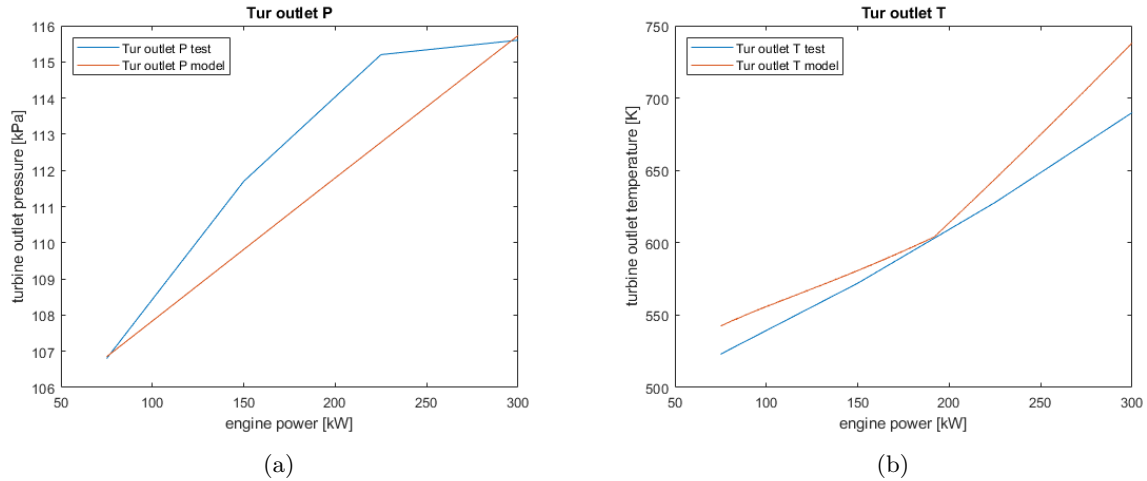


Figure 19: Turbine outlet pressure (a) and temperature (b)

Figure 20 shows the turbine flow vs pressure ratio. It can be seen that the model value is rather wrong. This is of course an effect of the error in the turbine pressures. The shape of the curve coming out of the model is due to the fact that the outlet pressure decreases, going from high to low engine power, and that the inlet pressure first remains constant (increasing slightly even) and then drops rather quick. This causes the pressure ratio and flow to increase first and then drop back down again. As this process happens over time in the model, the curve gets this weird shape as it is being plotted it into the figure. The flow range of the turbine does comply with the tested data, but all in all as long as the turbine pressures are not correct looking at this figure is not really useful.

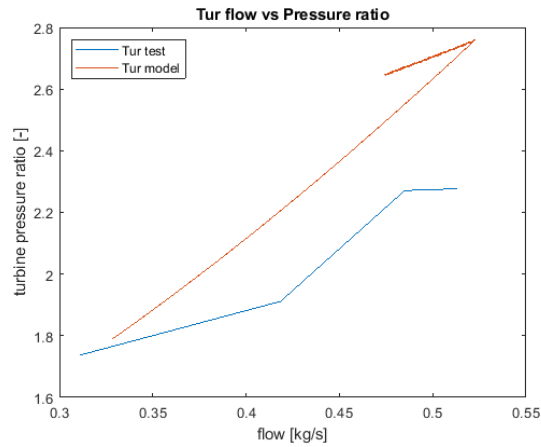


Figure 20: Turbine flow vs. pressure ratio

Fuel

For the fuel flows, figure 21a, a similar conclusion can be made as for the propeller curve. At low engine loads the fuel flows in the model are lower and only at high engine loads they become higher. Looking at the specific fuel consumption's in figure 21b it can again be seen that the both increase at low loads. This trend is being captured by the model although not in the same way as for the tested engine. Again a more in depth analysis of the fuel consumption of the tested engine will be done in section 4.2.3, but as stated for the propeller curve the fuel consumption and the combustion efficiency of the tested engine would need more research in order to implement them correctly into the model.

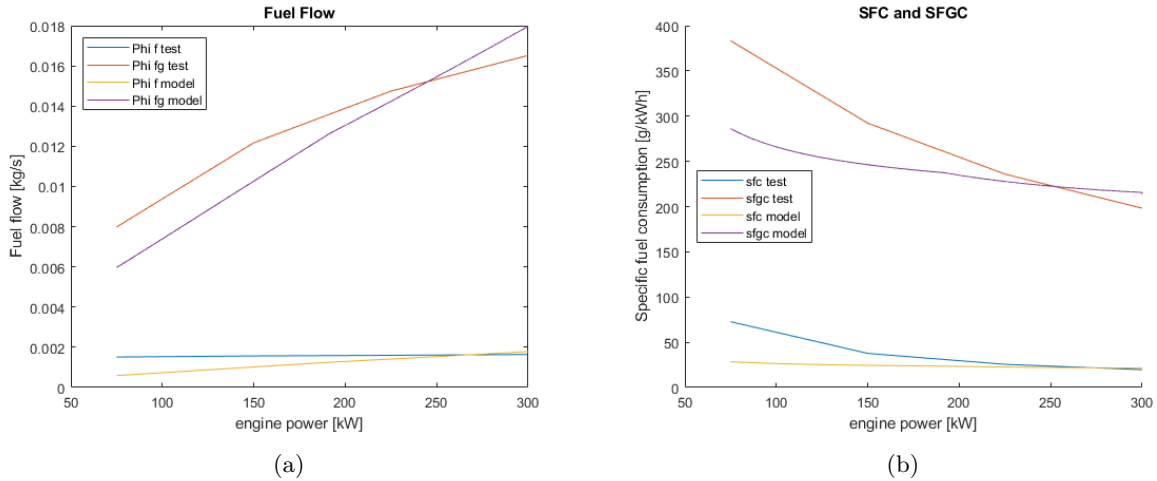


Figure 21: Fuel flows (a) and specific fuel and specific gaseous fuel consumption (b)

This concludes the calibration part of the matching of the dual-fuel MVFP model. For both the propeller and generator curve it was found that the turbine inlet pressure is calculated too high within the model and that the fuel consumption and the dual-fuel combustion need more investigation. However most other parameters are matching rather well at the moment. As mentioned the thermal loading of the engine will be a limiting factor when applying back-pressure. As the turbine temperatures within the model and the pressures and temperatures at the inlet side of the engine (and therefore the input in the cylinder) are matching well it was chosen to continue with the model as it is. But it does mean that there is room for improvement in the model and more research is necessary to improve it.

3.3 Verification of the dual-fuel MVFP model

After the calibration of the dual-fuel MVFP model, it was run with the same added back-pressure values as was done during the experiments in order to verify the model. There were two cases with added back-pressure, a low and a high variant. This section will show these results, first for the propeller curve in section 3.3.1 and then for the generator curve in section 3.3.2. The operating points that were used during the experiments can be found in figure 55.

3.3.1 Propeller curve

This section will describe the results for the propeller curve for the two experimentally tested cases with added back-pressure. The order of the results will be the same as in section 3.2, so following the flow through the engine. As the engine limits were reached at an earlier point now more back-pressure was added, the maximum power during the experiments was 254 kW instead of 300 kW.

Engine power

Figure 22 shows the engine power vs rpm for both cases. It is clear that the engine output at the shaft from the model ('Pb model') is the same as it was for the tested engine, so the engine output of the model is still correct.

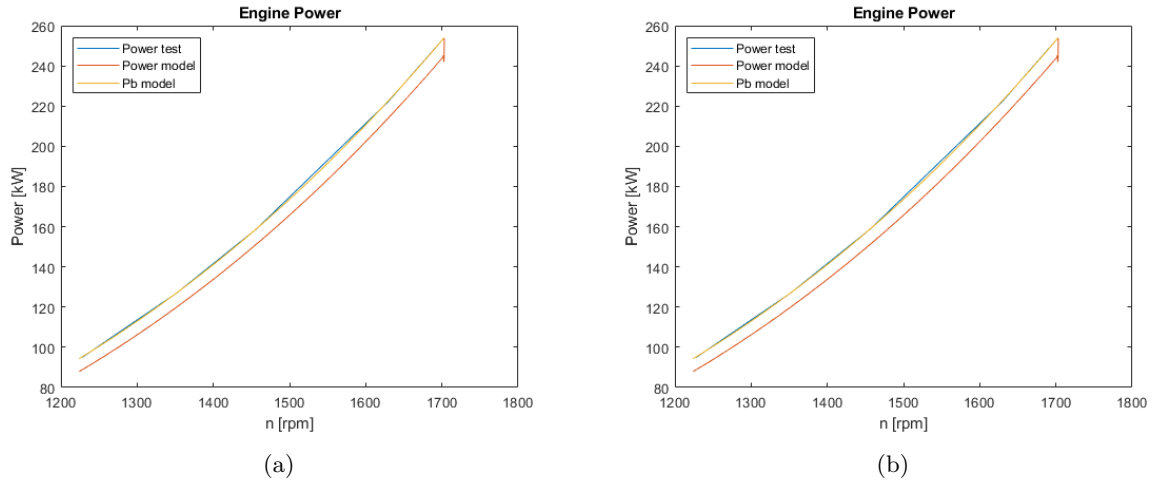


Figure 22: Engine power for low (a) and high (b) back-pressure

Compressor

The compressor outlet pressure for both cases have the same trend, being somewhat lower than the tested engine. This is the same as was found during the calibration. It has to be said that the difference in compressor outlet pressure during the experiments was very small, as can be seen in figure 57a. The problem with a too high turbine inlet pressure in the model which deteriorates the turbocharger performance is still present, so therefore the compressor outlet pressure is not perfect, but still good enough. Adding more back-pressure does not seem to enhance this issue for the compressor and the error is not too large.

The compressor outlet temperature (figure 24) matches fine, with only a small difference at low loads, but this is an effect of the too low pressure coming out of the compressor.

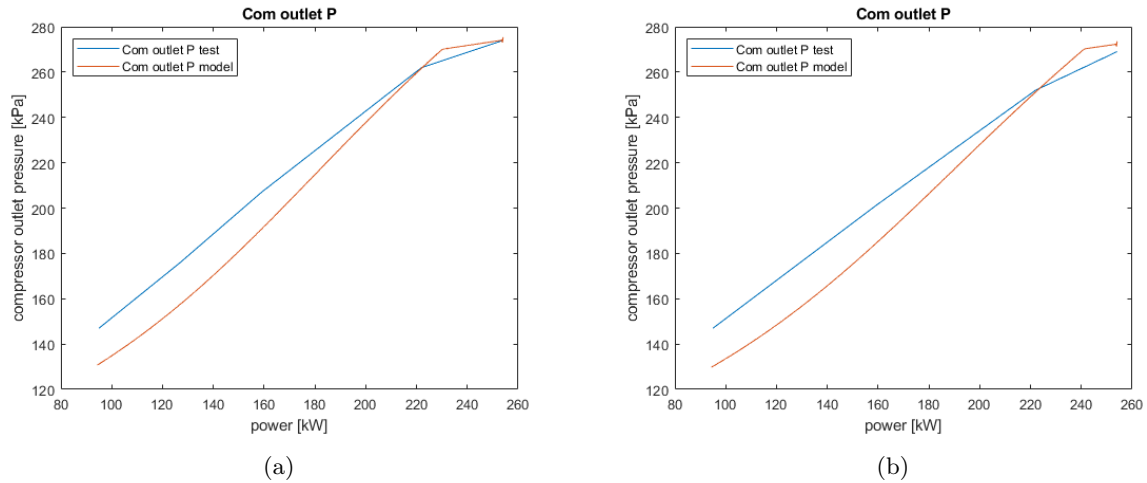
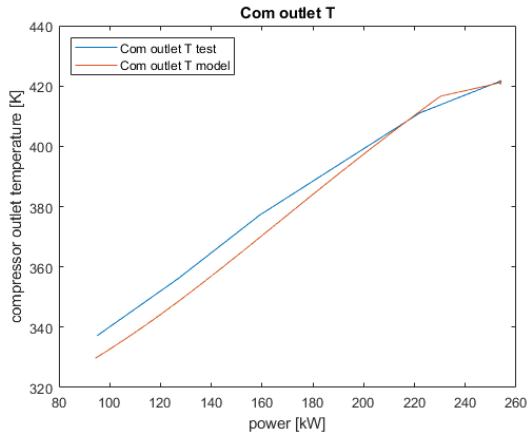
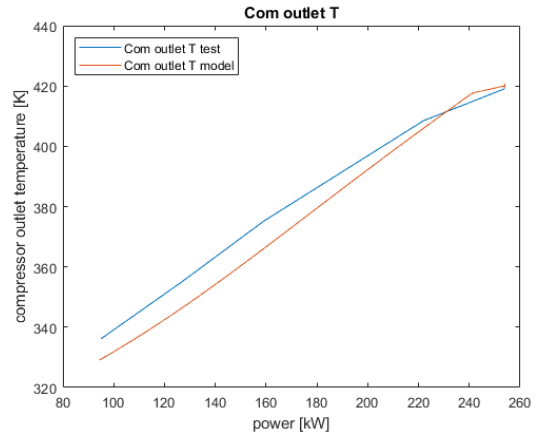


Figure 23: Compressor outlet pressure for low (a) and high (b) back-pressure



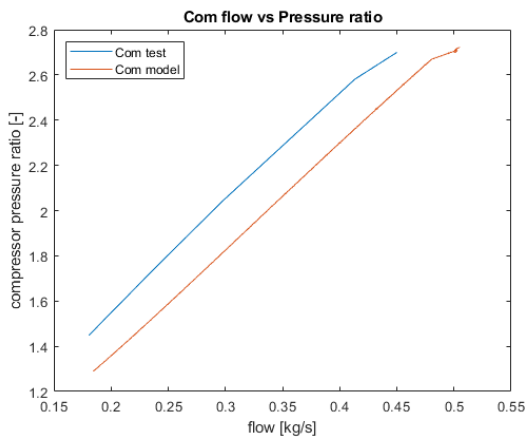
(a)



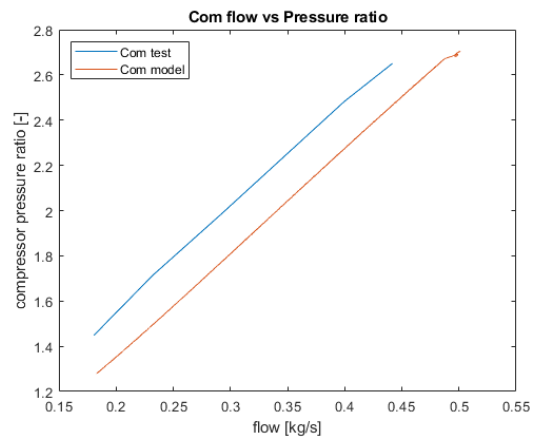
(b)

Figure 24: Compressor outlet temperature for low (a) and high (b) back-pressure

Looking at figure 25 the same issue as before can be seen. There is an error between the model results and the experimental results, however the shift in the flow vs pressure ratio (although it is small) is the same for both. So the model does capture this effect well. Figure 26 shows that for both cases the air swallow characteristic of the compressor and engine still matches.

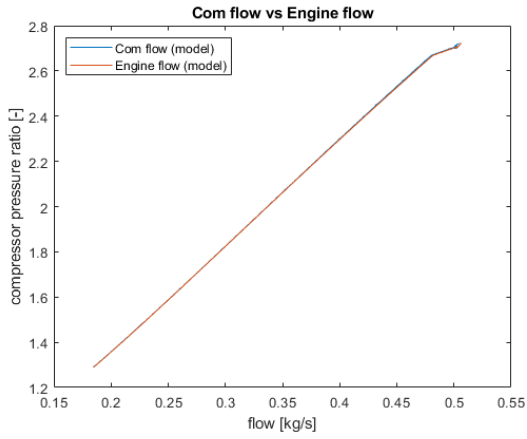


(a)

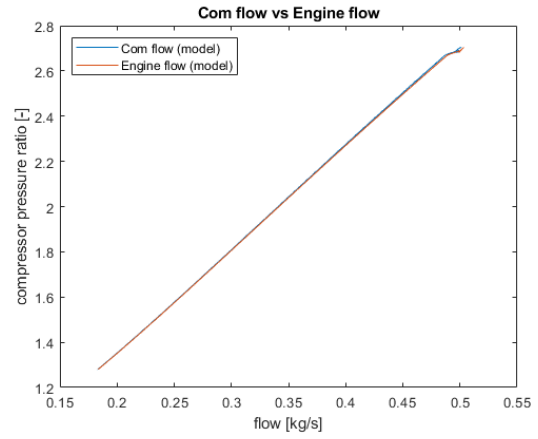


(b)

Figure 25: Compressor flow vs. pressure ratio for low (a) and high (b) back-pressure



(a)

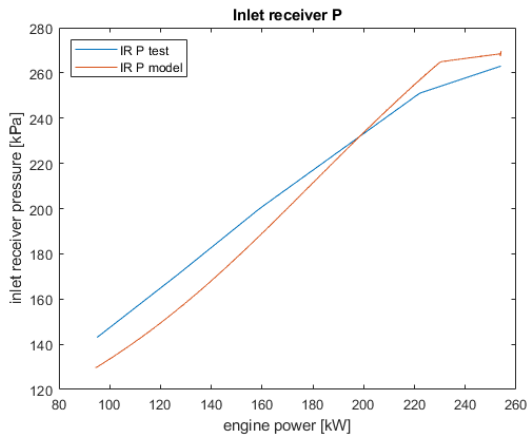


(b)

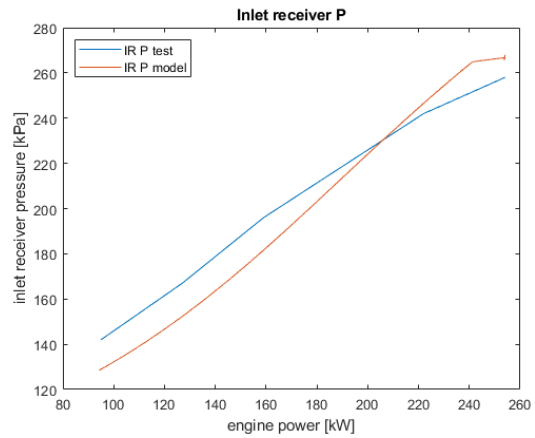
Figure 26: Compressor vs. Engine flow for low (a) and high (b) back-pressure

Inlet receiver

The error in compressor outlet pressure means that the inlet receiver pressure will be off as well. This can be seen in figure 27 where a similar trend as for the compressor can be found. However the error is not too large. The temperature of the inlet receiver seems to have a large error at low loads, but this difference is only a few degrees so this is not really an issue and will not cause large errors in other parts of the model.



(a)



(b)

Figure 27: Inlet receiver pressure for low (a) and high (b) back-pressure

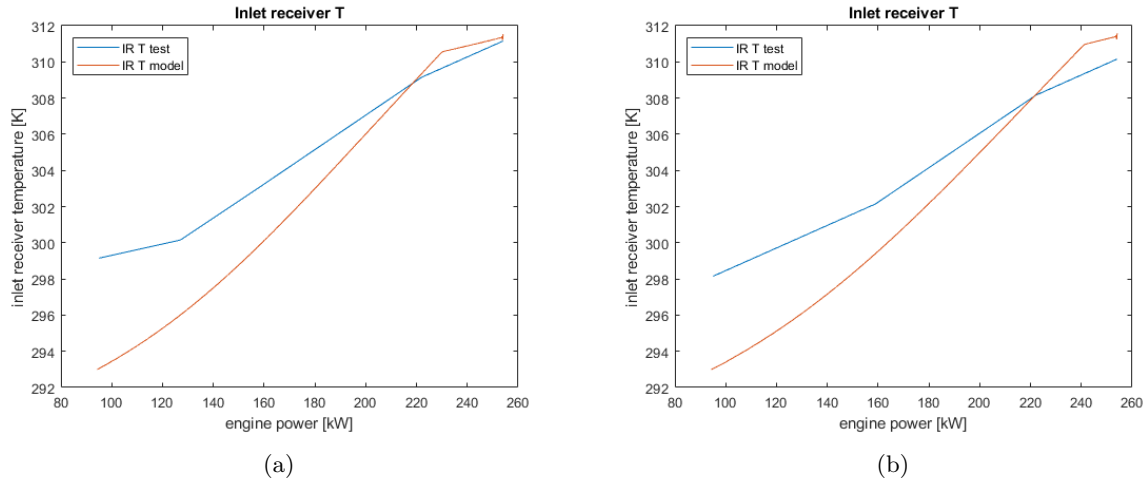


Figure 28: Inlet receiver temperature for low (a) and high (b) back-pressure

In-cylinder: Seiliger parameters

Figure 29 shows that the maximum in-cylinder pressure matches pretty good for both cases, so this verifies the calibration of the Seiliger parameter a. For the Seiliger parameter b verification the same conclusion as during the calibration can be made. That although the heat input is for the most part higher than for the experiments, the turbine inlet temperature does not get a too large error (around 6 % maximal), so this parameter works well too.

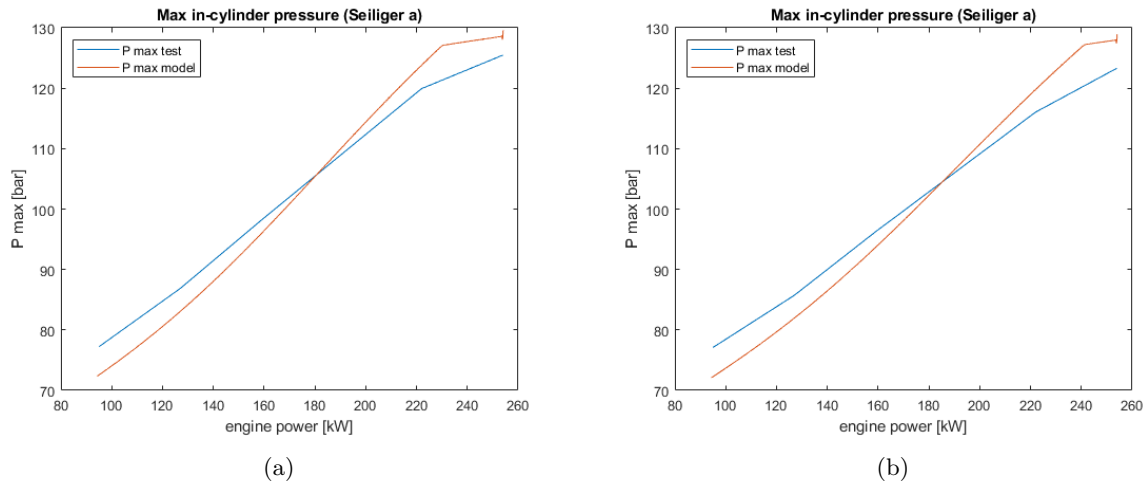


Figure 29: Maximum in-cylinder pressure for low (a) and high (b) back-pressure

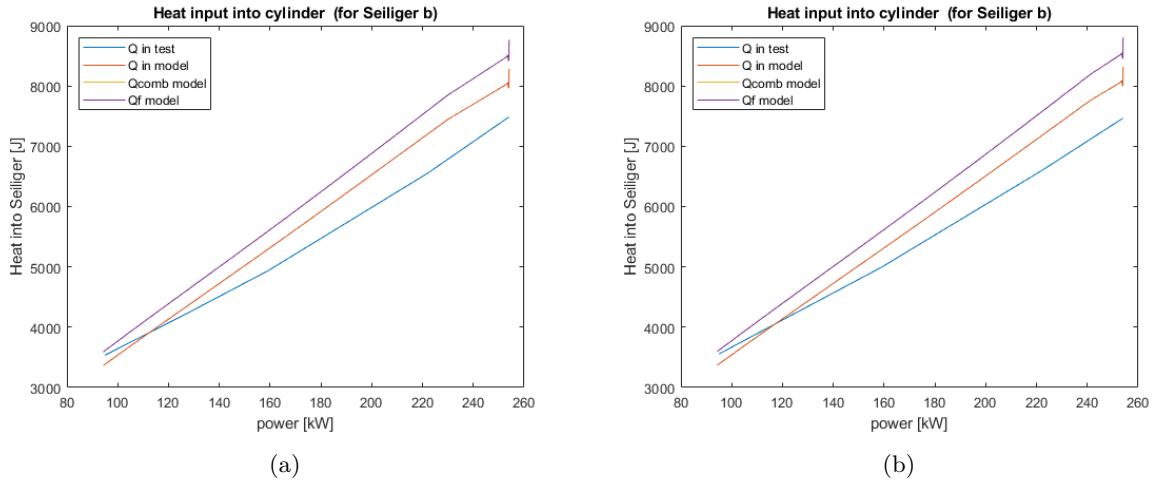


Figure 30: Heat input for Seiliger cycle for low (a) and high (b) back-pressure

Turbine

The turbine inlet pressure still has the issue that it is too high at high engine loads of course, but it does match at the low loads. And the change in outcome between the two tested cases (although they are very small) is captured by the model. As mentioned earlier the turbine inlet temperature is still matching rather well (figure 32), with a maximum error of 5-6% at the lowest engine power. And here too the model captures the trends really well.

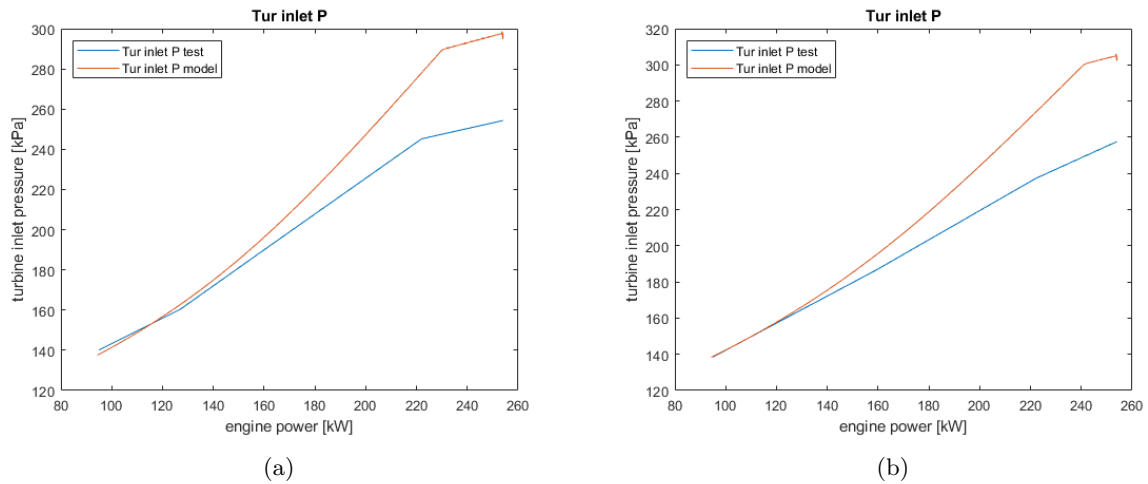


Figure 31: Turbine inlet pressure for low (a) and high (b) back-pressure

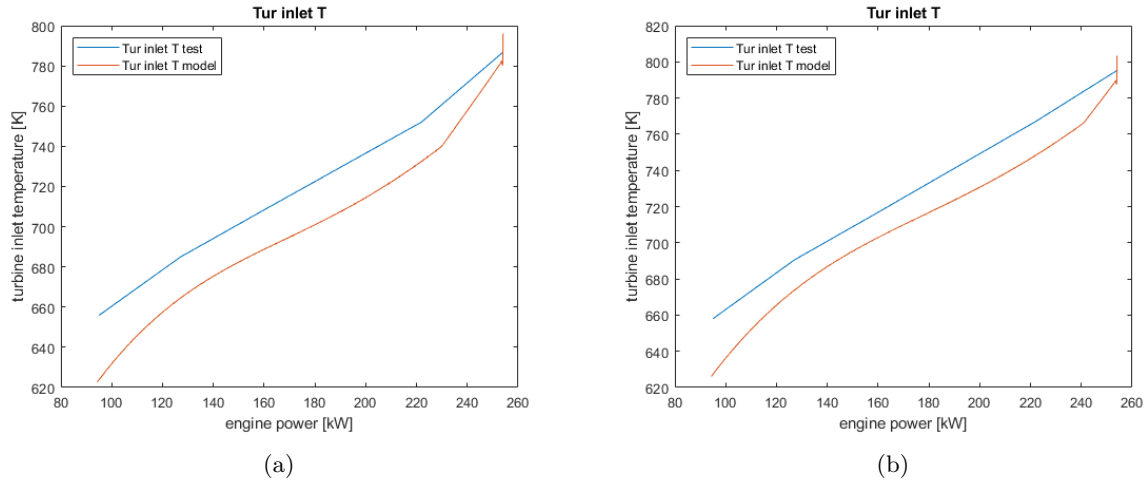


Figure 32: Turbine inlet temperature for low (a) and high (b) back-pressure

There still is a small difference between the measured turbine outlet pressure and what comes out of the model. Again for the model this is an input value and as stated earlier, during the experiments the change in absolute back-pressure between the tested points was not constant (which is hard to capture in the model). The turbine outlet temperature still works very well although the model shows a certain curvature in the graph at low loads until the waste-gate opens which the experimental results do not show so well. However this error is not so large and the sharp increase in temperature for the range when the waste-gate is opened is captured really well by the model.

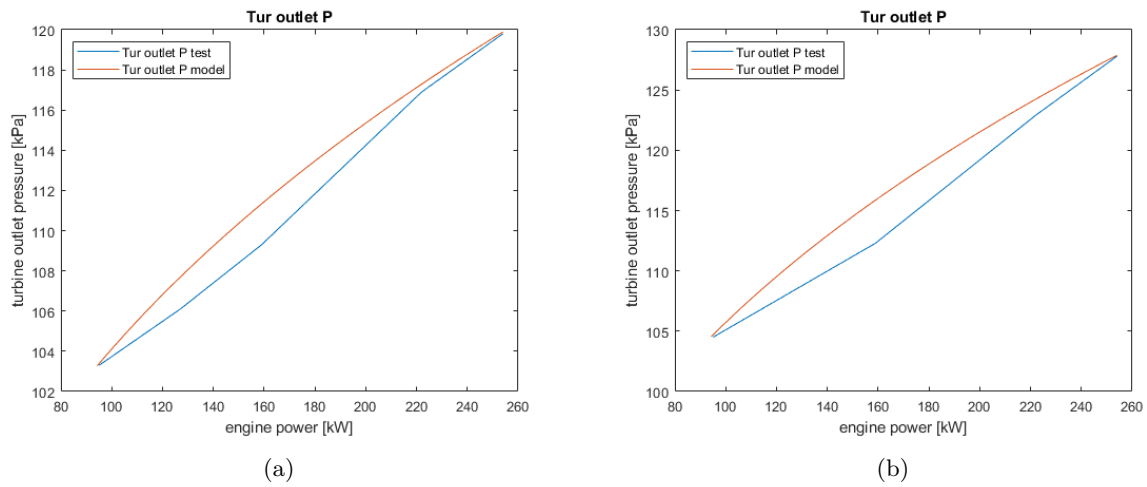


Figure 33: Turbine outlet pressure for low (a) and high (b) back-pressure

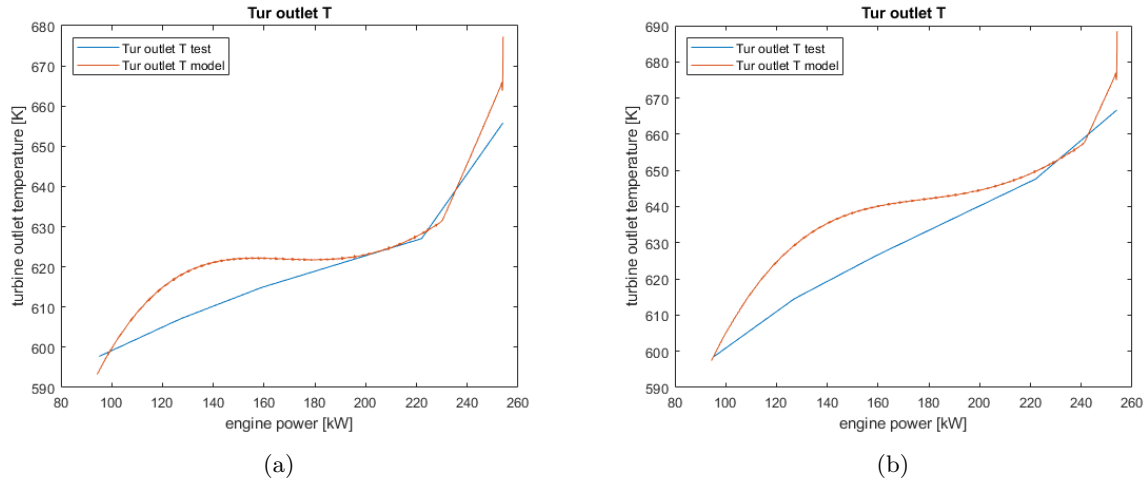


Figure 34: Turbine outlet temperature for low (a) and high (b) back-pressure

The turbine flow vs pressure ratio in figure 35 is matching well at low flows, but as the turbine inlet pressure starts to rise above the measured values, so overshoots the pressure ratio in these figures too. But it shows that at low engine loads (and thus lower flows) the turbine works fine in the model for the propeller curve.

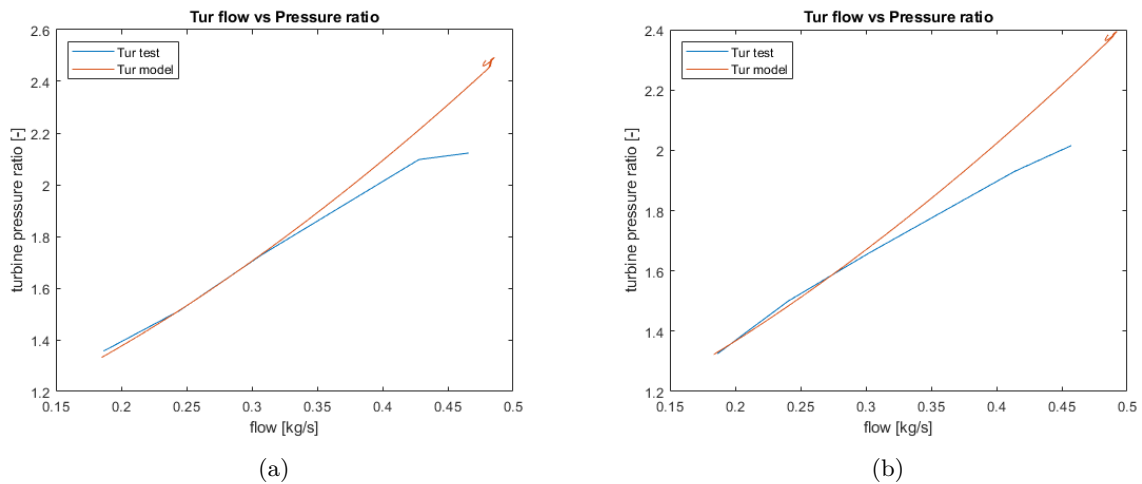


Figure 35: Turbine flow vs. pressure ratio for low (a) and high (b) back-pressure

Fuel

The fuel flows seem to match rather well, with the exception of the hump in the gaseous fuel flow at part load conditions for the engine. This same hump can be seen in the SFGC graph in figure 37. As mentioned earlier there seems to be a change in (combustion) efficiency over the engine power range, so this is a returning issue making it very difficult to get the fuel flows and specific fuel consumption's right. However the model seems to capture the change in fuel flows as back-pressure is increased so this gives reason to believe that the calibration was done right.

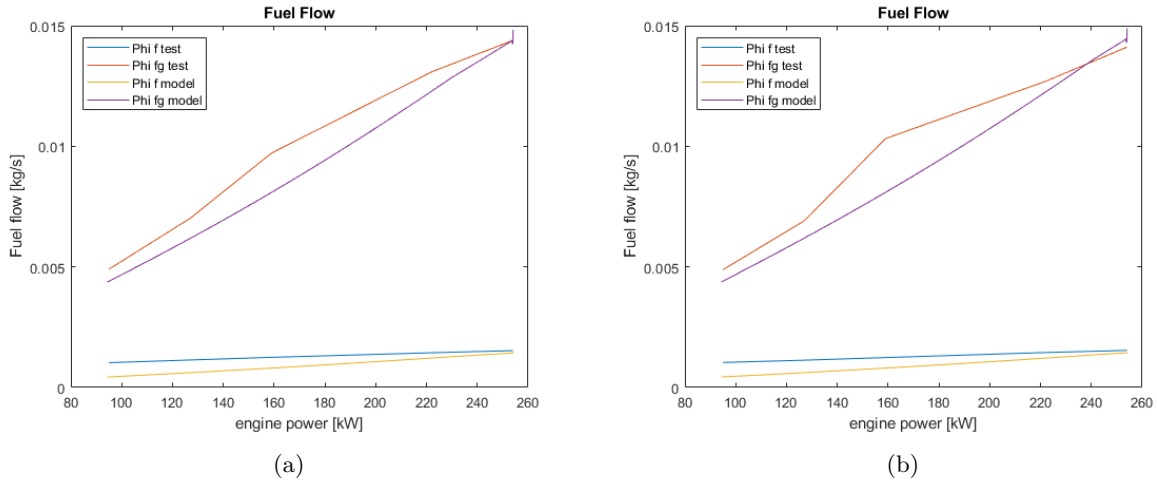


Figure 36: Fuel flows for low (a) and high (b) back-pressure

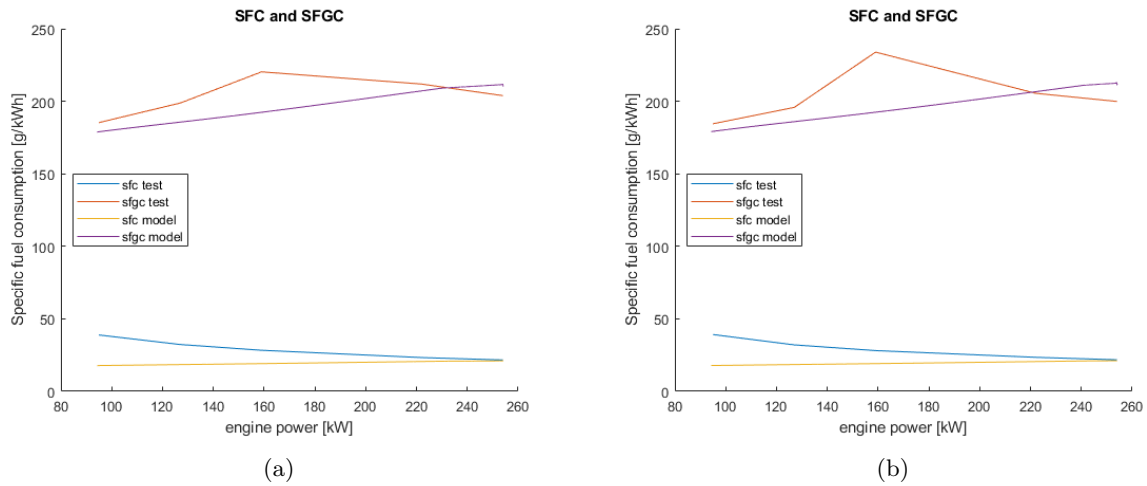


Figure 37: Specific fuel and Specific gaseous fuel consumption for low (a) and high (b) back-pressure

3.3.2 Generator curve

In this section the results from the generator curve for the cases with added back-pressure will be shown. Again increasing the back-pressure meant that the engine limits were reached at an earlier point than the maximum continuous rating, so the maximal engine power that could be reached during the experiments for the generator curve is 245 kW instead of 300 kW. At the end a conclusion about the verification will be made.

Engine power

In figure 38 it can be seen that the output of the model is still the same as for the tested engine, so this model output is indeed calibrated correctly.

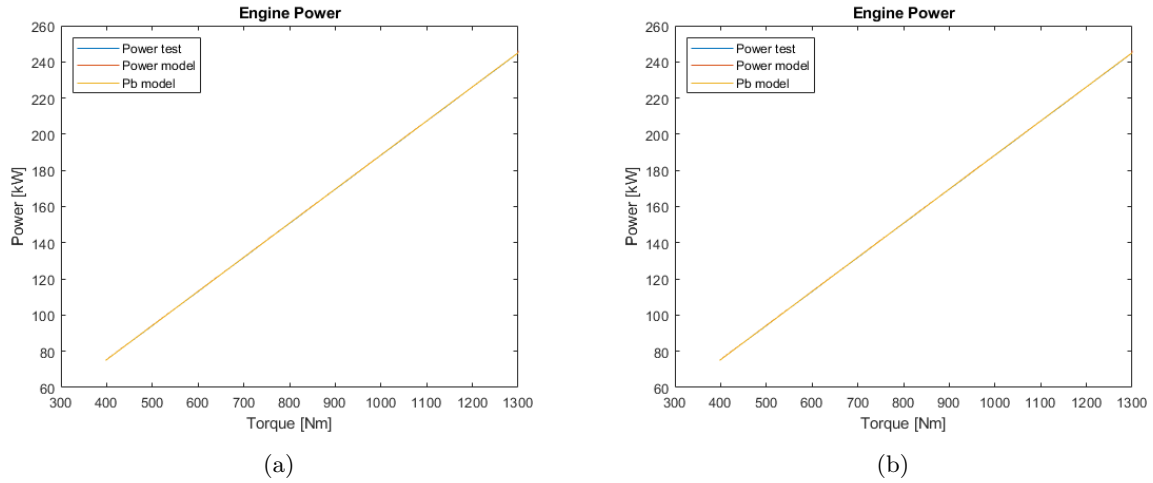


Figure 38: Engine power for low (a) and high (b) back-pressure

Compressor

For the compressor output pressure and temperature it can be seen in figures 39 and 40 that this still matches quite well. The trends are captured nicely and the error between the model and the experimental data is not too big as to cause large errors in the other components of the engine. As mentioned earlier there were only a few points experimentally tested along the generator curve, so the lack of data points may cause the error to look bigger than it in fact is (as the data points are connected linearly).

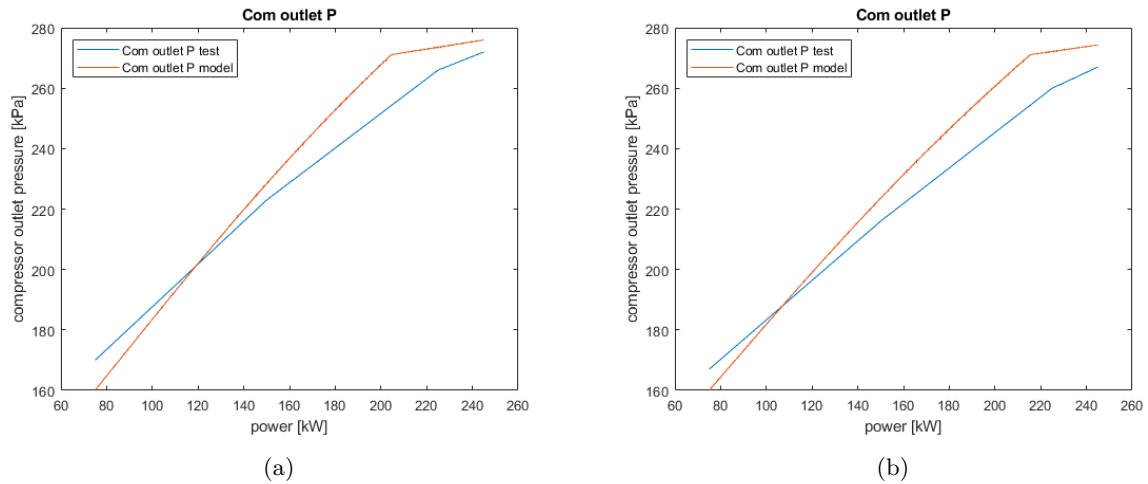
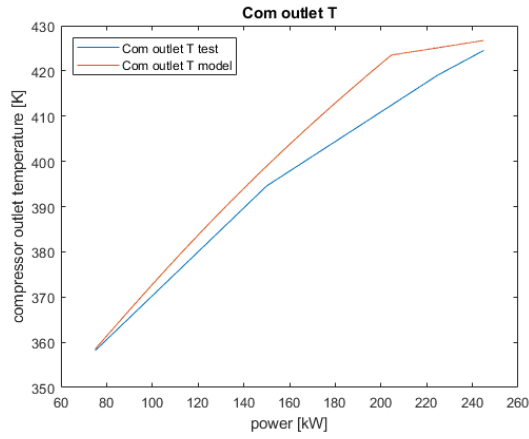
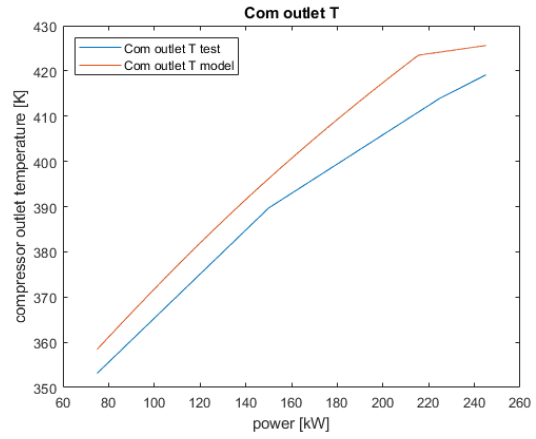


Figure 39: Compressor outlet pressure for low (a) and high (b) back-pressure



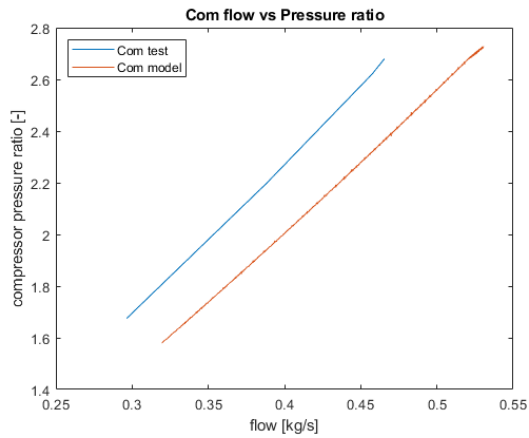
(a)



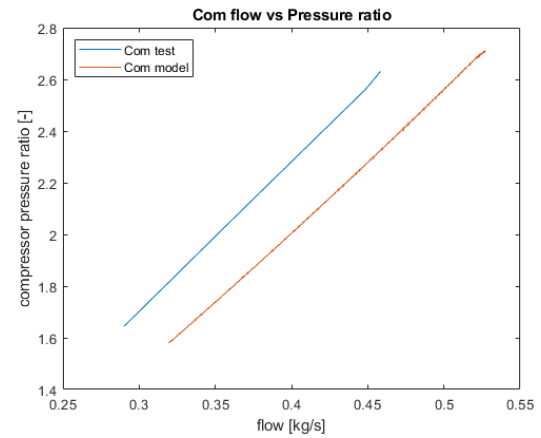
(b)

Figure 40: Compressor outlet temperature for low (a) and high (b) back-pressure

There is still a difference between the measured compressor flow vs pressure ratio and what comes out of the model, but this difference is the same as it was during the calibration. And the shift between these cases and the case with no added back-pressure seems to be the same for the model and the tested engine, see figure 41. In figure 42 it can be seen that the air swallow characteristic of the engine and the compressor matches for these cases as well.



(a)



(b)

Figure 41: Compressor flow vs. pressure ratio for low (a) and high (b) back-pressure

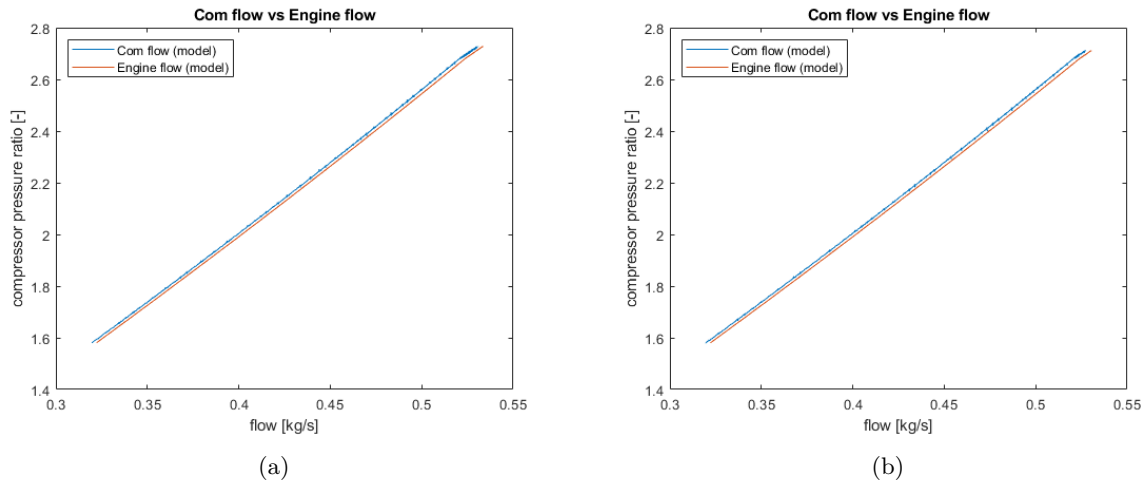


Figure 42: Compressor vs. Engine flow for low (a) and high (b) back-pressure

Inlet receiver

For the inlet receiver it can be seen in figures 43 and 44 that for the cases with increasing back-pressure the model still delivers rather good results, so here too it seems that the calibration was performed in a satisfactory manner. The difference in temperature is still only a couple degrees. The pressure trend seems to be captured nicely with only at part load a larger difference between model and test results, again coming partially from the lack of data points during the tests.

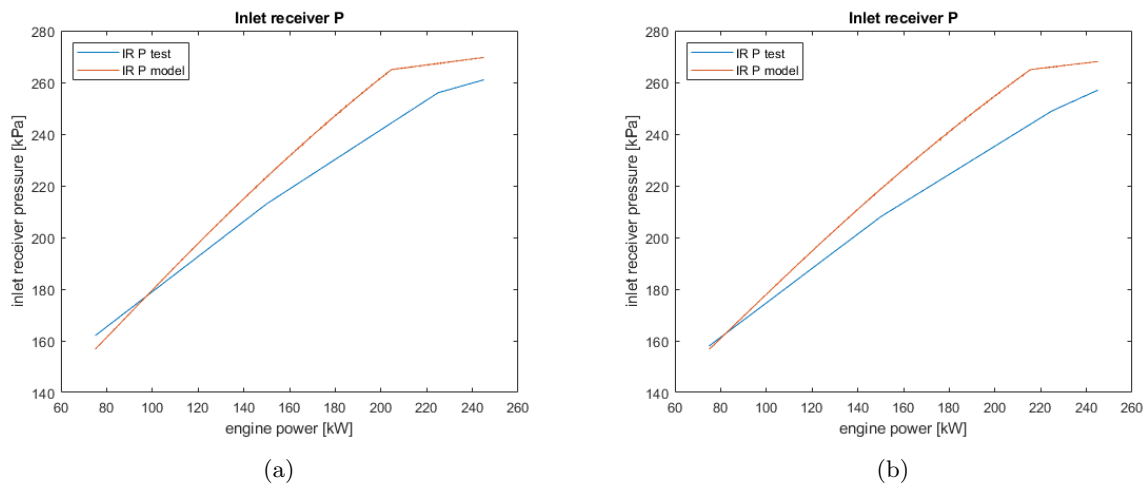


Figure 43: Inlet receiver pressure for low (a) and high (b) back-pressure

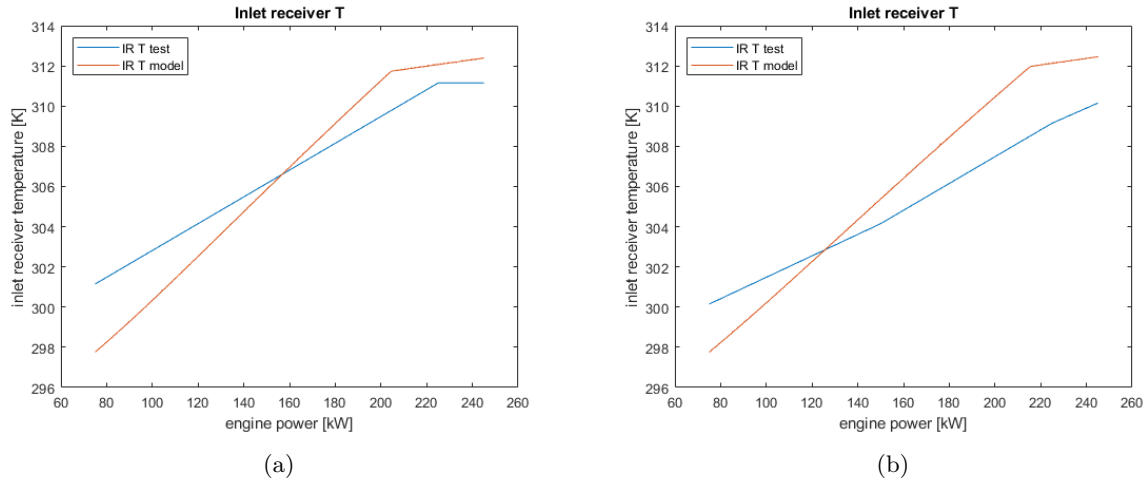


Figure 44: Inlet receiver temperature for low (a) and high (b) back-pressure

In-cylinder: Seiliger parameters

For the Seiliger parameters a similar conclusion can be made as during the calibration of the generator curve. The maximum in-cylinder pressure does not deviate much from the experimental data. And although the heat input is higher than calculated for the tested engine, the turbine inlet temperature is matching really good, so this verifies that these parameters were implemented rather well.

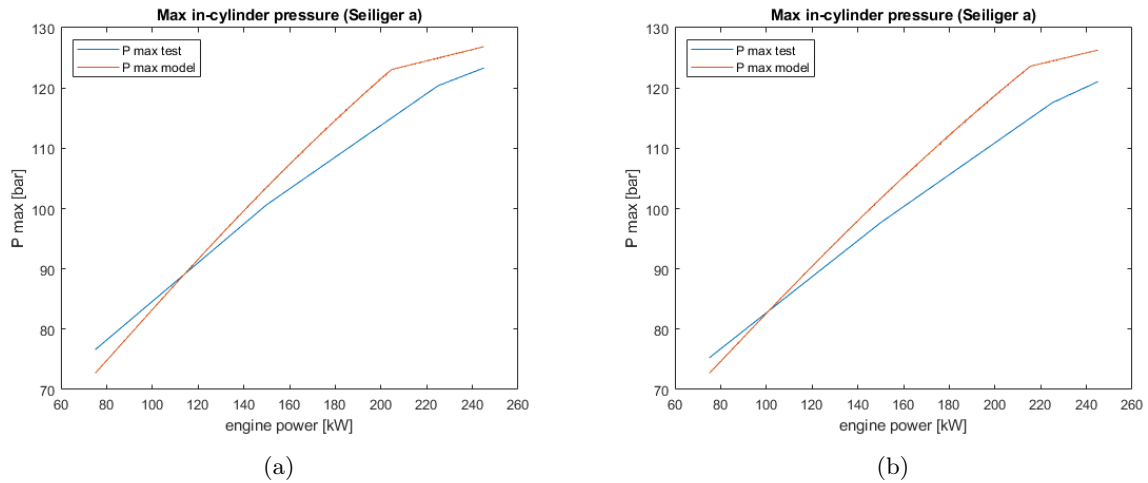


Figure 45: Maximum in-cylinder pressure for low (a) and high (b) back-pressure

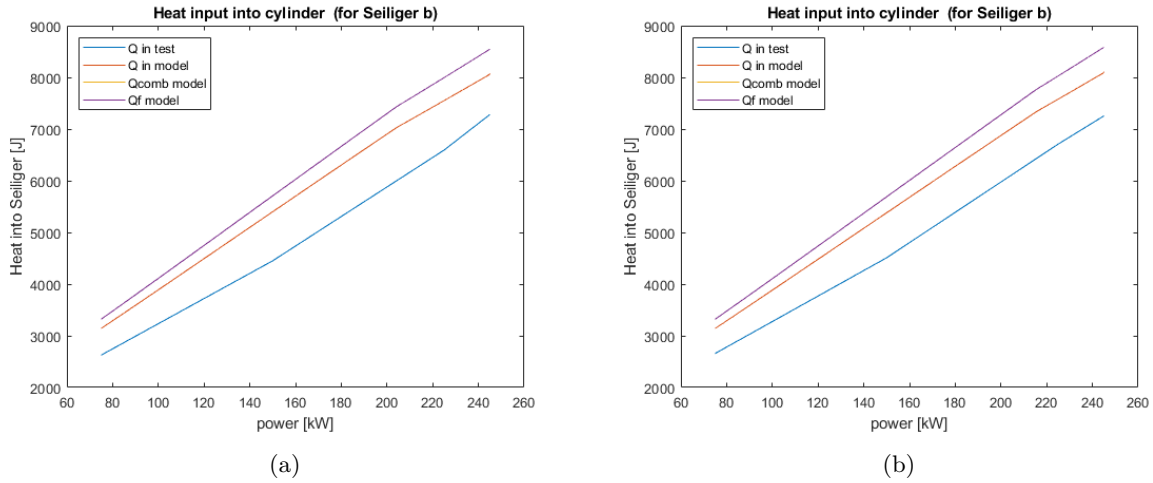


Figure 46: Heat input for Seiliger cycle for low (a) and high (b) back-pressure

Turbine

The problem with the turbine inlet pressure is of course still present in the model, this can be seen in figure 47. The turbine inlet temperature however in figure 48 is matching quite well. The turbine outlet pressure during the experiments with low added back-pressure, see figure 49a, is a little strange as it was measured to be higher at 225 kW than 245 kW, but this was probably a measurement error. But other than that the outlet pressures are pretty similar for these cases. The turbine outlet temperature is also matching well as can be seen in figure 50. All together these results verify the input parameters of the turbine, with the exception of the inlet pressure but this is a reoccurring problem in the model.

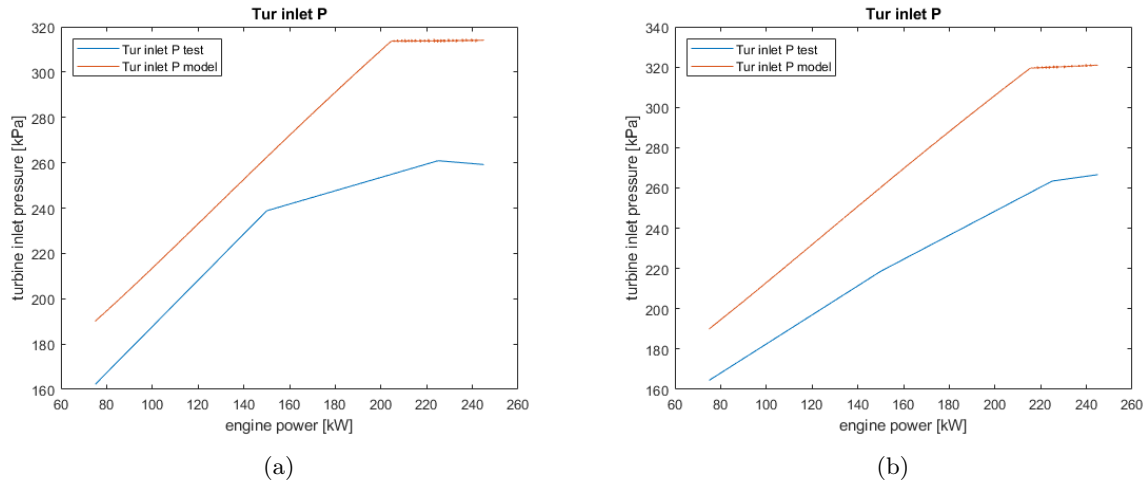
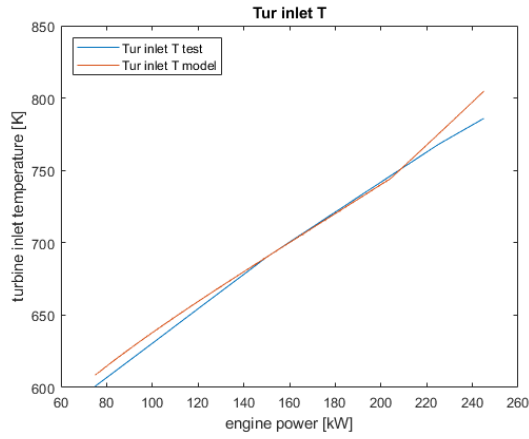
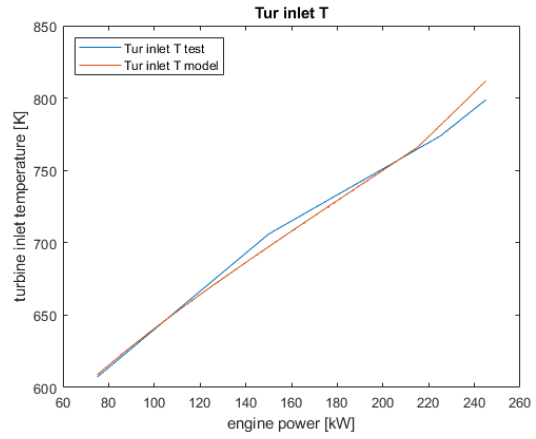


Figure 47: Turbine inlet pressure for low (a) and high (b) back-pressure

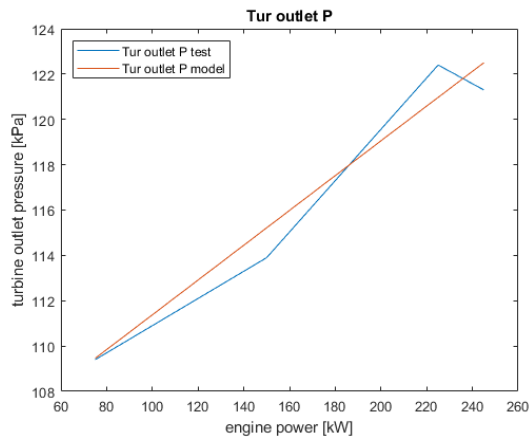


(a)

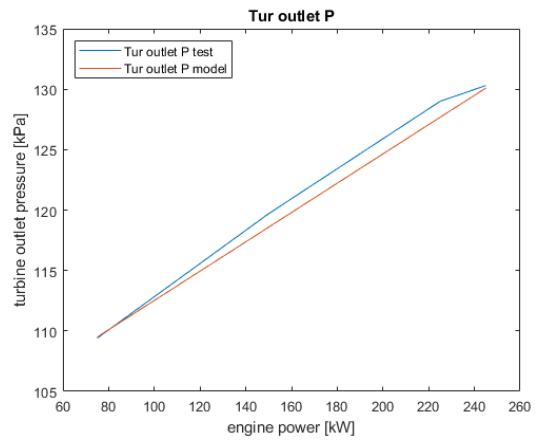


(b)

Figure 48: Turbine inlet temperature for low (a) and high (b) back-pressure

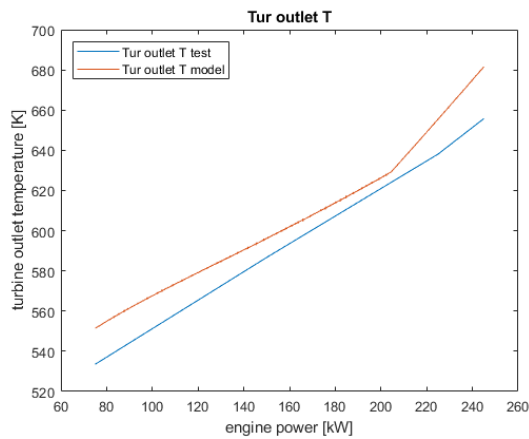


(a)

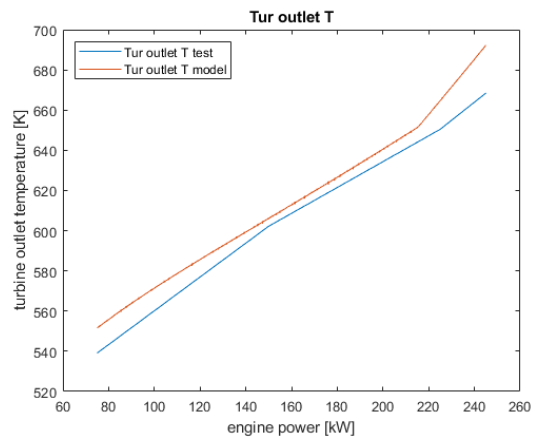


(b)

Figure 49: Turbine outlet pressure for low (a) and high (b) back-pressure



(a)



(b)

Figure 50: Turbine outlet temperature for low (a) and high (b) back-pressure

Due to the turbine inlet pressure issues the output of the model when looking at the turbine flow vs pressure ratio in figure 51 do not match at all. But as stated during the calibration results of the

generator curve, as long as this turbine inlet pressure is so far off, looking at these figures is not very useful.

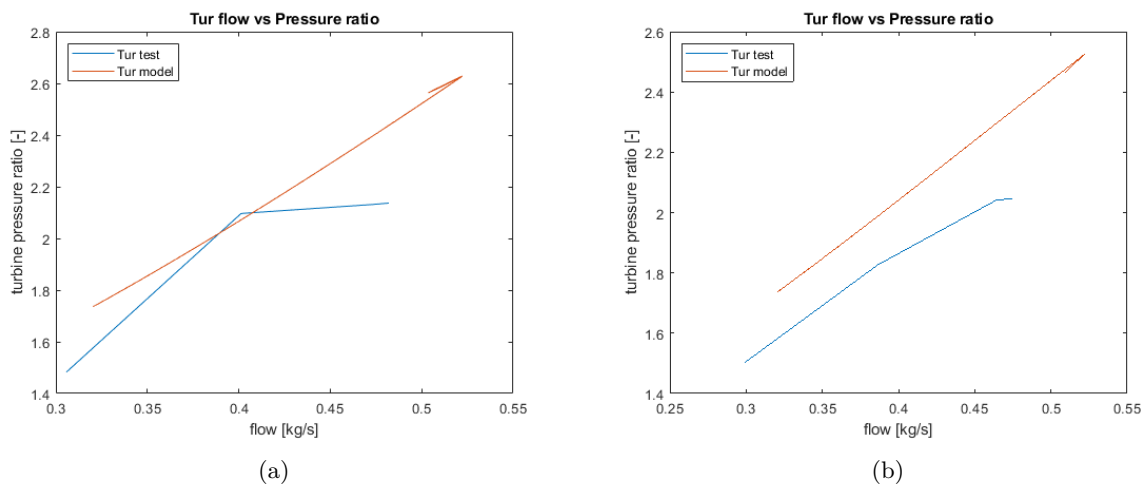


Figure 51: Turbine flow vs. pressure ratio for low (a) and high (b) back-pressure

Fuel

The fuel flows for both cases are too low in the model except at full power, see figure 52. This also causes the SFC and SFGC in figure 53 to be too low. However this issue was also found and explained during the calibration phase, so it is not surprising that this issue is seen here as well.

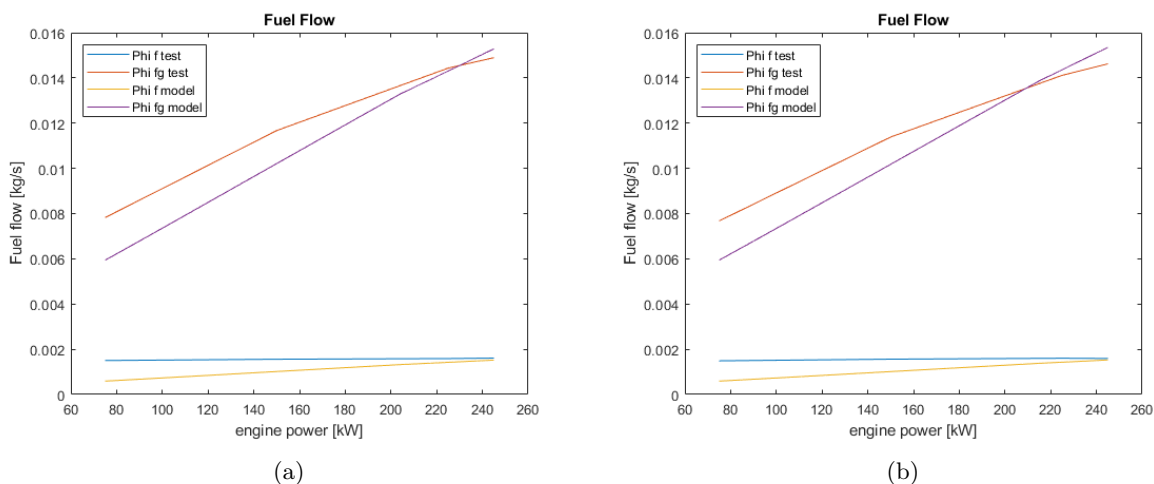


Figure 52: Fuel flows for low (a) and high (b) back-pressure

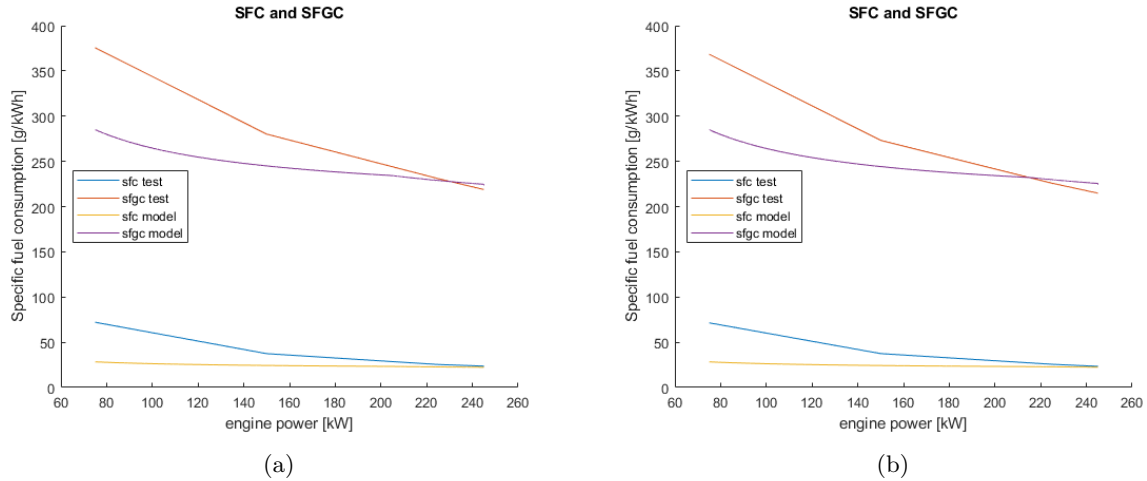


Figure 53: Specific fuel consumption and Specific gaseous fuel consumption for low (a) and high (b) back-pressure

Overall it can be seen that the same issues that were found during the calibration of the model appear here as well. But increasing the back-pressure does not seem to worsen these issues and the other engine parameters are still matching in a satisfactory manner. This concludes the verification part of the matching procedure. Although there are some issues in the model and there is definitely room for improvement, for this thesis the important engine parameters are the temperatures (especially those of the turbine) as these are the limiting factor for the engine when the back-pressure is increased. Since these engine parameters are matched it was chosen to continue with the model as it is. It can now be used to run with higher levels of back-pressure than could be done experimentally. The trends the engine parameters will show after running these test will be the basis for choosing the critical engine parameters when looking at the engine limits. This will be done in chapter 5. Then in chapter 6 the model will be used to test other points in the engine envelope as to get a better inside into the area's in this envelope were the engine limits are reached first.

4 Experiments

In this chapter the experiments performed at Harbin Engineering University will be described. In section 4.1 the experiment set-up will be described, as well as the collected data. This section will also highlight some issues that came up during the experiments and the influence on the collected data. As can be seen in figure 55 the experiments were conducted along the propeller and generator curve. So in section 4.2 the experimental results from the propeller curves will be discussed and in section 4.3 the results from the generator curves. And finally in section 4.4 the most important conclusions from the experimental results will be described.

4.1 Experiment set-up and collected data

In order to study the effects of back-pressure a combination of experiments and simulations will be used. These experiments were already carried out at Harbin Engineering University, on a YC6K dual-fuel, 6 cylinder 300 kW engine. The performance of this engine was measured at different loads and engine speeds along the propeller and generator curves, against three different cases of back-pressure. These three cases were no external back-pressure, low back-pressure and high back-pressure. The back-pressure was controlled by a butterfly valve in the exhaust after the turbine. Figure 54 shows the specifications of the dual-fuel engine and figure 55 shows the operating points of the engine for the three cases of back-pressure. The set-up of the experiment can be seen in figure 56.

Specification	Unit	Value
Engine Type	-	YC 6K
Supply mode of diesel fuel	-	High pressure common rail
Injection mode of gas	-	Single point
Valve overlap	deg	
Rated power	kW	300
Rated speed	rpm	1800
Bore	mm	129
Stroke	mm	155
Length of Connecting Rod	mm	250
Num. of Cylinder	-	6
Compression ratio	-	16.5
Maximum Pressure	bar	
Mean effective pressure	bar	16.45

Figure 54: Engine specification

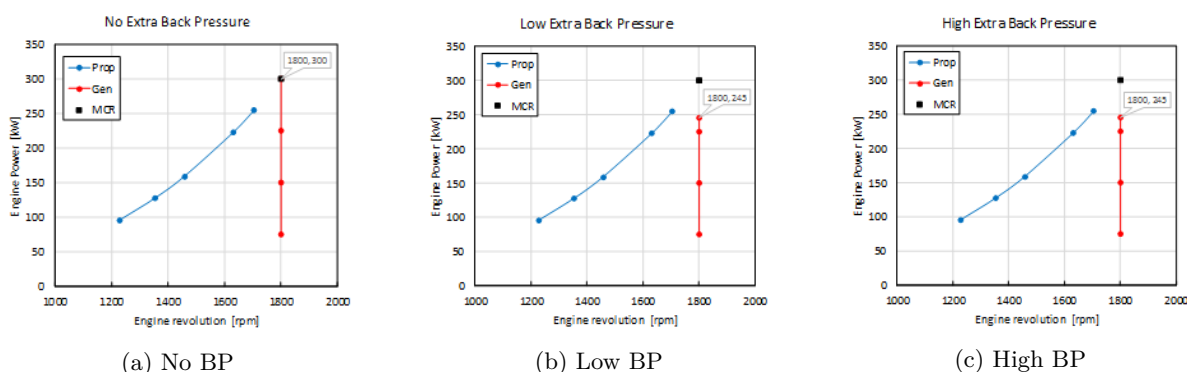


Figure 55: Operating points

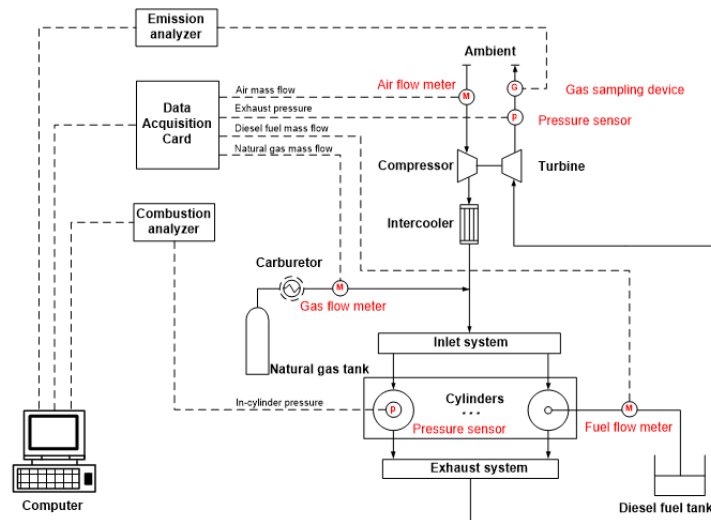


Figure 56: Experiment setup

At each of the operating points, for all cases of back-pressure, engine parameters were measured such as pressures and temperatures (both within the cylinder and of engine components), air-flow and fuel-flow. Also the composition of the exhaust gas was measured. The in-cylinder pressure data was recorded over 200 cycles at each point and saved using a crank angle scale and for each cycle the combustion data was recorded as well.

During the experiments some issues were noticed which require attention. The most important ones are summarised below.

- The position of the butterfly valve could be adjusted manually (on the housing) and remotely (electric actuator). It was not possible in the control room to monitor the exact open/close position of the valve, nor to reproduce this position at a later stage. The adjustment of the valve position is by open/close commands. During the experiments it was decided to establish measurement series based on one specific position of the back-pressure valve. The valve position was established by defining a back-pressure at a certain engine condition, which meant that at lower loads the back-pressure had a lower absolute level.
- The engine seems relatively insensitive to back-pressure: small changes in temperatures, pressures and emissions are observed. The inlet receiver temperature did not change at all with back-pressure, so no back-flow observed. However, due to the fact that the back-pressure valve was set to one specific position (see the point above), some of the operating points had pretty similar conditions. For instance for the lowest point on the propeller curve, the back-pressure the engine experienced was almost atmospheric pressure even with the back-pressure valve in use. This means that the results for this point were almost equal to the case with no back-pressure.
- Even with an open exhaust valve (which is the no back-pressure setting) the engine had an absolute back-pressure of 1.15 bar at full load. That means an over-pressure of 1.5 meter water column (mwc) related to ambient pressure, which is quite high related to literature. This over-pressure may be caused by the fact that the exhaust pipe had a long length and that a particle filter was installed in the system. This back-pressure at full load may already be higher than the allowable conditions given by the engine manufacturer. During the experiment, an extra back-pressure of 1.5 mwc was established related to the nominal conditions, resulting in a test condition with a maximal back-pressure of 1.3 bar (absolute pressure).
- There was a constituency of 7 % hydrogen in the natural gas. That is a considerable amount, not always found in benchmark natural gas compositions.
- The details of the valve timing were not specified. This is a very relevant feature for the analysis of the experiment and the possible verification in the model. On the one hand: there was hardly any influence of back-pressure on charge pressure, no visible back-flow so the valve overlap may be quite small. On the other hand: there were methane emissions, so there may have been some

valve overlap. Although the methane emissions could also come from incomplete combustion of the natural gas.

4.2 Experimental results - Propeller curve

In this section the experimental results from the tests along the propeller curve will be discussed for the three cases of back-pressure. In order to see what effect the back-pressure has on the inlet side of the engine the compressor outlet pressure and temperature as well as the inlet receiver pressure and temperature are being looked at. For the effect on the outlet side the exhaust receiver and the turbine outlet temperatures and pressures are used. As the back-pressure increases the engine has to work harder to expel the combustion gasses (3)(5)(20). This will have an influence on the fuel consumption, which will be explained in section 4.2.3. Then the effects on the emissions from the engine will be discussed.

Three important notes need to be made when looking at the figures in this section:

- As the back-pressure is increased, the engine can no longer run at the nominal point of the engine (300 kW at 1800 rpm). This is due to the fact that the limits of the engine are reached at an earlier point. The limit was the maximum allowable temperature of 650 degrees Celsius before the turbine. That is why the lines for the cases with back-pressure stop at a power of 254 kW.
- As explained in section 4.1, due to the way the experiments were conducted, at lower engine powers the absolute back-pressure the engine experiences is almost equal to ambient pressure. So part load conditions always had less absolute back-pressure then at full load. That is why some of the lines in the figures converge towards the low power range.
- The engine had an absolute back-pressure of 1.15 bar at full load with the exhaust valve open (this is the no back-pressure test). The amount of absolute back-pressure for the 'high' case was 1.3 bar and for the 'low' case 1.23 bar at full load. This means that the difference in back-pressure between the cases is quite low, so therefore the difference in results might be small.

4.2.1 Inlet side

As the back-pressure increases the pressure in the exhaust will increase, leading to a lower pressure ratio across the turbine. Because of this lower pressure ratio the turbocharger speed will decrease and therefore the charge pressure build up by the compressor will be lower. This in term will lead to a lower inlet receiver pressure (3)(20). Figure 57 shows the compressor outlet pressure and temperature for the 3 cases of back-pressure. In the first figure the pressure drop, as back-pressure increases, can indeed be seen. The second figure shows that the compressor outlet temperature also decreases as back-pressure increases, although only by a few degrees. Figure 57a also shows that at a certain engine power the increase in compressor outlet pressure becomes less. This is the effect of the waste-gate, which by-passes a part of the flow around the turbine (22).

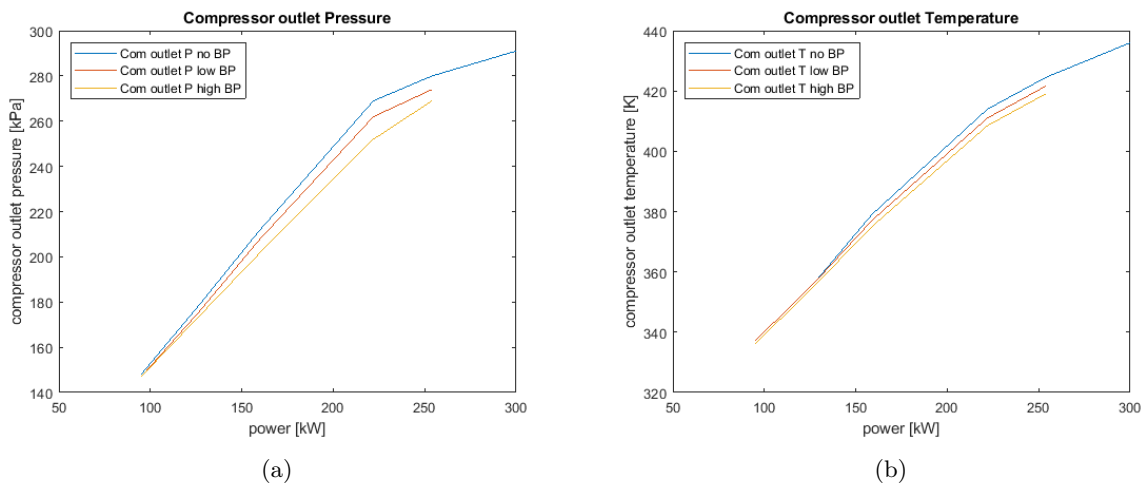


Figure 57: Compressor outlet pressure (a) and temperature (b) for 3 cases of back-pressure

Figure 58 shows the inlet receiver pressure and temperature. The higher the back-pressure the lower the inlet receiver pressure, as was expected from the literature (3)(20). Looking at the temperature the measured difference between the 3 cases is only 1 degree, so there is no real change here.

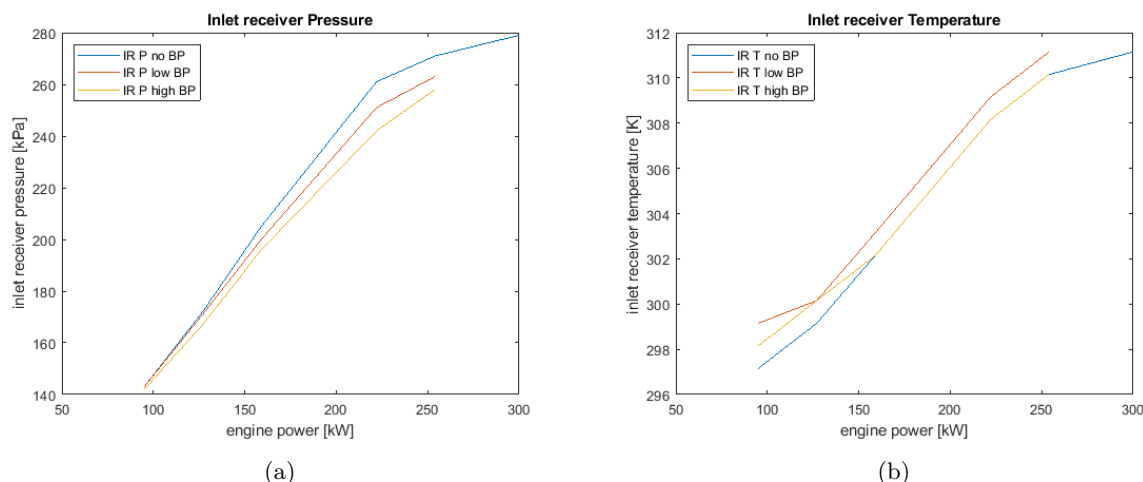


Figure 58: Inlet receiver pressure (a) and temperature (b) for 3 cases of back-pressure

4.2.2 Exhaust side

As the (back-)pressure in the exhaust increases, so will the exhaust receiver temperature. This can be seen in figure 59b. Here too the change in temperature as the back-pressure is increased is very small. From literature it is known that as back-pressure increases the engine has to work harder to expel the combustion gasses (3)(5)(20). This would mean that at the same load more fuel needs to be combusted if the back-pressure is increased. If more fuel is combusted the exhaust receiver temperature will rise as well. However, as will be show in section 4.2.3, the fuel consumption for the tested engine does not behave like the literature suggests. So the rise in exhaust receiver temperature is probably only due to the higher pressure in the exhaust side of the engine, which increases the thermal loading.

Looking at the pressures in the exhaust side, it can be seen that the exhaust receiver pressure (figure 59a) remains almost constant for all cases of back-pressure. As mentioned before the flattening of the pressure curve at a certain engine power is due to the fact that at this power the waste-gate becomes active and by-passes part of the flow around the turbine (22). The turbine outlet pressure (figure 60a) does increase with increasing back-pressure, which is logical as the valve to control the back-pressure is installed after the turbine. This figure also shows that the applied back-pressure is indeed not constant for each tested case. Together with the (almost) constant pressure in the exhaust receiver, it follows that the pressure ratio across the turbine will decrease as the back-pressure is increased, which was expected from the literature. The turbine outlet temperature (figure 60b) also increases when the back-pressure is increased. This is due to the fact that the pressure at the turbine outlet is higher and the temperature of the gas going into the turbine is higher as well, so thermal loading is increased.

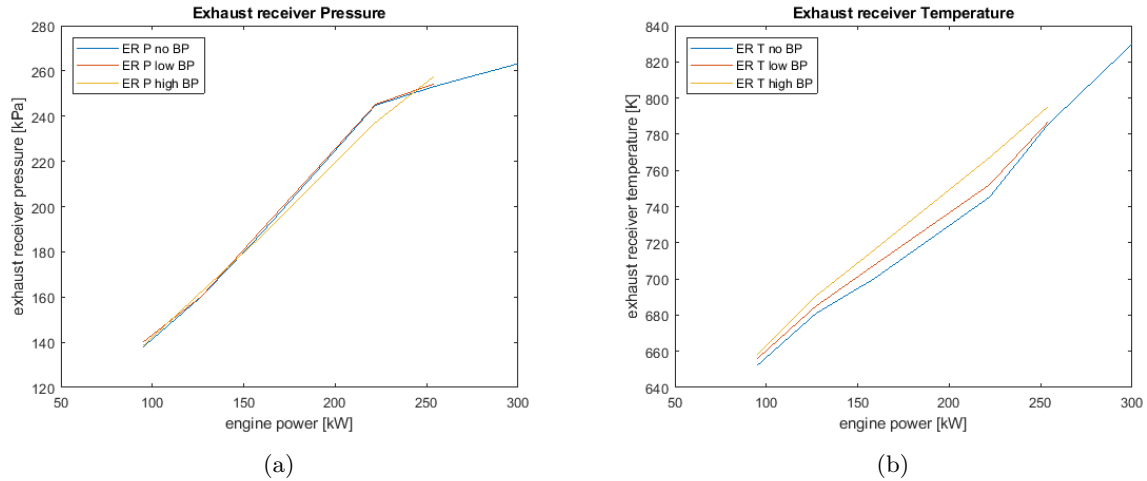


Figure 59: Exhaust receiver pressure (a) and temperature (b) for 3 cases of back-pressure

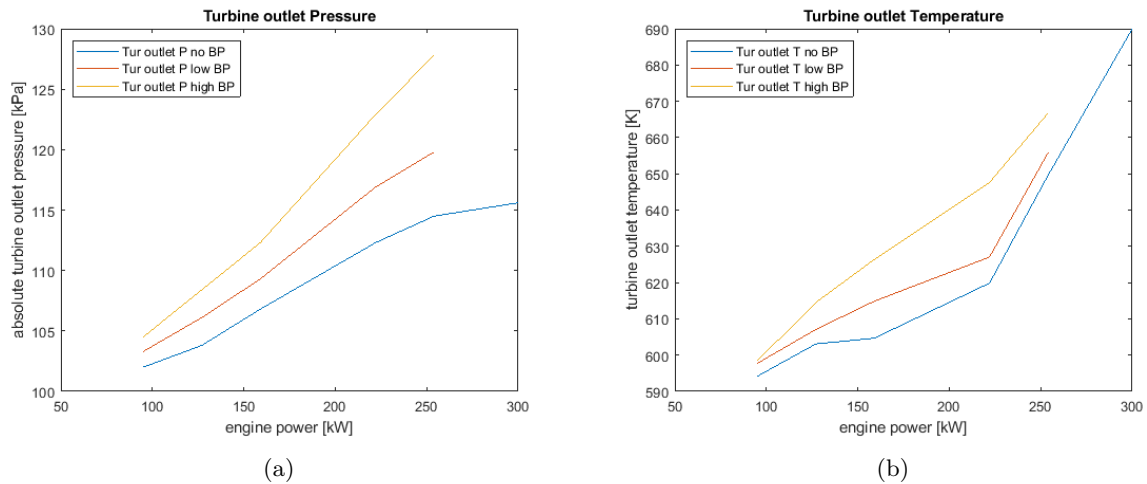


Figure 60: Absolute turbine outlet pressure (a) and temperature (b) for 3 cases of back-pressure

Overall when looking the inlet and outlet side, the recorded changes in pressures and temperatures are small. So it seems that this dual-fuel engine is relatively insensitive to back-pressure. But the engine limits, especially the maximal turbine inlet temperature, were reached rather quick, so relatively not a lot of extra added back-pressure could be applied to the tested engine. So therefore only small changes in outcome were to be expected. But the pressures and temperatures do behave (for the most part) as the literature suggested. Another thing that was noticed was that the pressure difference between the inlet side and the outlet side was very small, even for the no back-pressure case. So it seems that there is a risk of back-flow for this engine (especially if a large valve overlap would be chosen).

4.2.3 Fuel consumption

When the pressure in the exhaust system increases the engine needs to work harder to expel the combustion gasses from the cylinder. The literature so far suggests that in order to keep the same power output the fuel consumption needs to increase when the back-pressure increases (3)(5)(20). But as can be seen from figure 61 this is not true for the tested dual-fuel engine. The pilot fuel energy flow (figure 61a) is lower for both cases with added back-pressure. And for the gaseous fuel energy flow (figure 61b) there is only an increase at part load conditions for the engine. So it seems that the engine has a lower efficiency at part load.

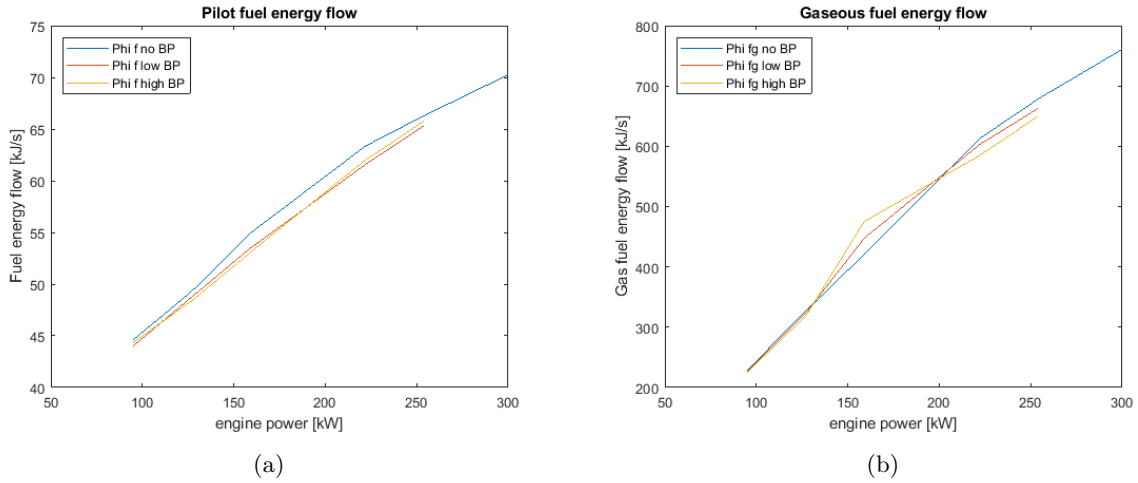


Figure 61: Pilot fuel energy flow (a) and gaseous fuel energy flow (b) for 3 cases of back-pressure

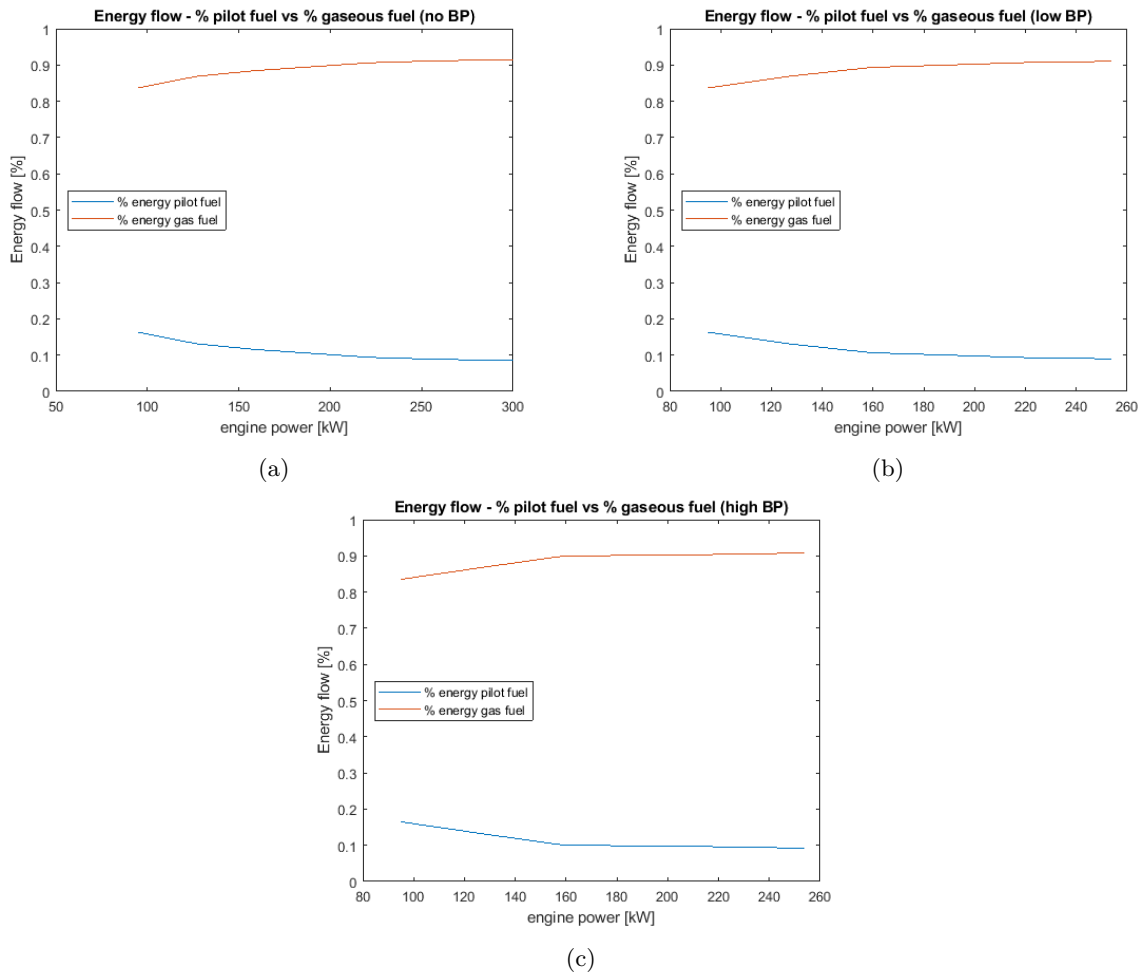


Figure 62: Pilot fuel energy vs Gaseous fuel energy for 3 cases of back-pressure

A similar trend as with the fuel energy flows can be seen when looking at the specific fuel consumption (SFC) and the specific fuel gas consumption (SFGC), see figure 63. Figure 63b shows the SFGC. It can be seen that for all cases the SFGC first increases, but at the high-power range it decreases again. So again it seems that the efficiency at part load conditions is lower for this engine. But, similar to the gaseous fuel energy flow, only at part load the SFGC is higher with increased back-pressure. So it seems that increasing the back-pressure leads to a better combustion of the gaseous fuel in the low- and high-

power range of the engine and a worse efficiency at part load conditions, which is contradictory to what was expected. What might be an explanation is that indeed the efficiency is lower at part load and with increasing back-pressure this effect becomes worse (therefore an increase in SFGC here). But at high loads the thermal loading of the engine increases, which might improve the combustion and lower the SFGC again.

The SFC (figure 63a) is higher in the low-power range, which is due to the fact that in this range a very lean mixture of air and gaseous fuel is fed to the engine which is hard to burn. This means that more pilot fuel is needed to combust this mixture (9)(10)(12)(13). This can also be seen in figure 62 where the % of energy coming from the pilot fuel and the gaseous fuel is shown for the 3 cases. It can be seen that in the high load region around 10% of the energy comes from the pilot fuel, but this increases in the low load region.

It was noticed that this 10% of energy coming from the pilot fuel is quite high, and again as the back-pressure is increased, the SFC is somewhat lower then the case with no back-pressure. This could indicate that the fuel calibration of the engine (which had only recently been converted to dual-fuel) might not have been perfect, which might also be an explanation for the improving efficiency with added back-pressure.

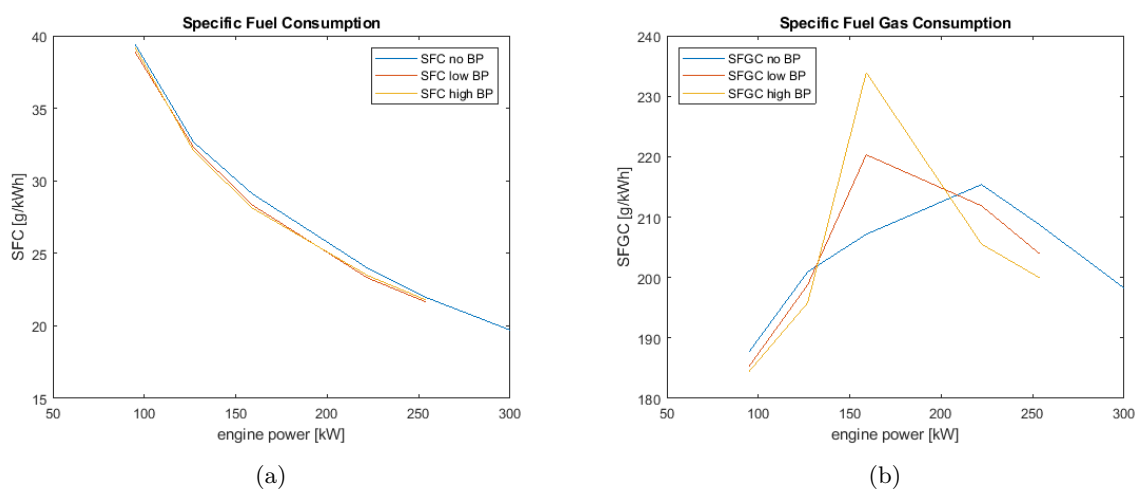


Figure 63: Specific fuel consumption (a) and specific fuel gas consumption (b) for 3 cases of back-pressure

4.2.4 Emissions

During the experiments the emissions were recorded as well. The results are summarised below. The pollutant emissions are given in both ppm and g/kWh.

O_2

As the engine power increases more fuel needs to be burned and therefore more air is needed. This can be seen in figure 64a where the incoming air flow is shown. The air flow for the cases with back-pressure is slightly lower. This happens because as the back-pressure increases in the exhaust, the pressure ratio across the turbine becomes smaller which decreases the turbocharger speed. This in term will lead to a lower compressor speed/efficiency and thus less air is put into the engine. Figure 64b show the amount of O_2 in the exhaust. Even though more air is coming into the engine as the engine power increases, the amount of oxygen in the exhaust goes down. So more oxygen is being used in the cylinder, which means that there is a better combustion at high loads. This is true for all tested cases. It is also clear that as the back-pressure is increased the amount of O_2 in the exhaust goes down. This reduction in O_2 can not only come from the fact that the incoming air and fuel flow (see section 4.2.3) is lower for these cases, as this difference is very small (especially in the low load region). So these results show an indication of improving combustion as back-pressure increases.

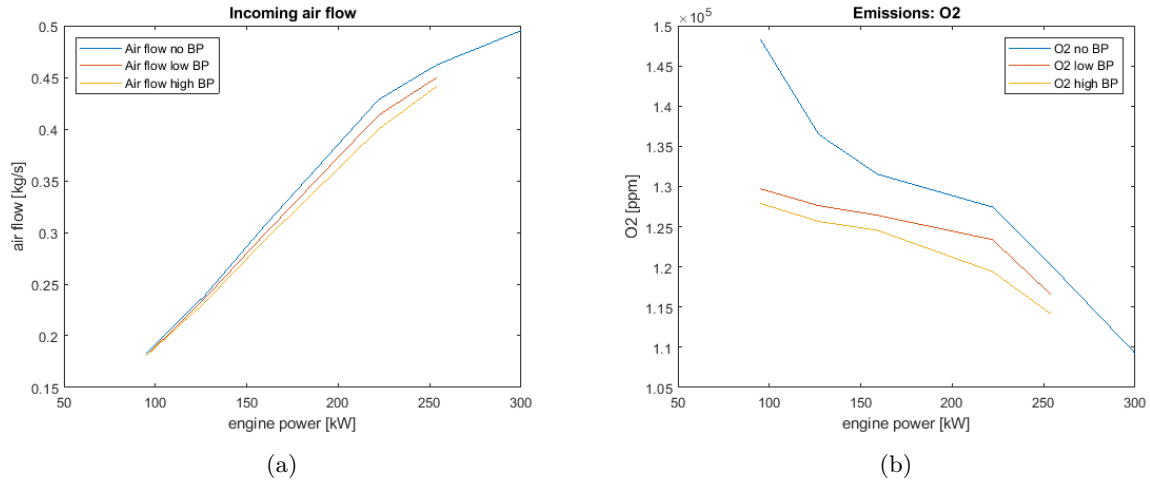


Figure 64: Incoming air flow (a) and O2 emissions (b) for 3 cases of back-pressure

CO

The amount of CO created by the engine is dependant on the amount of unburned gaseous fuel and the mixing temperature (12). At low loads there is bad fuel utilization as a very lean mixture of air and fuel is fed into the engine which is hard and slow to burn (9)(10)(12)(13). So therefore there are more CO emissions here than at full load, see figure 65. For the no back-pressure case the emissions at part load conditions are higher, which might be an effect of increased SFGC in this range. But as the load is increased the gaseous fuel utilization is improved and thus the CO emissions go down.

When comparing the 3 different cases, it can be seen that as back-pressure is increased, the amount of CO is higher at low loads, but improves quickly as the load increases. And the higher the back-pressure, the decrease in CO emissions is higher too. Again showing that there might be an improvement of combustion as the back-pressure is increased.

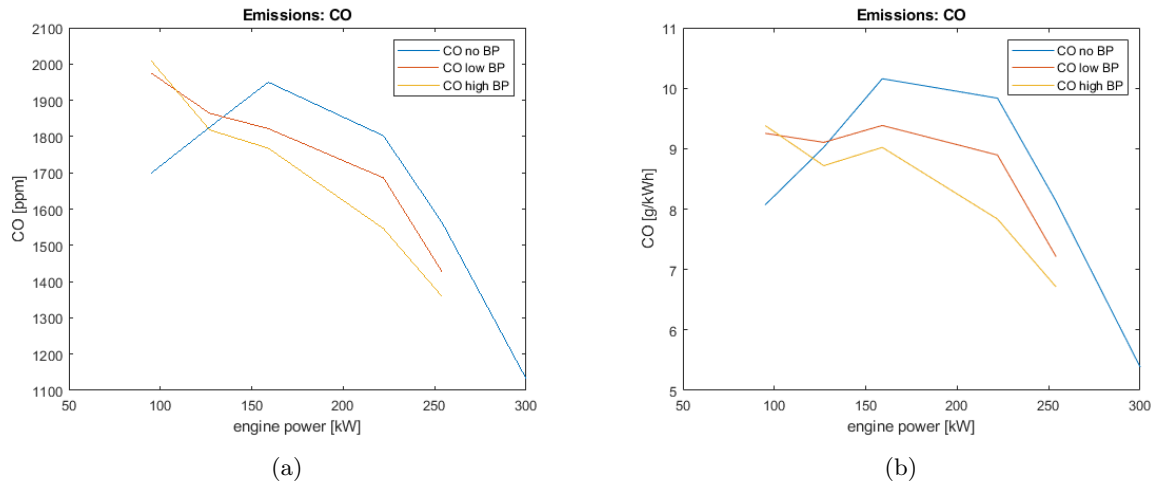


Figure 65: CO emissions in ppm (a) and g/kWh (b) for 3 cases of back-pressure

CO₂

If more fuel is combusted the amount of CO₂ will rise as more oxygen reacts with the carbon in the fuel. So with increasing engine power the amount of CO₂ rises as more fuel is combusted, see figure 66. In section 4.2.3 it was shown that the fuel flow for the cases with back-pressure is almost always lower than the case with no back-pressure. However, the amount of CO₂ is increased as the back-pressure is increased. So again the results are showing an improvement in combustion as the back-pressure rises.

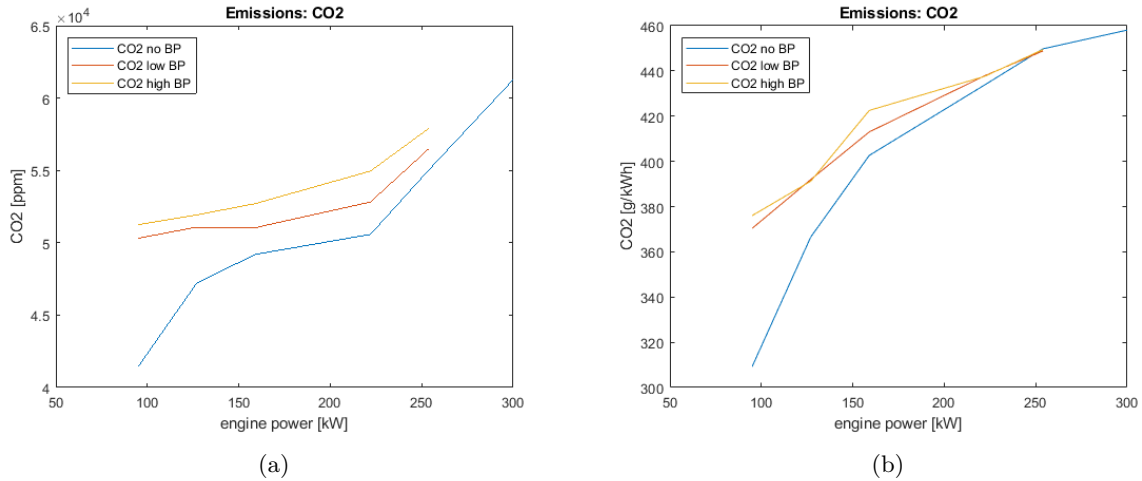


Figure 66: CO₂ emissions in ppm (a) and g/kWh (b) for 3 cases of back-pressure

NO_x

The formation of NO_x is due to two main reasons: a high oxygen concentration and/or a high charge temperature (12). At low loads there is a higher oxygen concentration so more NO_x will be formed. As the load increases the combustion efficiency will go up and there will be less oxygen left leading to lower NO_x emissions. This trend can be seen in figure 67 for all 3 cases. As the back-pressure increases the temperatures on the inlet receiver are (almost) equal, see figure 58b, so no real change in charge temperature. However, the temperatures in the exhaust increase with increasing back-pressure (figures 59b and 60b). Chemical reactions can still take place here and therefore the NO_x formation increases for the cases with back-pressure.

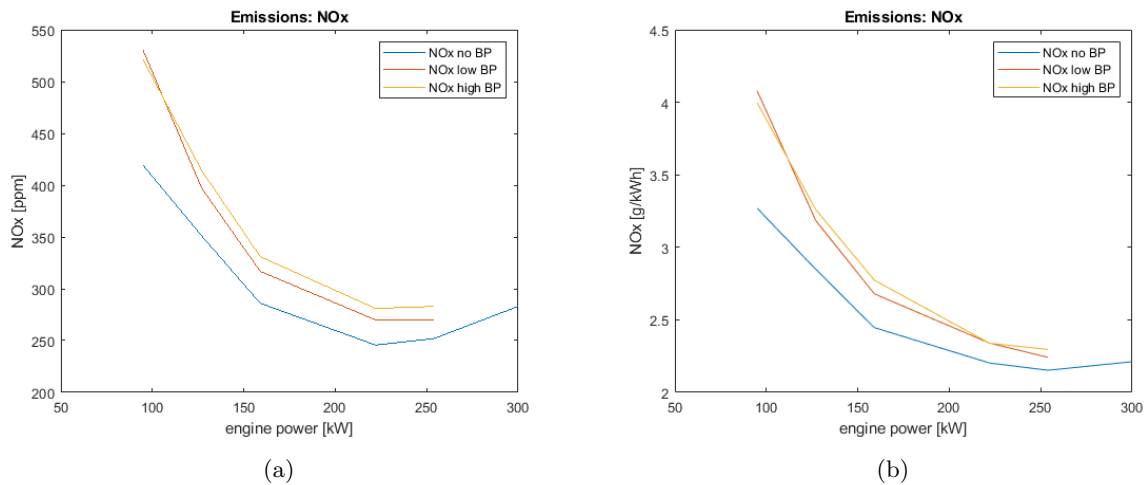


Figure 67: NO_x emissions in ppm (a) and g/kWh (b) for 3 cases of back-pressure

Unburned hydrocarbons

The unburned hydrocarbons (UHC) are a measure of how much of the gaseous fuel slips through the engine without being burned. In the low load region the combustion efficiency is lower and therefore the UHC emissions are higher here than at full power (9)(10)(12)(13). This can be seen in figure 68. The figure also clearly shows that at part load the UHC emissions are much higher, indicating that the combustion efficiency here is lower, similar to what was found for the SFGC in figure 63b. As the load increases more, so does the combustion efficiency and at a certain point the UHC emissions will go down. Figure 68 also shows that the UHC emissions decrease with increasing back-pressure (with the exception of the lowest tested engine power). This too suggests that the combustion is improved at higher back-pressures as the decrease in gaseous fuel flow is very small (at part load the gaseous fuel flow is in fact higher while UHC emissions remains lower).

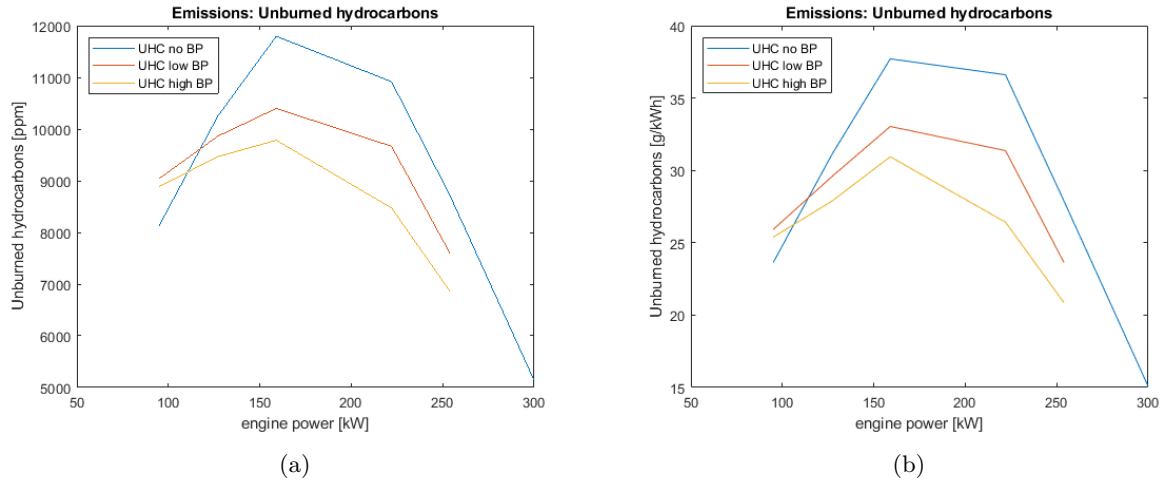


Figure 68: CO emissions in ppm (a) and g/kWh (b) for 3 cases of back-pressure

4.3 Experimental results - Generator curve

In this section the experimental results from the generator curve will be discussed. The same engine parameters as in section 4.2 for the propeller curve will be shown.

As in the previous section the following three notes need to be made when looking at the figures in this section:

- As the back-pressure is increased, the engine can no longer run at the nominal point of the engine (300 kW at 1800 rpm). This is due to the fact that the limits of the engine are reached at an earlier point. The limit was the maximum allowable temperature of 650 degrees Celsius before the turbine. That is why the lines for the cases with back-pressure stop at a power of 245 kW. (For the propeller curve this limit was reached at 254 kW, but the limit is now reached at an earlier point due to the higher rpm of the engine)
- As explained in section 4.1, due to the way the experiments were conducted, at lower engine powers the absolute back-pressure the engine experiences is lower. And the lower the engine power, the less difference in absolute back-pressure between the 3 tested cases. That is why some of the lines in the figures converge towards the low power range.
- The engine had an absolute back-pressure of 1.15 bar at full load with the exhaust valve open (this is the no back-pressure test). The amount of absolute back-pressure for the 'high' case was 1.3 bar and for the 'low' case 1.23 bar at full load. This means that the difference in back-pressure between the cases is quite low, so therefore the difference in results might be small.

4.3.1 Inlet side

As mentioned before in section 4.2.1 with increasing back-pressure the turbine becomes less efficient because the pressure ratio across the turbine becomes smaller. This leads to a lower turbine speed and this in turn leads to a lower compressor speed, which means that less charge pressure can be built up. This effect can indeed be seen in figure 69a, more clearly than in figure 57a in section 4.2.1. The lower compressor outlet pressure leads to a lower inlet receiver pressure, see figure 70a. Looking at the temperatures on the inlet side, the compressor outlet temperature (figure 69b) drops with increasing back-pressure, although this effect is mostly showing for the case with high back-pressure. This lower temperature is an effect of the lower pressure coming out of the compressor. For the inlet receiver there is no real change in temperature, similar to the results from the propeller curve.

Comparing these results to the results in section 4.2.1, it can be seen that the same effects happen with increasing back-pressure, which complies with previous research (3)(20). The only difference is that the pressures and temperatures at lower engine loads are higher for the generator curve, which is logical as the engine now runs at a higher rpm.

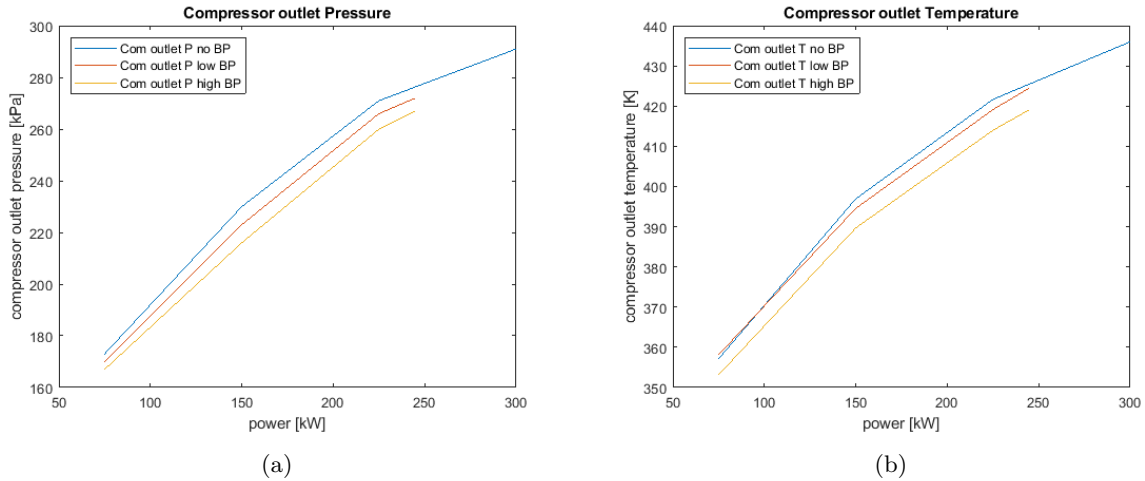


Figure 69: Compressor outlet pressure (a) and temperature (b) for 3 cases of back-pressure

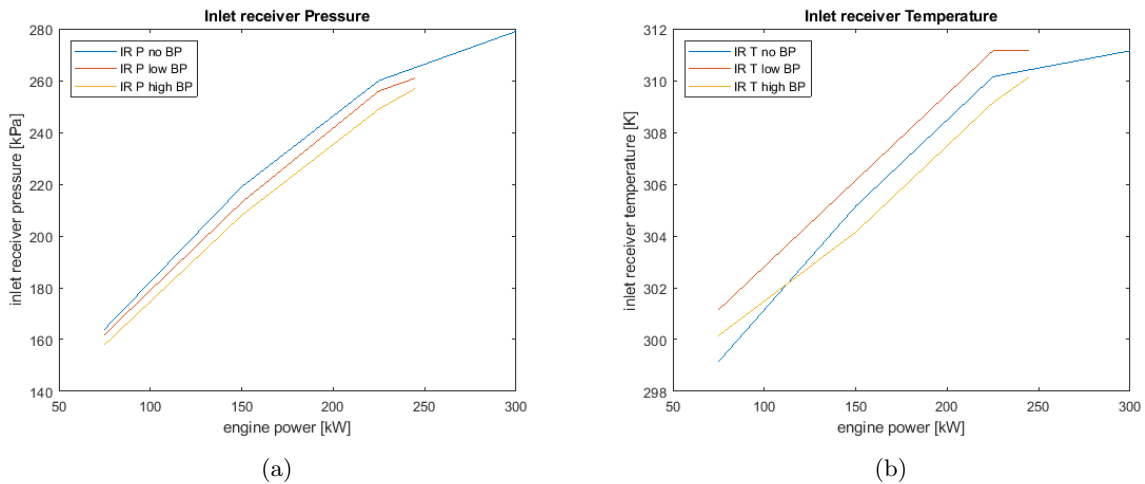


Figure 70: Inlet receiver pressure (a) and temperature (b) for 3 cases of back-pressure

4.3.2 Exhaust side

In figure 59a in section 4.2.2 it was shown that the exhaust receiver pressure did not change with increasing back-pressure. In figure 71a it can be seen that the exhaust receiver pressure for the 3 cases follow the similar trend, being lower at lower engine power and increasing until the waste-gate becomes active. This is similar to what was found for the propeller curve and makes sense as with increasing power the engine works harder which increases the pressures in the system. However the difference in figure 71a between the 3 tested cases of back-pressure is quite inconsistent. At the lowest tested engine power the exhaust receiver pressures for the cases with added back-pressure are (almost) the same, this is can be explained as the turbine outlet pressure for these cases at this point are (almost) the same (see figure 72a). But both are lower than the case with no added back-pressure which seems contradictory, as with a higher pressure in the exhaust system one would expect the pressure to be higher everywhere. This is true for higher engine powers, but here the pressure for the case with low back-pressure is higher then the other 2 cases. Also figure 71a shows that for the low back-pressure case the back-pressure at 245kW is slightly lower than just before that point, which is strange. So it seems that there might have been some inconsistencies in the measurements here during the experiments.

Looking at the temperatures, both the exhaust receiver and turbine outlet temperatures increase with increasing back-pressure. This complies with what was found for the propeller curve and with earlier research (3)(20), that with increasing back-pressure the engine needs to work harder to expel the combustion gasses and together with the increased pressure in the system this increases the temperatures and therefore the thermal loading.

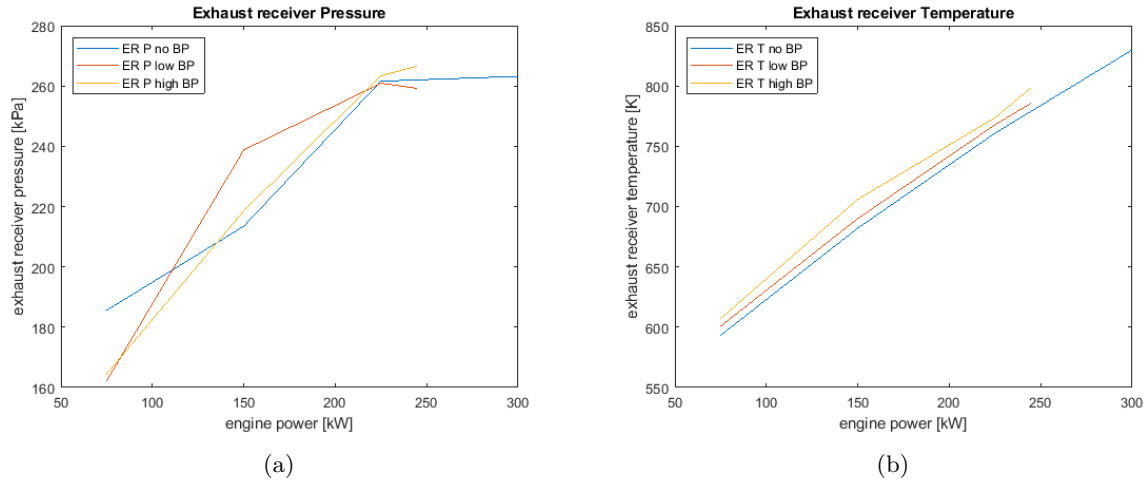


Figure 71: Exhaust receiver pressure (a) and temperature (b) for 3 cases of back-pressure

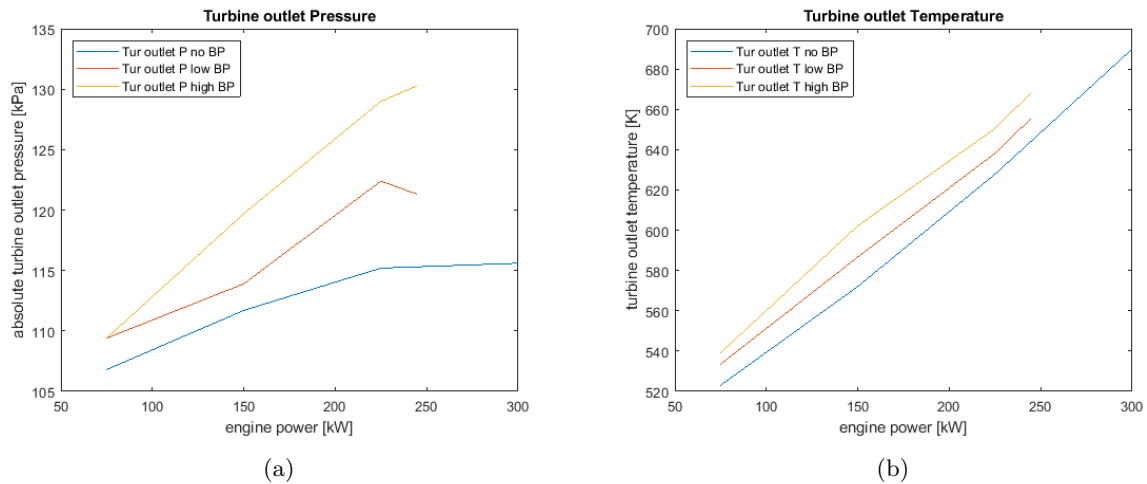


Figure 72: Absolute turbine outlet pressure (a) and temperature (b) for 3 cases of back-pressure

All together the pressures and temperatures for the generator curve behave similarly to what was found for the propeller curve and complies with previous research (3)(5)(20), although the exhaust receiver pressure is deviating slightly. Comparing inlet and outlet pressures it can be seen that the difference is very small, sometimes the pressure was measured to be higher at the outlet side. So for the generator curve too there is a risk of back-flow for this engine.

4.3.3 Fuel consumption

For the fuel energy flow, figure 73, the same conclusion can be made as for the propeller curve. Even though the literature suggest that with increasing back-pressure the fuel flow increases because the engine needs to work harder to expel the combustion gasses (3)(5)(20), for the tested dual-fuel engine this is not true. Both the pilot and gaseous fuel energy flow decrease with increasing back-pressure, although for the pilot fuel energy flow the difference is almost negligible. This can also be seen in figure 75a, which shows the SFC, where there is no real change between the tested cases. This figure does again show the trend that at low load more pilot fuel is being used, as was the case for the propeller curve. Comparing this SFC with the one for the propeller curve, it can be seen that the SFC for the generator curve is higher. So at this high constant rpm the total efficiency is lower.

Looking at the energy flow distribution between the pilot and gaseous fuel, figure 74, the same trend as for the propeller curve is found. At higher power the amount of energy coming from the pilot fuel is around 10 %, but this increases for the lower engine loads. This complies with what was found earlier that more pilot fuel is needed to start the combustion of the gaseous fuel in the lower load range.

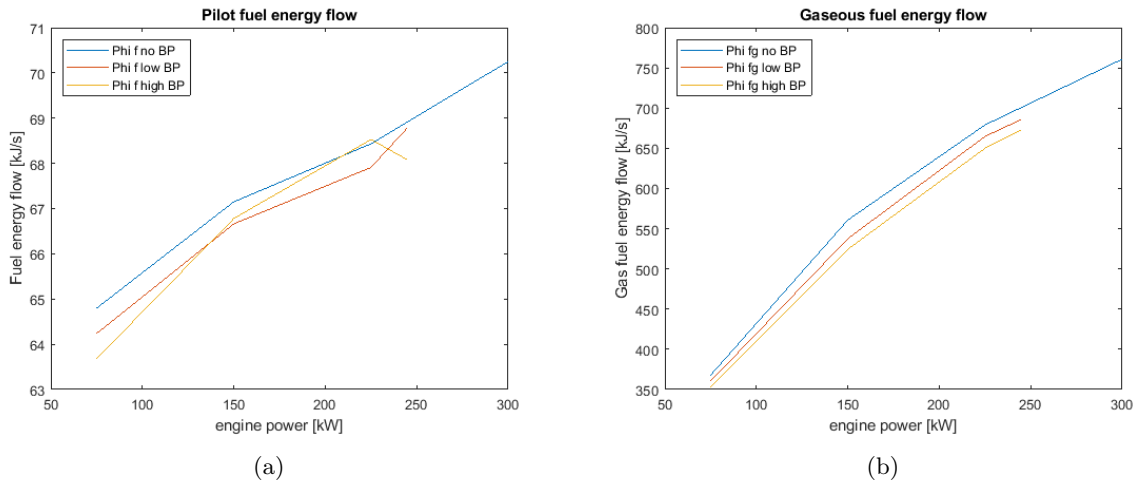


Figure 73: Pilot fuel energy flow (a) and gaseous fuel energy flow (b) for 3 cases of back-pressure

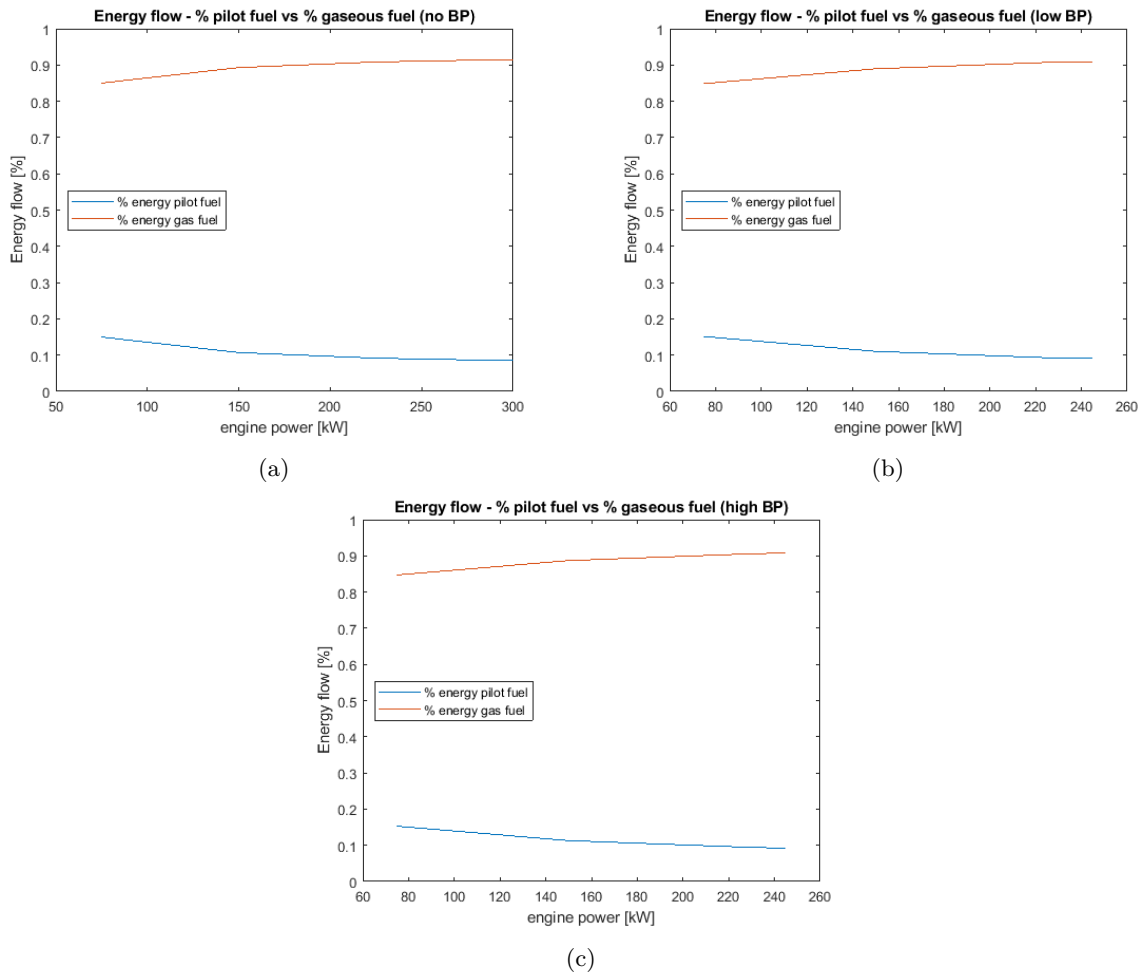


Figure 74: Pilot fuel energy vs Gaseous fuel energy for 3 cases of back-pressure

The SFGC, shown in figure 75b, decreases as the engine power increases, showing an improvement in efficiency at higher engine ratings. This is slightly different to what was found for the propeller curve, see section 4.2.3 and figure 63b, but this trend is the same as what was expected. Comparing this SFGC with that of the propeller curve it is seen that even though there seems to be a more consistent improvement of efficiency here, the SFGC for the propeller curve is lower. This complies with what is known for gas type engines, that at constant high rpm the efficiency is lower. What also can be seen is that the SFGC

becomes lower with increasing back-pressure, suggesting that there is an improvement in efficiency with increasing back-pressure for the tested engine (similar to what was found for the propeller curve).

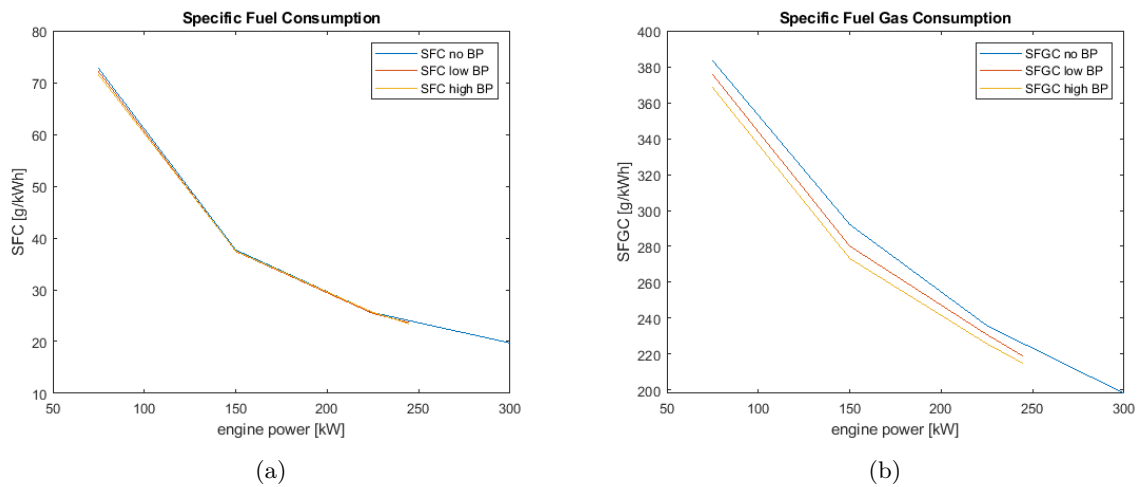


Figure 75: Specific fuel consumption (a) and specific fuel gas consumption (b) for 3 cases of back-pressure

4.3.4 Emissions

The same emissions were recorded as for the propeller curve, the results are shown below.



The incoming air flow rises as the engine power rises because more fuel needs to be burned. This is clearly shown in figure 76a. As mentioned earlier because the pressure ratio across the turbine drops with increasing back-pressure the turbocharger speed decreases and less air is being put into the engine. This drop in incoming air flow can also be seen in figure 76a. At higher engine powers more fuel needs to be burned, but the combustion efficiency of the mixture also improves, that is why the O_2 emissions go down as engine power increases, see figure 76b. Similar to the propeller curve, the O_2 emissions are lower for the cases with back-pressure. The conclusion is the same as in section 4.2.4, it is a combined effect of the lower incoming air flow and the seemingly improved efficiency at higher back-pressure (as was concluded in the previous section about fuel consumption).

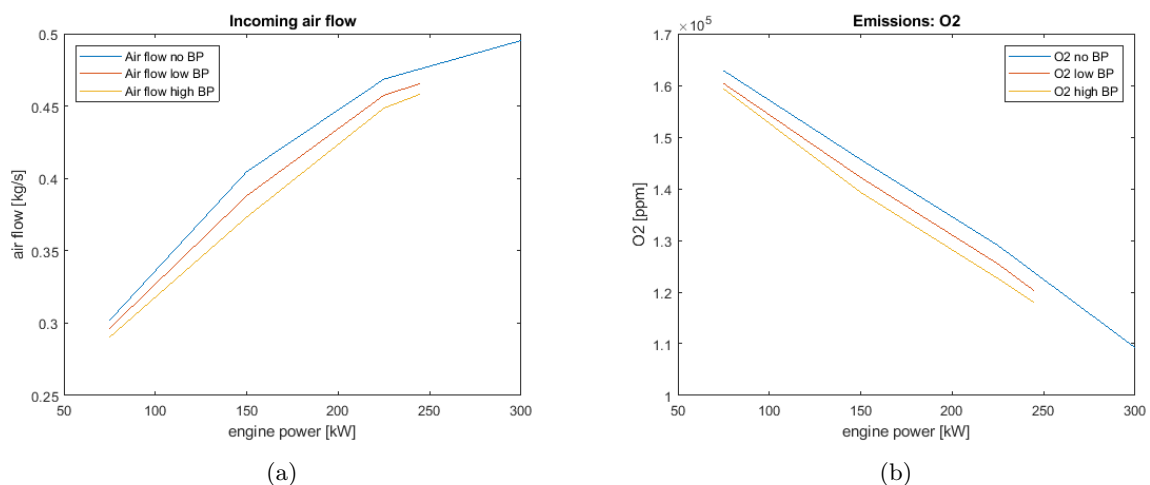


Figure 76: Incoming air flow (a) and O2 emissions (b) for 3 cases of back-pressure



From (12) it is known that the amount of CO in the exhaust is dependant on the amount of unburned gaseous fuel and the mixing temperature. At low loads the fuel utilization is lower than at high loads leading to higher CO emissions. Figure 77 shows this trend quite clearly. Similar to the propeller curve

results the CO emissions for the cases with added back-pressure are higher at low loads, although this difference is less for the generator curve. But at higher engine loads these emissions become lower than for the case with no added back-pressure, which complies with the conclusion from section 4.3.3 that there is an improvement in gaseous fuel utilization. If we compare the CO emissions with those of the propeller curve, the CO emissions for the generator curve are higher, which complies with the SFGC comparison between the two curves.

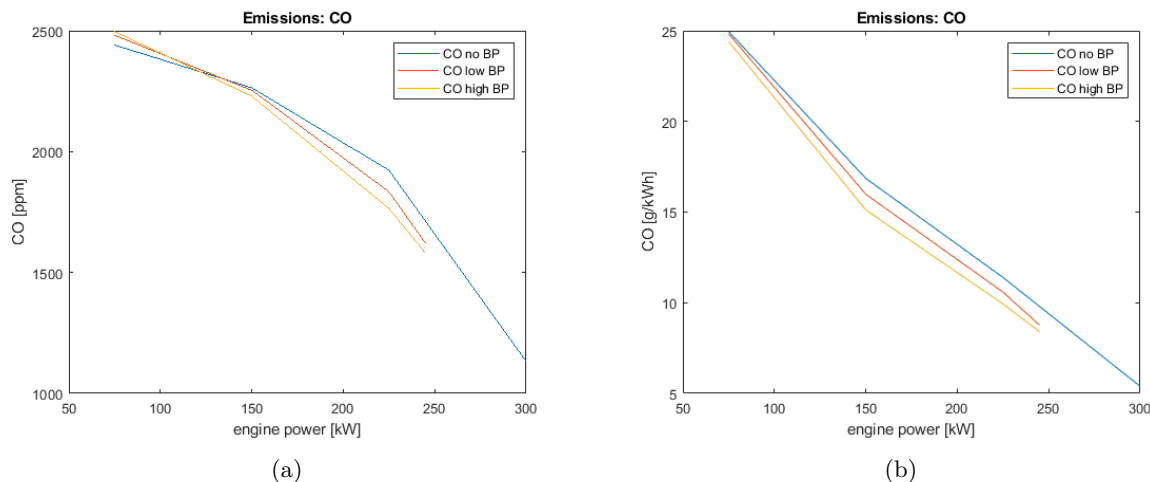


Figure 77: CO emissions in ppm (a) and g/kWh (b) for 3 cases of back-pressure

CO₂

If more fuel is being burned more CO₂ will be present in the exhaust. Fuel consumption increases with increasing engine loads and therefore the amount of CO₂, which can be seen in the figure below. For the cases with back-pressure the same conclusion can be made as before for the propeller curve: even though less fuel is being used the amount of CO₂ rises, suggesting that there is an improvement in the fuel utilization as back-pressure increases. Comparing with the CO₂ emissions from the propeller curve it can be seen that the emissions here are lower.

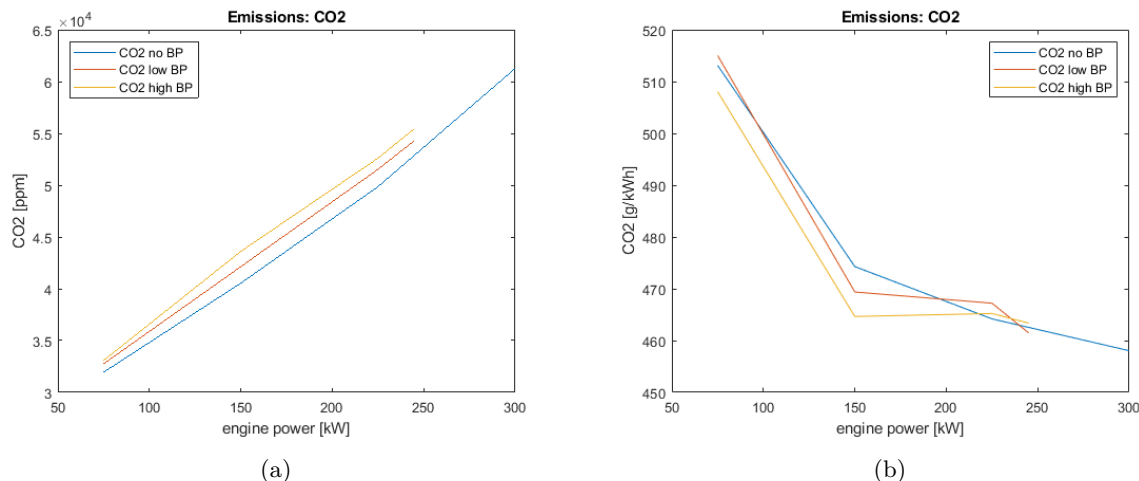


Figure 78: CO₂ emissions in ppm (a) and g/kWh (b) for 3 cases of back-pressure

NO_x

As stated earlier, the formation of NO_x is dependant on the O₂ concentration and the (charge) temperature (12). Although the oxygen concentration goes down (see figure 76b) figure 79 shows an increase in NO_x emissions, so this must be because the temperatures in the exhaust increase at these engine loads. The temperatures are also higher for the cases with back-pressure, so for those cases the NO_x emissions are higher too. This trend is very different to what was found for the propeller curve, however for the generator curve the NO_x emissions are lower for the whole power range.

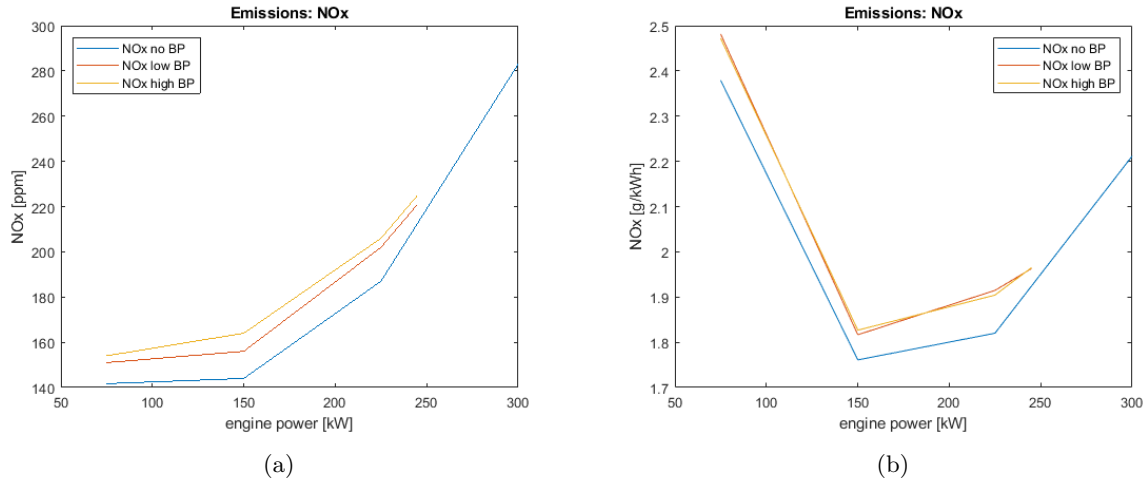


Figure 79: NO_x emissions in ppm (a) and g/kWh (b) for 3 cases of back-pressure

Unburned hydrocarbons

If more natural gas slips through the engine without being burned the amount of UHC emissions will be higher. From figure 80 it is clear that at lower loads the fuel utilization is worse than at higher loads since the UHC emissions are higher but the fuel flow is lower in this range. It also shows that the UHC emissions decrease with increasing back-pressure, which is due to the fact that the fuel flow is lower in these cases, but might also be an effect of improved combustion as was concluded before.

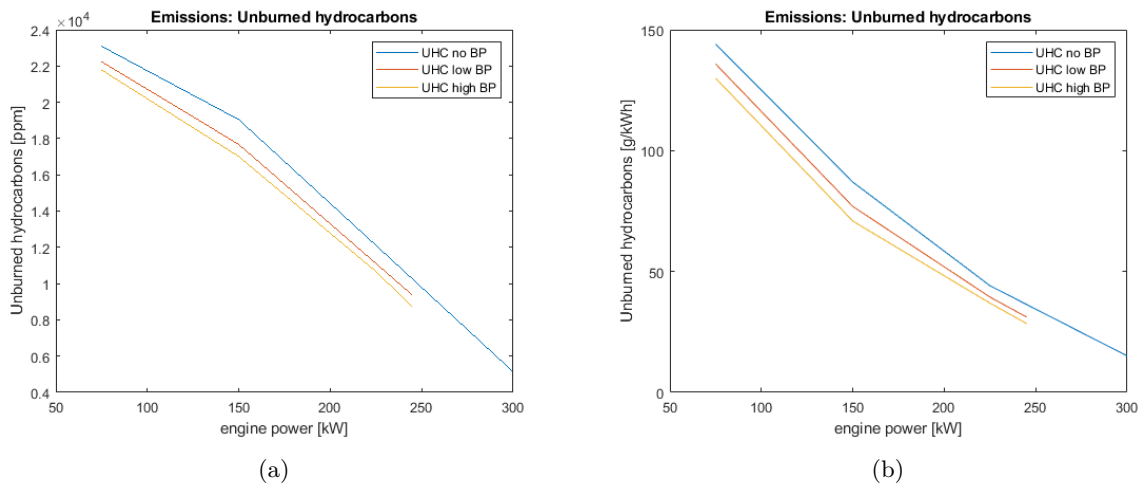


Figure 80: Unburned hydrocarbons emissions in ppm (a) and g/kWh (b) for 3 cases of back-pressure

4.4 Conclusion of experimental results

In the previous sections the results from the experiments were analysed. This section will shortly summarise the most important conclusions. For a more detailed explanation it is referred to read the concerning section.

- **Notes:** It is important to remember that a constant back-pressure could not be established during the experiments. So the engine experienced a lower absolute back-pressure at low loads than at high loads. The engine also had an absolute back-pressure of 1.15 bar at full load with the exhaust valve open, so only a small amount of back-pressure could be added for the other 2 cases. Therefore only small differences were found sometimes. This made a good comparison between cases sometimes a bit difficult
- **Pressures and temperatures:** On the inlet side of the engine the pressures and temperatures were measured to be lowered with increasing back-pressure as was expected as the higher back-pressure causes deterioration of turbocharger efficiency. On the outlet side of the engine the

exhaust receiver pressure results were a little off, probably due to issues during the experiments. The temperatures on the outlet side increased with increasing back-pressure as was expected. So overall the pressures and temperatures behaved as the literature suggested. What was noticed was the small difference in pressures between the inlet and outlet side of the engine, so there is a risk of back-flow for the tested engine.

- **Fuel:** At low loads more pilot fuel is being used by the engine. This was expected as literature suggested that the combustion of the gaseous fuel in this region is not so efficient, so more diesel is needed to start the combustion. What was contradictory to what was found so far is the decrease in fuel consumption as the back-pressure was increased. Whether this effect is indeed true for this type of engine and combustion improves due to the higher thermal loading, or that the tested engine (which only recently before the experiment was converted into a dual-fuel system) was not calibrated correctly, remains to be seen and more investigation is necessary. Another effect that was found is that the efficiency seems to change over the range of engine power for the propeller curve. It seems that the engine has a lower efficiency at part load conditions. At higher powers it improves again, maybe due to the higher thermal loading at these powers. Again more research with this type of dual-fuel engines is necessary to prove or explain this phenomena. The generator curve seems to have a much more constant improving efficiency over the range of engine power, but the specific fuel consumptions were higher than the generator curve. This does comply with how a gas-type engine behaves at high constant rpm.
- **Emissions:** Per tested case the emissions behaved as was expected over the range of engine powers. However comparing the 3 tested cases of back-pressure with one another and looking at them in combination with the fuel energy flows and the specific fuel flows, the emission results showed signs of improved combustion with increasing back-pressure.

5 Dual-fuel MVFP model extrapolation

In the previous chapter the results from the experiments were described. In this chapter the dual-fuel MVFP model will be used to run with higher levels of back-pressure than could be done experimentally. The outcomes are checked with literature and the experimental outcomes from chapter 4 to see if the same trends are found or not. Based on these findings some critical parameters will be selected as basis for limit cases for the next chapter.

For the model runs in this chapter the following choices were made:

- Even with the exhaust pipe fully opened, the tested engine had an absolute back-pressure of 1.15 bar at full load. This is rather high already and because of therefore only a small amount of extra back-pressure could be established during the experiments. This meant that only small differences in outcomes could be observed. The highest value of absolute back-pressure during the experiments was 1.3 bar. Starting from this level a maximum of 1 bar extra back-pressure will be added in the model. This is the equivalent of around 10 meter water column of added back-pressure, more would be an unrealistic amount of back-pressure for a maritime engine.
- As explained in section 4.1 during the experiments the back-pressure the engine experienced was not constant. This meant that at lower loads the difference between the tested cases were very small of even equal to each other, again giving only very small changes in results. The back-pressure level is now kept constant over the range of engine power for each run.
- The model runs, for both the propeller and generator curve, all start at the MCR point of the engine. During the experiments this could not be achieved due to the fact that engine limits were reached.
- The amount of back-pressure as indicated in the legends in each figure is the absolute back-pressure the engine is experiencing in the model runs.

By conducting the model runs in this way, bigger differences between the tested cases can be shown, giving more insight into the workings of this type of engine. And levels of back-pressure that can not be tested experimentally can now be used. Again the results will be shown by following the flow through the engine, ending with the fuel flow.

Compressor

In figure 81 it can be seen that the compressor outlet pressure decreases with increasing back-pressure. This is the same trend as was found for the experiments and complies with previous research. This is the effect of a decreasing pressure ratio across the turbine, which reduces the flow through the turbine. This leads to a lower turbocharger speed and therefore the compressor is not able to build-up more pressure in the system (3)(4)(5)(20). A side effect of this lower compressor outlet pressure is a lower temperature in this part of the engine, as can be seen in figure 82, as also found in chapter 4 and previous studies (3)(4)(5)(20).

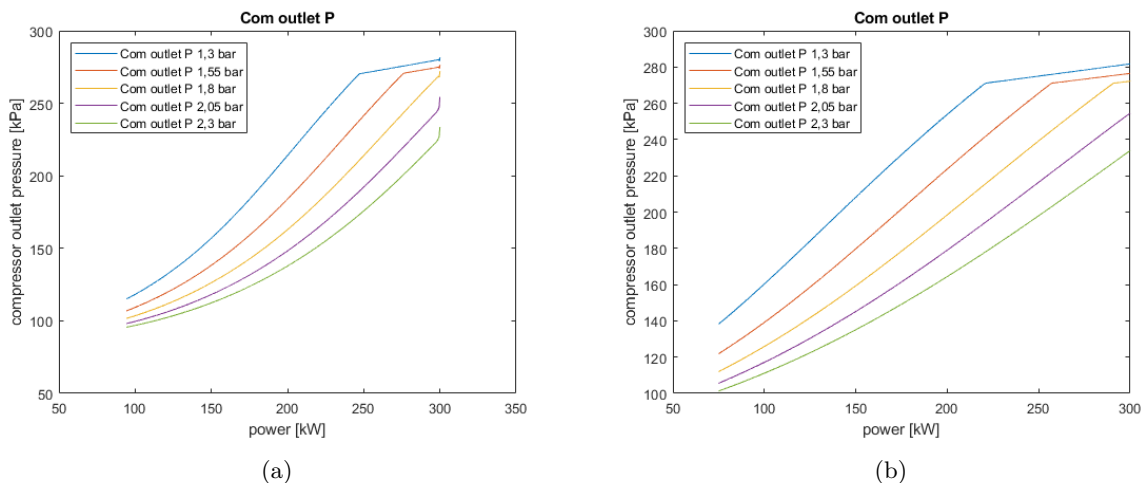


Figure 81: Compressor outlet pressure for propeller curve (a) and generator curve (b)

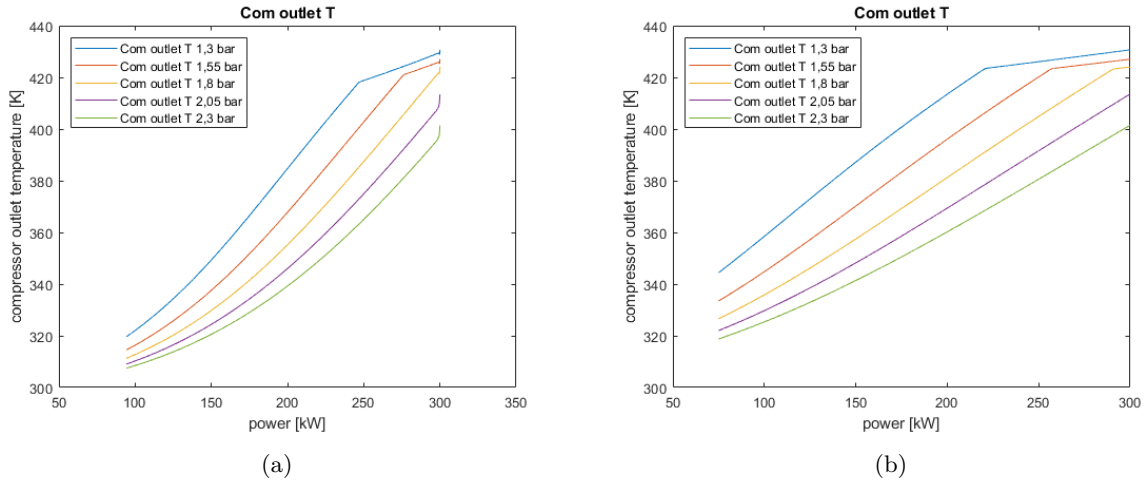


Figure 82: Compressor outlet temperature for propeller curve (a) and generator curve (b)

Inlet receiver

When the compressor outlet pressure decreases, so will the inlet receiver as can be seen in figure 83. This is logical and complies with what was found before. But what is more important to see here is that at a certain point the inlet receiver pressure at which the waste-gate becomes active (around 261 kPa) is no longer reached. This means that at the outlet side of the engine the waste-gate will not open. This will increase the flow through the turbine, but at the same time will lead to higher turbine inlet pressures and temperatures which may cause damage to the turbine.

Looking at the temperatures in figure 84 it can be seen that at high loads the temperatures are somewhat lower with increasing back-pressure, although the difference is very small. This was also found during the measurements of the experiments. What is different here is the increase in temperature for lower engine powers. This may be an effect of the increasing work the engine has to do and that this causes the model to calculate a higher heat pick-up in this element. Although it has to be said that the difference is only a few degrees between the different cases while the added back-pressure is quite significant, so it could almost be seen as constant as was found during the experiments.

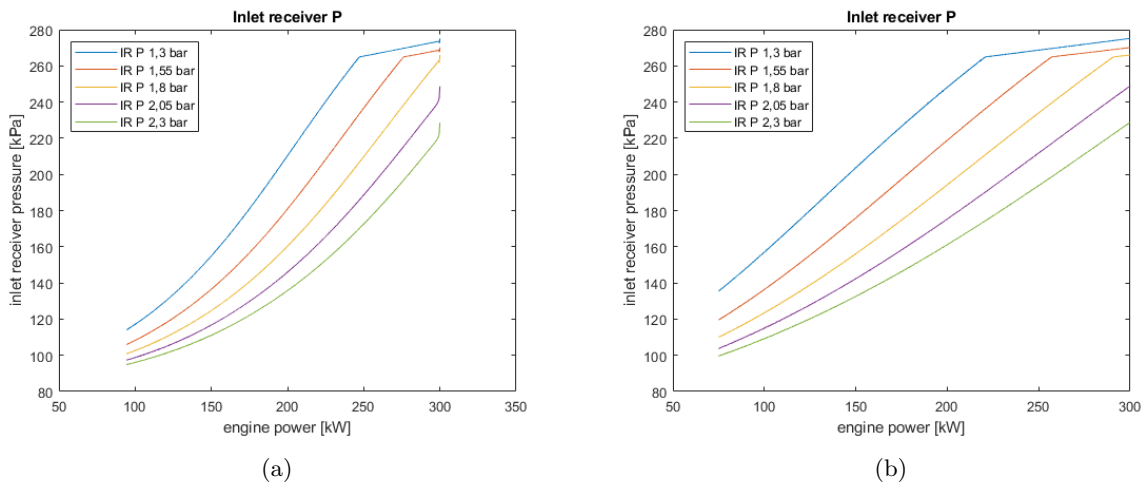


Figure 83: Inlet receiver pressure for propeller curve (a) and generator curve (b)

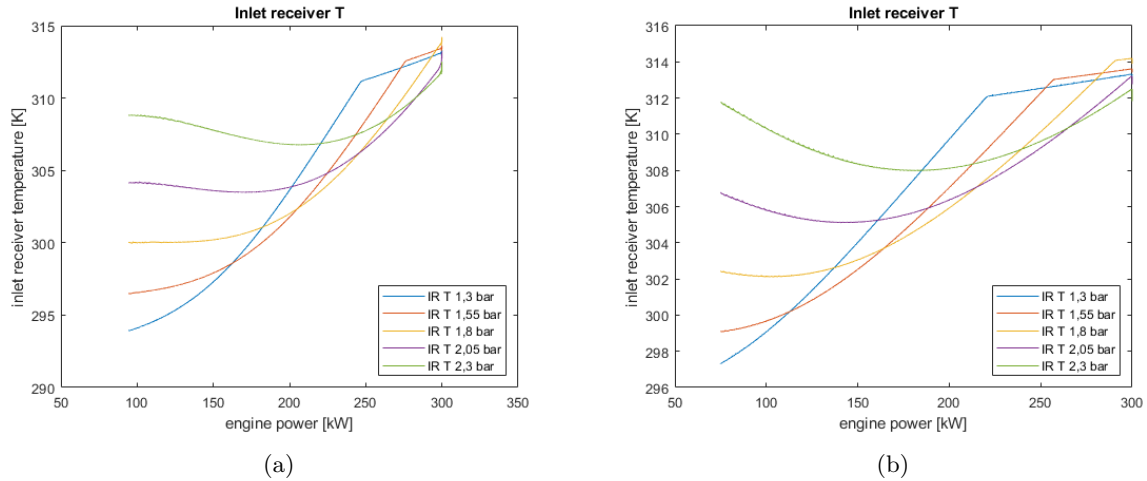


Figure 84: Inlet receiver temperature for propeller curve (a) and generator curve (b)

In-cylinder pressure

As the pressure on the inlet side decreases so will the pressure build-up in the cylinder. This can be seen in figure 85 where the maximum in-cylinder pressure is shown. This means that within the model, in order to keep the same engine power output, more fuel will need to be combusted to release the necessary energy. This, in combination with a lower air intake due to the lowered turbocharger performance, means that the air-fuel ratio will go down. If this becomes too low the engine will no longer work, so this is also an important limit for the engine performance.

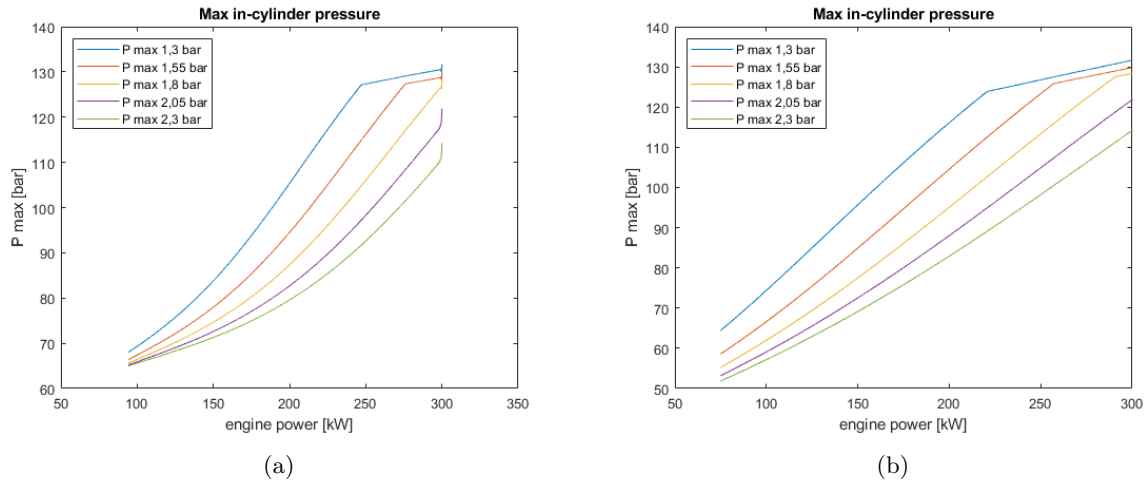
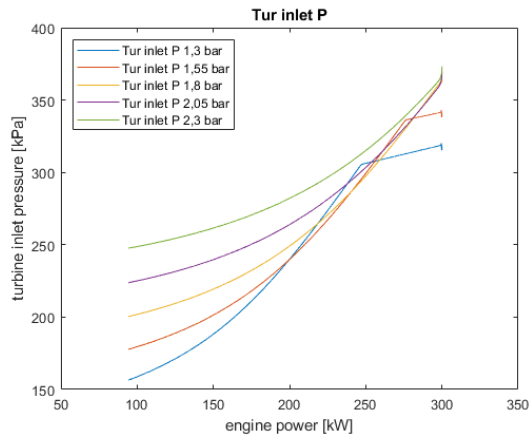


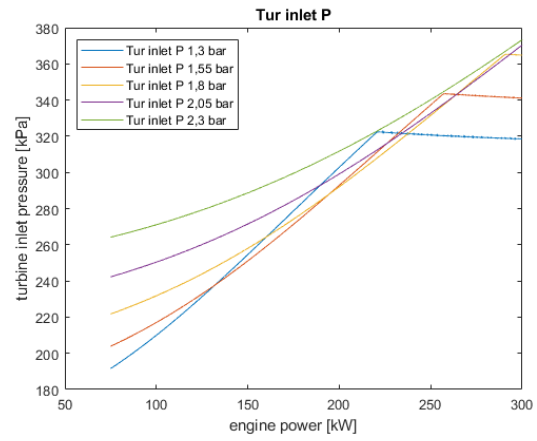
Figure 85: Maximum in-cylinder pressure for propeller curve (a) and generator curve (b)

Turbine

As the back-pressure increases, so do the pressures and the temperatures on the exhaust side of the engine. This can be seen in figures 86 to 88. These effects were also found during the experiments. The increase in back-pressure leads to a lower pressure ratio across the turbine, which causes a lower flow through the turbine. This in term leads to a higher pressure build-up before the turbine, which is also what was found earlier in earlier research (3)(4)(5)(20). Figure 86 also shows the effect of the waste-gate not opening for certain levels of back-pressure as the turbine inlet pressure keeps on increasing as no flow is by-passed. Figure 87 shows that the turbine inlet temperature can become very high. This high temperature can cause the turbine to be thermally overloaded and damage the turbine. So this is an important parameter for the engine limits when back-pressure is applied.

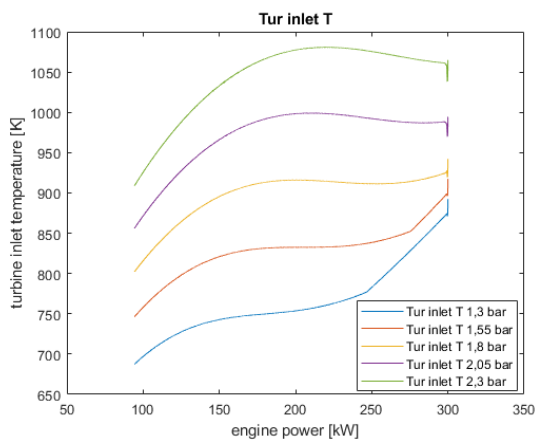


(a)

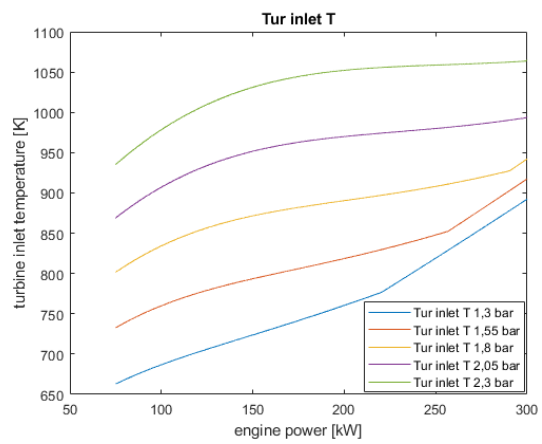


(b)

Figure 86: Turbine inlet pressure for propeller curve (a) and generator curve (b)

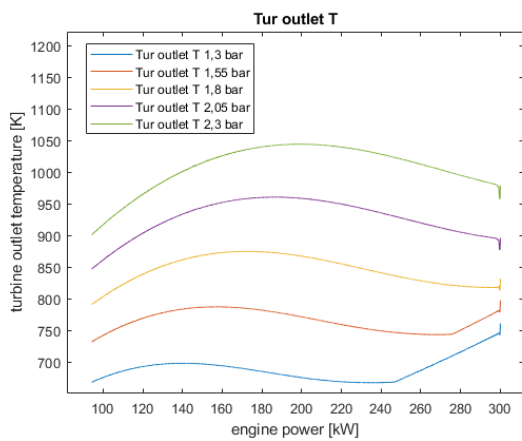


(a)

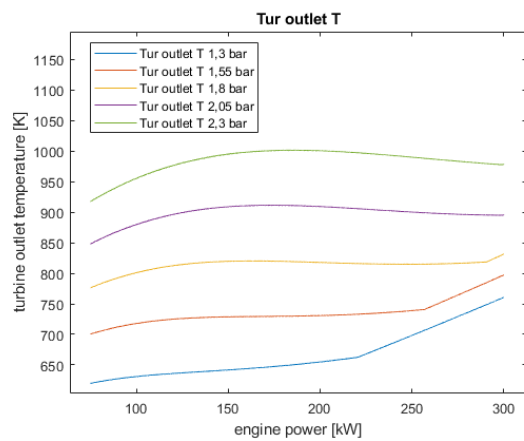


(b)

Figure 87: Turbine inlet temperature for propeller curve (a) and generator curve (b)



(a)



(b)

Figure 88: Turbine outlet temperature for propeller curve (a) and generator curve (b)

Exhaust valve

Previous studies have shown that the exhaust valve temperature is also an important parameter for the

thermal loading of the engine (3)(5)(20). This engine component can get very hot and may reach its maximum allowable temperature before other components. The heat pick-up of the exhaust valve is a combination of the heating during the blow-down process and the cooling during scavenging. In the MVFP model there is an estimator model for the exhaust valve temperature based on the temperatures of these processes (5). Figure 89 shows the results of this estimator model. Comparing these results with the turbine inlet temperature from figure 87, it can be seen that they follow the same trend but that the exhaust valve temperatures are much higher. So it may indeed be that the limit for this component is reached earlier. Therefore this engine parameter will also be taken into account in the next chapter.

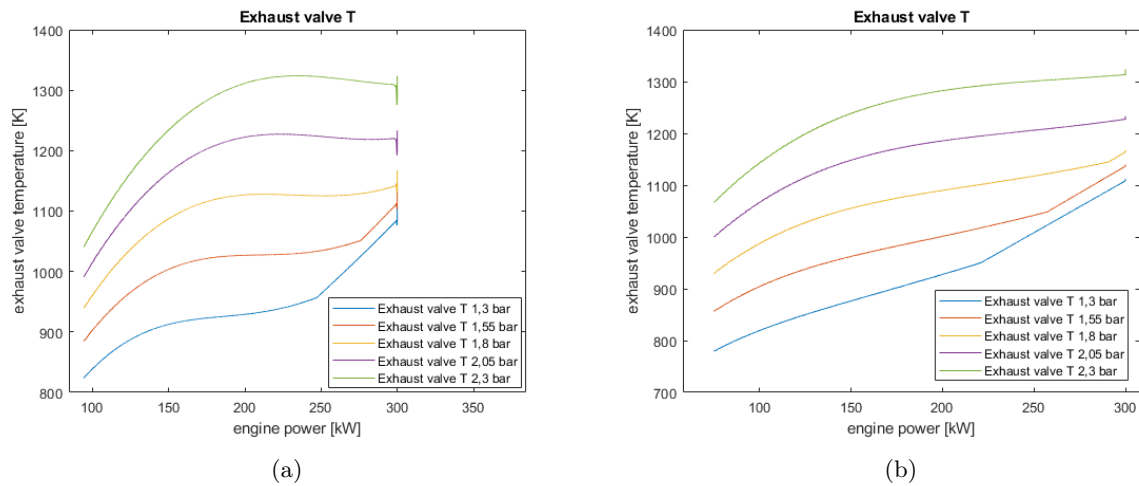


Figure 89: Exhaust valve temperature for propeller curve (a) and generator curve (b)

Fuel flows

With increasing back-pressure the engine has to work harder to expel its combustion gasses (3)(4)(5)(20). This in combination with a lower in-cylinder pressure leads to an increase in fuel consumption in order to keep the engine output the same. This effect on the fuel consumption was also found by the model results in figures 90 and 91. Although this complies with the literature, this effect was not found during the experiments where a lower fuel consumption was measured. But as stated before this effect can not be properly explained without further research.

The increase in fuel consumption in combination with a deteriorating turbocharger performance leads to a lower air-fuel ratio. If this becomes too low there will be incomplete combustion and the engine performance will go down. So again the air-fuel ratio is also an important limiting parameter for a dual-fuel engine under back-pressure.

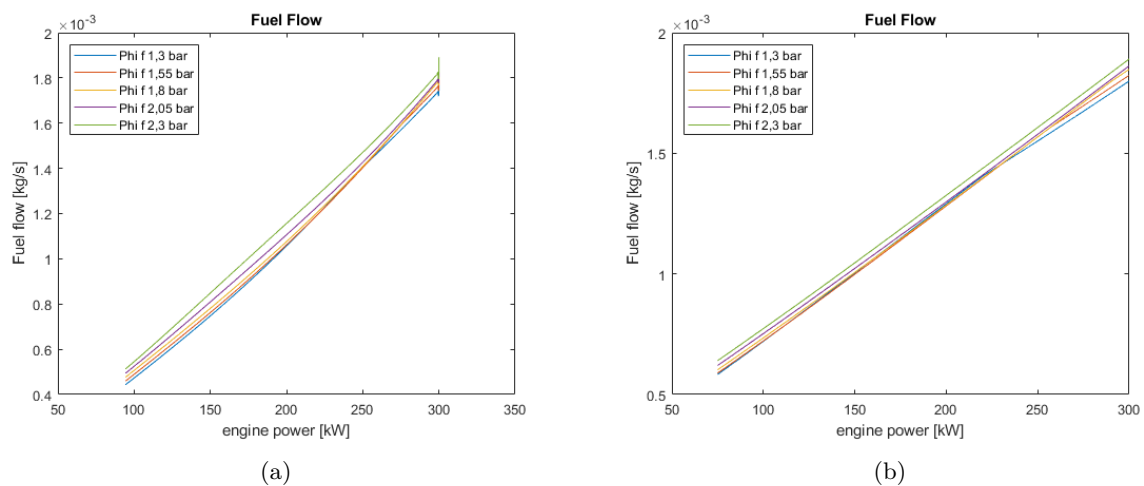


Figure 90: Pilot fuel flow for propeller curve (a) and generator curve (b)

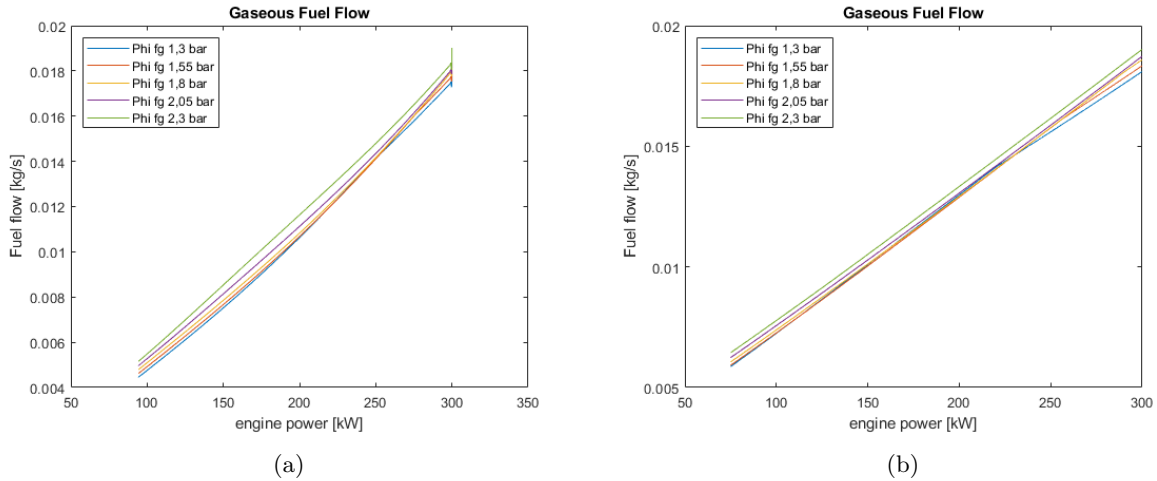


Figure 91: Gaseous fuel flow for propeller curve (a) and generator curve (b)

Altogether increasing the back-pressure in the model (and keeping it constant over the power range) delivers the same results as found in previous research and the experiments. As more back-pressure can be implemented in the model than during the experiments the changes become more pronounced. The only parameter that does not comply with the experimental results is the fuel flow, which according to the model does increase, but this effect does comply with the literature (3)(4)(5)(20). It was also found that this increase in the fuel flows in combination with a lower air intake due to a lower turbocharger performance can lead to too low air-fuel ratio's, which could be a limiting factor for the engine together with the thermal loading of the turbocharger. Therefore in the next chapter these two engine parameters will be used to find limit cases of back-pressure levels for this dual-fuel engine.

6 Limit cases

In this chapter the dual-fuel MVFP model will be used to find limit cases of back-pressure for the engine. First the engine envelope needs to be determined in order to know what the engine limits are without back-pressure. Based on the previous chapters it was found that the air-excess ratio, the outlet receiver temperature and the exhaust valve temperature were important parameters for the engine limits. The air-excess ratio is an indicator to see weather the fuel mixture can still be properly combusted, the outlet receiver temperature is an indicator of the thermal loading of the turbine and the exhaust valve temperature for the thermal loading of the engine (in combination with outlet receiver temperature). The effect of increasing back-pressure on these three parameters will be shown to see when they reach their limit values.

6.1 Engine envelope

Based on other experiments performed at Harbin University with the dual-fuel engine the engine envelope shown in figure 92 was developed. This engine envelope was developed over a wider range of engine rpm than the range that was taken during the experiments with back-pressure. In order to find the limit cases of back-pressure the simulations with added back-pressure were performed along the propeller curve. This curve can also be seen in figure 92 as well as the propeller curve that was used during the back-pressure experiments to show that they match.

In order to find the acceptable values for the air-excess ratio and the outlet receiver and exhaust valve temperature, the model was used to run at the maximum engine power for each rpm without back-pressure. This will give the minimum air-excess ratio and maximum outlet receiver and exhaust valve temperature that can be reached at the corresponding rpm. The results are shown in figure 93 as the black limit curves. For a gas type engine a too high air-excess ratio can cause the engine to misfire. The misfire limit for such an engine lays around an air-excess ratio of 2.4 (29). This limit is also shown in figure 93a.

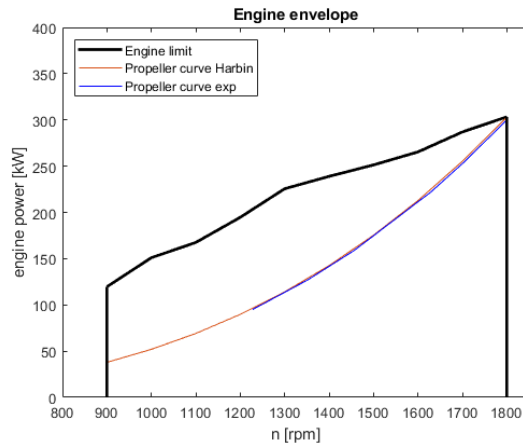


Figure 92: Engine envelope and propeller curve

6.2 Engine limits with back-pressure

After finding the limit values for air-excess ratio, outlet receiver temperature and exhaust valve temperature the model was used to simulate increasing back-pressure along the propeller curve. Increasing the back-pressure reduces the air intake and therefore the air-excess ratio, and also increases the temperatures in the outlet of the engine. This means that the engine limits will be reached at an earlier point, or to look at it a different way increasing back-pressure reduces the engine envelope as shown in figure 92. This means that the propeller curve may lay outside of the engine envelope and the engine can no longer produce the necessary power. The limit curves shown in figure 93a are the minimum air-excess ratio as calculated by the model for the given engine envelope and the maximum air-excess ratio to avoid misfire (this value of 2.4 was found in (29)). So the air-excess ratio curves should lay between these limits. The limits shown in figures 93b and 93c are the maximum outlet receiver and exhaust valve temperatures for the engine. This means that the outlet receiver and exhaust valve temperature curves should lay below these limits in order for the engine to be able to cope with the back-pressure level.

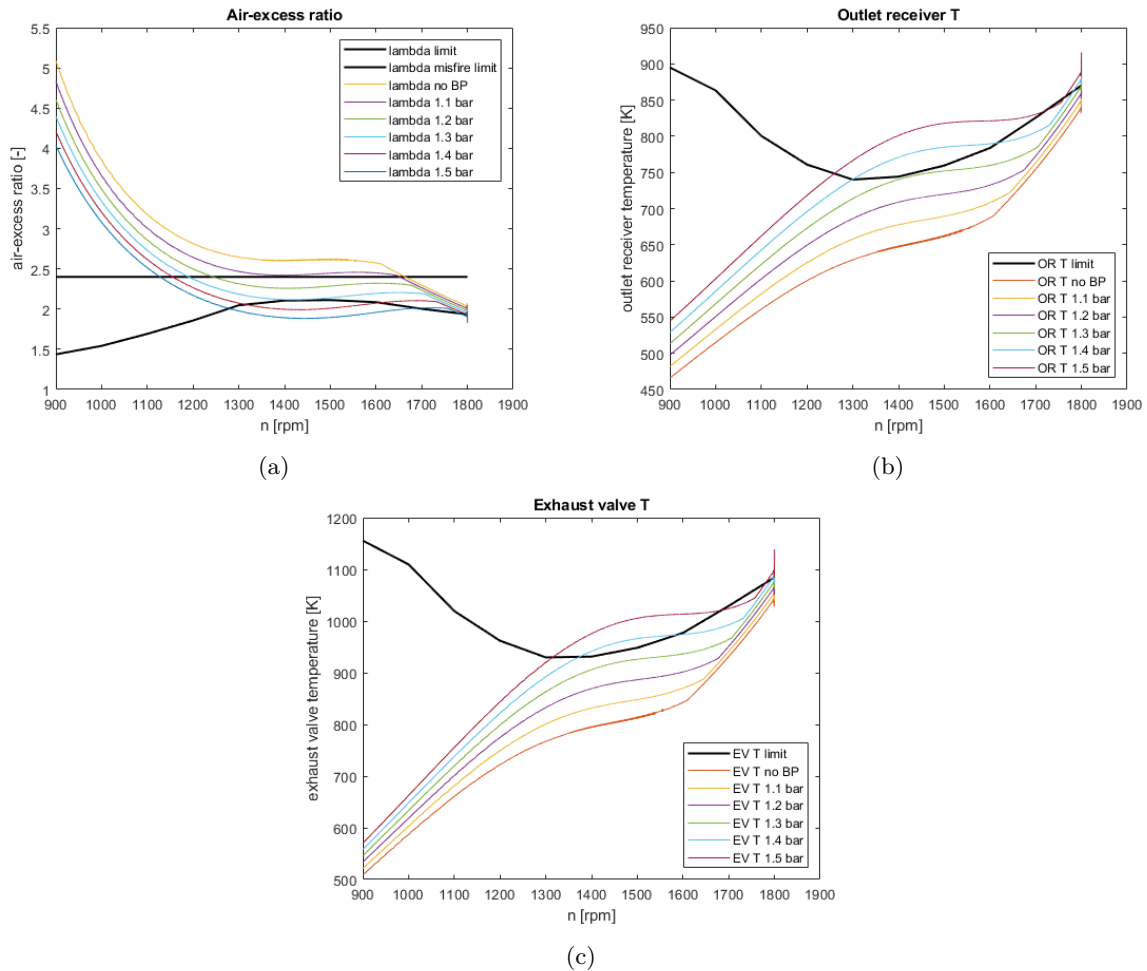


Figure 93: Engine limits and back-pressure effect on air-excess ratio (a), outlet receiver temperature (b) and exhaust valve temperature (c)

The trend of decreasing air-excess ratio and increasing temperatures at the outlet when the back-pressure is increased can clearly be seen in figure 93. Looking at the temperatures it also shows that in the current model the engine is able to cope with back-pressure up to an absolute back-pressure of 1.3 bar. If the back-pressure is increased more the temperatures are getting too high at part load conditions first and later at full power the limits are being reached as well. What also can be seen is that the limit for the outlet receiver temperature is reached before the limit of the exhaust valve temperature. So for the thermal loading the outlet receiver seems to be the more important parameter if a certain control system is implemented to prevent the engine from being overloaded.

Looking at figure 93a it can be seen that the margin for the air-excess ratio is quite narrow. As stated before the fuel flows in the current model are not matching, which has an influence on the calculated air-excess ratio's. For instance it seems that the air-excess ratio for the no back-pressure case at part load lays above the misfire limit, while during the experiments no misfire occurred. However the model does show that with increased back-pressure (and therefore a decreasing air-excess ratio) at part load the air-excess ratio could become too low. The air-excess ratio's at low load are getting quite high for a gas type engine. This might come due to the fact that the current model uses a too low fuel flow at this point, especially for the pilot fuel, which means that in reality the air-excess ratio's at low loads are somewhat lower than calculated. Also as seen during the experiments at lower loads more pilot fuel is used. This means that at low loads a dual-fuel type engine starts to behave more like a diesel engine than a gas engine, which means that the misfire limit in this range might not be applicable (so the increase in air-excess ratio at low loads might not become an issue). All together it shows that the air-excess ratio is an important parameter for the engine limits. So implementing a certain control system to keep the air-excess ratio within the limits might be necessary.

As stated earlier the model is not perfect and can be improved upon. Changing the model will also have an influence on the results in this chapter, so drawing hard conclusions about the exact limits for the

tested engine is difficult at this point. Also changing engine parameters such as valve timing or the type of turbocharger will change the limit curves and the point at which they are being reached. However this part does show that the model can be used in this way to look for engine limits which can not be done experimentally.

7 Conclusions and recommendations

For this master thesis an experimental and model based investigation was performed to see what influence static back-pressure has on the performance and emissions of a dual-fuel engine. For this purpose an existing Mean Value First Principle (MVFP) model was adopted to a dual-fuel MVFP model and matched to the engine that was used for the experiments. The experiments helped with gaining insight into the behaviour of a dual-fuel engine under back-pressure and the model could then be used to see what would happen at back-pressure levels that could not be performed experimentally. Below the main conclusions from this research are summarised and some recommendations for further research are given.

7.1 Conclusions

For clarity the conclusions from the experiments and from the model investigation are separated.

Experiments

- Increasing the back-pressure decreases the pressures and temperatures on the inlet side of the engine. On the outlet side the pressures and temperatures increased. So for the thermal loading of the engine, the outlet parameters are more important.
- The difference between inlet and outlet pressures was small, so there is a risk of back-flow for the tested engine when there is a (large) valve overlap. This could create issues, especially at high levels of back-pressure.
- At low loads there is an increase in pilot fuel consumption. At these loads the gaseous fuel is harder to combust, so more pilot fuel is needed to start the ignition.
- Increasing the back-pressure decreased the fuel consumption, with the exception of the gaseous fuel flow at part load conditions for the propeller curve. This lower fuel consumption was not expected but may be a result of the higher thermal loading of the engine at higher levels of back-pressure.
- For the propeller curve it was found that the efficiency of the tested engine at part load conditions was lower than at low or high power. Again the higher thermal loading at high power might improve the efficiency, and at lower power the engine experienced a lower absolute back-pressure which leads to somewhat distorted results. For the generator curve the change in efficiency was more constant over the power range, but the specific fuel consumptions were always higher than for the propeller curve.
- Increasing the back-pressure showed lower emissions of O₂, CO, and unburned hydrocarbons and higher emissions of CO₂ and NO_x. Looking at the emissions in combination with the fuel flows, some of the emissions showed signs of improved combustion efficiency with increasing back-pressure.

Dual-fuel MVFP model

- The changes to turn the existing MVFP model into a dual-fuel model were implemented successfully. The formula's that were used to calculate the properties of the gaseous fuel and its stoichiometric gas were based on the volume fractions of the gaseous fuel and its base elements, so other types of gaseous fuel can be used as well.
- The matching of the model was not perfect as the turbine inlet pressure at higher engine powers was calculated too high. This problem could not be fully resolved at the time, but since the other parameters matched well (also when back-pressure was increased) it was chosen to continue, also because the parameters that were seen as important for the engine limits did match well.
- The model was able to work with higher levels of back-pressure than could be reached during the experiments. These back-pressures could now be kept constant (which was not the case during the experiments), to see what happens at these levels. The model showed the same trends for pressures and temperatures (so it works quite well) but they were more pronounced than the results from the experiments. The only difference between the model and the experiments was that the model does calculate an increasing fuel consumption with increasing back-pressure, as the literature so far suggested. The high levels of back-pressure also showed that at a certain level the waste-gate

is not activated anymore, leading to high pressures and temperatures before the turbine and a high exhaust valve temperature. It also showed that the air-excess ratio was an important limiting factor for the engine.

- It was also shown how the model could be used to define acceptable limits of back-pressure for the engine. The air-excess ratio, exhaust valve temperature and turbine inlet temperature were selected as the limiting parameters for the engine under back-pressure. Their limit values were calculated with the model based on the engine envelope, without back-pressure applied. Then the model was used to run along the propeller curve with increased back-pressure to see when these limits were reached. The problems first occur at part load conditions and then at full power as well. It also showed that the air-excess ratio at low power might increase to a too high level for a gas type engine.

7.2 Recommendations

Below some recommendations for improvements or further research are listed.

- As stated earlier the model was not matched perfectly as the turbine inlet pressure becomes too high at high engine powers, so there is some room for improvement here. For the purpose of this research this was not a big problem, but for further use it might be necessary to investigate what happens here.
- During the experiments the absolute back-pressure the engine experienced was not constant. This gave some issues during the matching phase. For instance it made it quite difficult to get the exact turbine outlet pressure, leading to other errors at other places in the model. Performing other back-pressure experiments with a truly constant back-pressure might help for a better matching procedure. Also having more experimental data can help with further improvements in the model and show to what extent the model at this moment works correctly.
- In this thesis the focus was on the constant back-pressure effects. The next step could be to see what happens with a fluctuating back-pressure (as initiated by waves) on a dual-fuel engine.
- During the experiments the fuel flows were measured to decrease with increasing back-pressure. This phenomena did not comply with the literature so far and was hard to explain. So far the conclusions were that either the increased thermal loading plays a role on the gaseous fuel combustion or that the tested engine was not calibrated perfectly. So more research into the combustion of dual-fuel (with more focus on the in-cylinder process) might be useful to explain what really happens here. This will also help to improve the dual-fuel MVFP model as a better combustion efficiency model can be implemented. This may also help to get a better matching fuel consumption within the model.
- The gaseous fuel that was used was composed of different elements, but mainly methane. It might also be interesting to see what happens with other types of gaseous fuel.
- The model simulations were performed for a constant turbocharged, 4-stroke engine with no valve overlap. It would also be interesting to see what happens when engine components are changed within the model, for instance a pulse turbocharger or a large valve overlap.

References

- [1] IMO: Greenhouse Gas Emissions. <http://www.imo.org/en/OurWork/Environment/PollutionPrevention/AirPollution/Pages/GHG-Emissions.aspx>, (Accessed on 02/04/2020).
- [2] Visser, K. GasDrive - TKI Water Research Program funded by STW, *LNG fuelling System Integration: a novel approach*. Presentation at Innovation Day at TU Delft, 2015.
- [3] Singh, J. *Experimental and simulated investigations of marine Diesel engine performance against dynamic back pressure at varying sea-states due to underwater exhaust systems*. TU Delft, 2019.
- [4] Hield, P. *The Effect of Back Pressure on the Operation of a Diesel Engine*. Maritime Platforms Division, DSTO Defence Science and Technology Organisation (Australia), 2011.
- [5] Sapra, H.; Godjevac, M.; Visser, K.; Stapersma, D.; Dijkstra, C. *Experimental and simulation-based investigations of marine diesel engine performance against static back pressure*. Elsevier, Applied Energy 204: 78-92, 2017.
- [6] Karuppusamy, P.; Senthil, D. R. *Design, analysis of flow characteristics of catalytic converter and effects of backpressure on engine performance*. IJREAT International Journal of Research in Engineering and Advanced Technology, Volume 1, Issue 1, ISSN 2320-8791, 2013.
- [7] Joardder, M. U. H.; Roy, M. M.; Uddin, S. *Effect of Engine Backpressure on the Performance and Emissions of a CI Engine*. The 7th Jordanian International Mechanical Engineering Conference (JIMEC'7), 2010.
- [8] Mustafi, N.; Raine, R.; Verhulst, S. *Combustion and emissions characteristics of dual fuel engine operated on alternative gaseous fuels*. Elsevier, Fuel 109: 669-678, 2013.
- [9] Carlucci, A. P.; de Risi, A.; Laforgia, D.; Naccarato, F. *Experimental investigation and combustion analysis of a direct injection dual-fuel diesel-natural gas engine*. Elsevier, Energy 33: 256-263, 2007.
- [10] Kusaka, J.; Okamoto, T.; Daisho, Y.; Kihara, R.; Saito, T. *Combustion and exhaust gas emission characteristics of a diesel engine dual-fueled with natural gas*. Elsevier, JSAE review 21: 489-496, 2000.
- [11] Karim, G. A. *A review of combustion processes in the dual fuel engine - the gas diesel engine*. Pergamon Press Ltd., Prog. Energy Combust. Sci. Vol 6: pp 277-285, 1980.
- [12] Lounici, M. S.; Loubar, K.; Tarabet, L.; Balistrrou, M.; Niculescu, D.; Tazerout, M. *Towards improvement of natural gas-diesel dual fuel mode: An experimental investigation of performance and exhaust emissions*. Elsevier, Energy 64: 200-211, 2014.
- [13] Carlucci, A. P.; Laforgia, D.; Saracino, R.; Toto, G. *Combustion and emissions control in diesel-methane dual fuel engines: The effects of methane supply method combined with variable in-cylinder charge bulk motion*. Elsevier, Energy Conversion and Management: 3004-3017, 2011.
- [14] Yuo, J.; Liu, Z.; Wang, Z.; Wang, D.; Xu, Y.; Du, G.; Fu, X. *The exhausted gas recirculation improved brake thermal efficiency and combustion characteristics under different intake throttling conditions of a diesel/natural gas dual fuel engine at low loads*. Elsevier, Fuel 266 117035, 2020.
- [15] You, J.; Liu, Z.; Wang, Z.; Wang, D.; Xu, Y. *Impact of natural gas injection strategies on combustion and emissions of a dual fuel natural gas engine ignited with diesel at low loads*. Elsevier, Fuel 260: 116414, 2019.
- [16] Lee, C.; Pang, Y.; Wu, H.; Nithyanandan, K.; Liu, F. *An optical investigation of substitution rates on natural gas/diesel dual-fuel combustion in a diesel engine*. Elsevier, Applied Energy 261: 114455, 2020.
- [17] Yousefi, A.; Guo, H.; Birouk, M.; Liko, B. *On greenhouse gas emissions and thermal efficiency of natural gas/diesel dual-fuel engine at low load conditions: Coupled effect of injector rail pressure and split injection*. Elsevier, Applied Energy 242: 216-231, 2019.

- [18] Wang, Z.; Zhao, Z.; Wang, D.; Tan, M.; Han, Y.; Liu, Z.; Dou, H. *Impact of pilot diesel ignition mode on combustion and emissions characteristics of a diesel/natural gas dual fuel heavy-duty engine*. Elsevier, Fuel 167: 248-256, 2015.
- [19] Geertsma, R. D.; Negenborn, R. R.; Visser, K.; Loonstijn, M. A.; Hopman, J. J. *Pitch control for ships with diesel mechanical and hybrid propulsion: Modelling, validation and performance quantification*. Elsevier, Applied Energy 206: 1609-1631, 2017.
- [20] Sapra, H. *Study of effects on performance of a Diesel engine due to varying back pressure for an underwater exhaust system*. TU Delft, 2015.
- [21] Stapersma, D. *Lecture notes WB4408A Diesel Engines Volume 1, Performance analysis*; TU Delft, 2010.
- [22] Stapersma, D. *Lecture notes WB4408A Diesel Engines Volume 2, Turbocharging*; TU Delft, 2010.
- [23] Stapersma, D. *Lecture notes WB4408B Diesel Engines Volume 3, Combustion*; TU Delft, 2010.
- [24] Stapersma, D. *Lecture notes WB4408B Diesel Engines Volume 4, Emissions and Heat Transfer*; TU Delft, 2010.
- [25] Ding, Y. *Characterising combustion in Diesel engines using parameterised finite stage cylinder process models*. Ph.D. thesis, TU Delft, published by VSSD, 2011.
- [26] Ding, Y.; Sui, C.; Li, J. *An Experimental Investigation into Combustion Fitting in a Direct Injection Marine Diesel Engine*. MDPI, Applied Sciences 8, 2489, 2018.
- [27] Sui, C.; Song, E.; Stapersma, D.; Ding, Y. *Mean value modelling of diesel engine combustion based on parameterized finite stage cylinder process*. Elsevier, Ocean Engineering 136: 218-232, 2017.
- [28] Sapra, H.; Godjevac, M.; de Vos, P.; van Sluijs, W.; Linden, Y.; Visser, K. *Hydrogen-natural gas combustion in a marine lean-burn SI engine: A comparative analysis of Seiliger and double Wiebe function-based zero-dimensional modelling*. Elsevier, Energy conversion and Management 207: 112494, 2020.
- [29] Georgescu, I. *Characterising the transient behaviour of dual-fuel engines*. TU Delft, 2013.
- [30] Westhoeve, J. A. *Hybrid electrical turbocharging, improving the loading capability and efficiency of a dual fuel engine*. TU Delft, 2018.

List of Figures

1	Mean Value First Principle model (5)	10
2	Seiliger cycle and parameters	11
3	Flow chart of procedure to obtain Seiliger parameters (26)	11
4	Engine power	18
5	Compressor outlet pressure (a) and temperature (b)	18
6	Compressor flow vs. engine flow (a) and compressor flow vs. pressure ratio (b)	19
7	Inlet receiver pressure (a) en temperature (b)	19
8	Maximum in-cylinder pressure (a) and heat input into Seiliger cycle (b)	20
9	Turbine inlet pressure (a) and temperature (b)	21
10	Turbine outlet pressure (a) and temperature (b)	21
11	Turbine flow vs. pressure ratio	22
12	Fuel flows (a) and specific fuel and specific gaseous fuel consumption (b)	22
13	Engine power	23
14	Compressor outlet pressure (a) and temperature (b)	23
15	Compressor flow vs. engine flow (a) and compressor flow vs. pressure ratio (b)	24
16	Inlet receiver pressure (a) en temperature (b)	24
17	Maximum in-cylinder pressure (a) and heat input into Seiliger cycle (b)	25
18	Turbine inlet pressure (a) and temperature (b)	25
19	Turbine outlet pressure (a) and temperature (b)	26
20	Turbine flow vs. pressure ratio	26
21	Fuel flows (a) and specific fuel and specific gaseous fuel consumption (b)	27
22	Engine power for low (a) and high (b) back-pressure	28
23	Compressor outlet pressure for low (a) and high (b) back-pressure	28
24	Compressor outlet temperature for low (a) and high (b) back-pressure	29
25	Compressor flow vs. pressure ratio for low (a) and high (b) back-pressure	29
26	Compressor vs. Engine flow for low (a) and high (b) back-pressure	30
27	Inlet receiver pressure for low (a) and high (b) back-pressure	30
28	Inlet receiver temperature for low (a) and high (b) back-pressure	31
29	Maximum in-cylinder pressure for low (a) and high (b) back-pressure	31
30	Heat input for Seiliger cycle for low (a) and high (b) back-pressure	32
31	Turbine inlet pressure for low (a) and high (b) back-pressure	32
32	Turbine inlet temperature for low (a) and high (b) back-pressure	33
33	Turbine outlet pressure for low (a) and high (b) back-pressure	33
34	Turbine outlet temperature for low (a) and high (b) back-pressure	34
35	Turbine flow vs. pressure ratio for low (a) and high (b) back-pressure	34
36	Fuel flows for low (a) and high (b) back-pressure	35
37	Specific fuel and Specific gaseous fuel consumption for low (a) and high (b) back-pressure	35
38	Engine power for low (a) and high (b) back-pressure	36
39	Compressor outlet pressure for low (a) and high (b) back-pressure	36
40	Compressor outlet temperature for low (a) and high (b) back-pressure	37
41	Compressor flow vs. pressure ratio for low (a) and high (b) back-pressure	37
42	Compressor vs. Engine flow for low (a) and high (b) back-pressure	38
43	Inlet receiver pressure for low (a) and high (b) back-pressure	38
44	Inlet receiver temperature for low (a) and high (b) back-pressure	39
45	Maximum in-cylinder pressure for low (a) and high (b) back-pressure	39
46	Heat input for Seiliger cycle for low (a) and high (b) back-pressure	40
47	Turbine inlet pressure for low (a) and high (b) back-pressure	40
48	Turbine inlet temperature for low (a) and high (b) back-pressure	41
49	Turbine outlet pressure for low (a) and high (b) back-pressure	41
50	Turbine outlet temperature for low (a) and high (b) back-pressure	41
51	Turbine flow vs. pressure ratio for low (a) and high (b) back-pressure	42
52	Fuel flows for low (a) and high (b) back-pressure	42
53	Specific fuel consumption and Specific gaseous fuel consumption for low (a) and high (b) back-pressure	43
54	Engine specification	44
55	Operating points	44

56	Experiment setup	45
57	Compressor outlet pressure (a) and temperature (b) for 3 cases of back-pressure	46
58	Inlet receiver pressure (a) and temperature (b) for 3 cases of back-pressure	47
59	Exhaust receiver pressure (a) and temperature (b) for 3 cases of back-pressure	48
60	Absolute turbine outlet pressure (a) and temperature (b) for 3 cases of back-pressure	48
61	Pilot fuel energy flow (a) and gaseous fuel energy flow (b) for 3 cases of back-pressure	49
62	Pilot fuel energy vs Gaseous fuel energy for 3 cases of back-pressure	49
63	Specific fuel consumption (a) and specific fuel gas consumption (b) for 3 cases of back-pressure	50
64	Incoming air flow (a) and O2 emissions (b) for 3 cases of back-pressure	51
65	CO emissions in ppm (a) and g/kWh (b) for 3 cases of back-pressure	51
66	CO ₂ emissions in ppm (a) and g/kWh (b) for 3 cases of back-pressure	52
67	NO _x emissions in ppm (a) and g/kWh (b) for 3 cases of back-pressure	52
68	CO emissions in ppm (a) and g/kWh (b) for 3 cases of back-pressure	53
69	Compressor outlet pressure (a) and temperature (b) for 3 cases of back-pressure	54
70	Inlet receiver pressure (a) and temperature (b) for 3 cases of back-pressure	54
71	Exhaust receiver pressure (a) and temperature (b) for 3 cases of back-pressure	55
72	Absolute turbine outlet pressure (a) and temperature (b) for 3 cases of back-pressure	55
73	Pilot fuel energy flow (a) and gaseous fuel energy flow (b) for 3 cases of back-pressure	56
74	Pilot fuel energy vs Gaseous fuel energy for 3 cases of back-pressure	56
75	Specific fuel consumption (a) and specific fuel gas consumption (b) for 3 cases of back-pressure	57
76	Incoming air flow (a) and O2 emissions (b) for 3 cases of back-pressure	57
77	CO emissions in ppm (a) and g/kWh (b) for 3 cases of back-pressure	58
78	CO ₂ emissions in ppm (a) and g/kWh (b) for 3 cases of back-pressure	58
79	NO _x emissions in ppm (a) and g/kWh (b) for 3 cases of back-pressure	59
80	Unburned hydrocarbons emissions in ppm (a) and g/kWh (b) for 3 cases of back-pressure	59
81	Compressor outlet pressure for propeller curve (a) and generator curve (b)	61
82	Compressor outlet temperature for propeller curve (a) and generator curve (b)	62
83	Inlet receiver pressure for propeller curve (a) and generator curve (b)	62
84	Inlet receiver temperature for propeller curve (a) and generator curve (b)	63
85	Maximum in-cylinder pressure for propeller curve (a) and generator curve (b)	63
86	Turbine inlet pressure for propeller curve (a) and generator curve (b)	64
87	Turbine inlet temperature for propeller curve (a) and generator curve (b)	64
88	Turbine outlet temperature for propeller curve (a) and generator curve (b)	64
89	Exhaust valve temperature for propeller curve (a) and generator curve (b)	65
90	Pilot fuel flow for propeller curve (a) and generator curve (b)	65
91	Gaseous fuel flow for propeller curve (a) and generator curve (b)	66
92	Engine envelope and propeller curve	67
93	Engine limits and back-pressure effect on air-excess ratio (a), outlet receiver temperature (b) and exhaust valve temperature (c)	68

List of Tables

1	Composition of natural gas used as fuel	12
2	Properties of both fuel types	13
3	Properties of the stoichiometric gasses from both fuel types	13